U.S. Department
of Transportation

**Federal Railroad
Administration**

Analysis of Accelerations Measured During Full-Scale Tank Car Impact Tests

Office of Research
and Development
Washington, DC 20590

DOT/FRA/ORD 07/08

Final Report
April 2007

REPORT DOCUMENTATION PAGE

Form Approved
OMB No. 0704-0188

1. AGENCY USE ONLY (LEAVE BLANK)	2. REPORT DATE	3. REPORT TYPE AND DATES COVERED
	April 2007	Final Report April 2007

4. TITLE AND SUBTITLE
Analysis of Accelerations Measured During Full-Scale Tank Car Impact Tests

5. FUNDING NUMBERS
RR28/DB034

6. AUTHOR(S)
Lyons, Matthew L.; Riddell, William T.; Koch, Kevin W.

7. PERFORMING ORGANIZATION NAME(S) AND ADDRESS(ES)
U.S. Department of Transportation
Research and Special Programs Administration
John A. Volpe National Transportation Systems Center
55 Broadway
Cambridge, MA 02142-0193

8. PERFORMING ORGANIZATION REPORT NUMBER
DOT VNTSC-FRA-07-03

9. SPONSORING/MONITORING AGENCY NAME(S) AND ADDRESS(ES)
U.S. Department of Transportation
Federal Railroad Administration
Office of Research and Development
1120 Vermont Avenue, NW–Mail Stop 20
Washington, DC 20590

10. SPONSORING/MONITORING AGENCY REPORT NUMBER
DOT/FRA/ORD-07/08

11. SUPPLEMENTARY NOTES

12A. DISTRIBUTION/AVAILABILITY STATEMENT
This document is available to the U.S. public through the National Technical Information Service, Springfield, VA 22161.
This document is also available on the FRA Web site at www.fra.dot.gov.

12B. DISTRIBUTION CODE

13. ABSTRACT (MAXIMUM 200 WORDS)

Tank car impact responses were investigated using accelerometers mounted at various locations on a tank car. Several tests were run with both a full and an empty tank car, and varying the tank car impact speed. The data from the accelerometers went through a power spectral density (PSD) analysis for the longitudinal and vertical directions. The results from PSD analyses were compared with the peak coupler force and the dominant draft gear mechanism, also obtained from the data.

The results showed that the dominant draft gear mechanism had a marked effect on the response of the tank car, and, as speed and energy increased, the draft gear mechanism changed. For the empty tank car impact test results, in longitudinal acceleration signals, a frequency of 0 Hz and a range of frequencies above 300 Hz were present in PSD analyses; in vertical acceleration signals, a frequency of 13 Hz was present in PSD analyses, coinciding with the first axial mode of a simply supported cylinder. For the full tank car impact test results, in the vertical acceleration signals, two distinct peaks, at 5 Hz and 26 Hz, were present.

14. SUBJECT TERMS
tank car, shock response spectrum, acceleration, impact, power spectral density

15. NUMBER OF PAGES
100

16. PRICE CODE

17. SECURITY CLASSIFICATION OF REPORT	18. SECURITY CLASSIFICATION OF THIS PAGE	19. SECURITY CLASSIFICATION OF ABSTRACT	20. LIMITATION OF ABSTRACT
Unclassified	Unclassified	Unclassified	

METRIC/ENGLISH CONVERSION FACTORS

ENGLISH TO METRIC	METRIC TO ENGLISH
LENGTH (APPROXIMATE)	**LENGTH (APPROXIMATE)**
1 inch (in) = 2.5 centimeters (cm)	1 millimeter (mm) = 0.04 inch (in)
1 foot (ft) = 30 centimeters (cm)	1 centimeter (cm) = 0.4 inch (in)
1 yard (yd) = 0.9 meter (m)	1 meter (m) = 3.3 feet (ft)
1 mile (mi) = 1.6 kilometers (km)	1 meter (m) = 1.1 yards (yd)
	1 kilometer (km) = 0.6 mile (mi)
AREA (APPROXIMATE)	**AREA (APPROXIMATE)**
1 square inch (sq in, in^2) = 6.5 square centimeters (cm^2)	1 square centimeter (cm^2) = 0.16 square inch (sq in, in^2)
1 square foot (sq ft, ft^2) = 0.09 square meter (m^2)	1 square meter (m^2) = 1.2 square yards (sq yd, yd^2)
1 square yard (sq yd, yd^2) = 0.8 square meter (m^2)	1 square kilometer (km^2) = 0.4 square mile (sq mi, mi^2)
1 square mile (sq mi, mi^2) = 2.6 square kilometers (km^2)	10,000 square meters (m^2) = 1 hectare (ha) = 2.5 acres
1 acre = 0.4 hectare (he) = 4,000 square meters (m^2)	
MASS - WEIGHT (APPROXIMATE)	**MASS - WEIGHT (APPROXIMATE)**
1 ounce (oz) = 28 grams (gm)	1 gram (gm) = 0.036 ounce (oz)
1 pound (lb) = 0.45 kilogram (kg)	1 kilogram (kg) = 2.2 pounds (lb)
1 short ton = 2,000 pounds (lb) = 0.9 tonne (t)	1 tonne (t) = 1,000 kilograms (kg)
	= 1.1 short tons
VOLUME (APPROXIMATE)	**VOLUME (APPROXIMATE)**
1 teaspoon (tsp) = 5 milliliters (ml)	1 milliliter (ml) = 0.03 fluid ounce (fl oz)
1 tablespoon (tbsp) = 15 milliliters (ml)	1 liter (l) = 2.1 pints (pt)
1 fluid ounce (fl oz) = 30 milliliters (ml)	1 liter (l) = 1.06 quarts (qt)
1 cup (c) = 0.24 liter (l)	1 liter (l) = 0.26 gallon (gal)
1 pint (pt) = 0.47 liter (l)	
1 quart (qt) = 0.96 liter (l)	
1 gallon (gal) = 3.8 liters (l)	
1 cubic foot (cu ft, ft^3) = 0.03 cubic meter (m^3)	1 cubic meter (m^3) = 36 cubic feet (cu ft, ft^3)
1 cubic yard (cu yd, yd^3) = 0.76 cubic meter (m^3)	1 cubic meter (m^3) = 1.3 cubic yards (cu yd, yd^3)
TEMPERATURE (EXACT)	**TEMPERATURE (EXACT)**
[(x-32)(5/9)] °F = y °C	[(9/5) y + 32] °C = x °F

QUICK INCH - CENTIMETER LENGTH CONVERSION

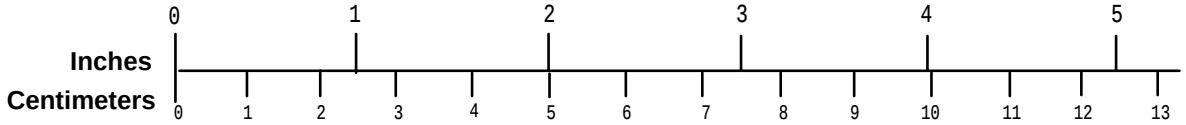

QUICK FAHRENHEIT - CELSIUS TEMPERATURE CONVERSION

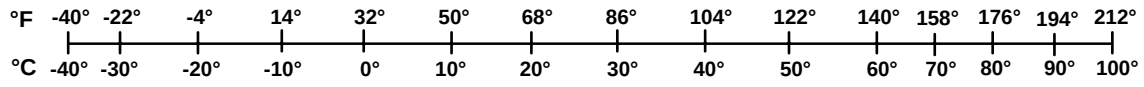

For more exact and or other conversion factors, see NIST Miscellaneous Publication 286, Units of Weights and Measures. Price $2.50 SD Catalog No. C13 10286

Updated 6/17/98

Preface

The tests that are described in this report resulted from a cooperative effort between industry groups and Federal agencies. The Tank Car Operating Environmental Task Force was established by the Association of American Railroads (AAR)–Chemical Manufacturers Association–Railway Progress Institute (RPI) liaison team to oversee this project. This project was funded by RPI, AAR, and the Federal Railroad Administration (FRA) Office of Research and Development.

The analysis discussed in this report was performed as part of the Tank Car Structural Integrity Program sponsored by FRA's Office of Research and Development.

The FRA Office of Research and Development tank car safety program manager is Mr. Jose Pena. Union Tank Car Company (or ACF) donated the tank car. Mr. Al Henzi facilitated this donation. Mr. Jim Rader (FRA-Office of Safety) helped with the historical aspects of the introduction and supplied the photograph for Figure 1. Mr. Keith Smith, of Southwest Research Institute, formerly of Transportation Technology Center, Inc. (TTCI), was responsible for much of the original vision and direction of the project. Thanks also to Todd Treichel, of RPI-AAR, and Christopher Barkan, University of Illinois, for support of this project.

Table of Contents

List of Figures vii

List of Tables x

Executive Summary 1

1. Introduction 3

2. Experimental Procedure 5

2.1 Test Configuration 5
2.2 Equipment 5
2.3 Instrumentation 7

3. Experimental Observations 9

3.1 Draft Gear Behavior 9
3.2 Longitudinal Coupler Forces 11
3.3 Measured Accelerations 12

4. Analysis of Results 17

4.1 Analysis of Measured Accelerations 17
4.2 Calculation of Anticipated Natural Frequencies 31
4.3 PSD Results 34
4.4 Displacements 35

5. Discussion 39

5.1 Draft Gear Mechanism 39
5.2 Coupler Force, Impact Speed, and Draft Gear Mechanism 39
5.3 PSD Analyses 40
5.4 The Relationship of PSD Results to Natural Frequencies 41

6. Summary and Conclusions 43

References 45

Appendix A. PSD Results of Empty Car Impact Tests 47

Appendix B. PSD Results of Full Car Impact Tests 71

Acronyms 85

List of Figures

Figure 1. A Sill Pad on a Tank Car–The Arrow Points to a Crack that Was Caused by High Coupler Forces Resulting from an Over-Speed Impact 3

Figure 2. Configuration of Impact Tests–With the Brakes Applied on the Hopper Car at the End of the Consist 5

Figure 3. Dimensions of the Tank Car Used in the Impact Tests.....6

Figure 4. Schematic of Draft Gear Used for Test.....7

Figure 5. Location of Accelerometers on Tank Car Body.....8

Figure 6. Coupler Force Plotted Against Time for Empty Tank Car Impacts at (a) 4.5 mph, (b) 6.1 mph, and (c) 7.4 mph, Representing Spring, Stick-Slip, and Solid Load Transfer Mechanisms, Respectively 10

Figure 7. Coupler Force Plotted Against Time for Full Tank Car Impacts at (a) 2.5 mph, (b) 4.2 mph, and (c) 7.5 mph, Representing Spring, Stick-Slip, and Solid Load Transfer Mechanisms, Respectively 11

Figure 8. Peak Longitudinal Coupler Forces Plotted Against Impact Velocity for an Empty and Full Tank Car.....12

Figure 9. Vertical Accelerations Measured at Location 6 for Three Solid Impacts of an Empty Tank Car at (a) 8.0 mph (1052 kips Peak Coupler Force), (b) 7.8 mph (970 kips Peak Coupler Force), and (c) 7.9 mph (1004 kips Peak Coupler Force) .13

Figure 10. Longitudinal Accelerations Measured at Location 6 for Three Solid Impacts of an Empty Tank Car at (a) 8.0 mph (1052 kips Peak Coupler Force), (b) 7.8 mph (970 kips Peak Coupler Force), and (c) 7.9 mph (1004 kips Peak Coupler Force).....14

Figure 11. Vertical Accelerations Measured from Location 6 for Three Solid Impacts of a Full Tank Car at (a) 7.4 mph (1347 kips Peak Coupler Force), (b) 7.2 mph (1276 kips Peak Coupler Force), and (c) 7.5 mph (1375 kips Peak Coupler Force).....15

Figure 12. Longitudinal Accelerations Measured from Location 6 for Three Solid Impacts of a Full Tank Car at (a) 7.4 mph (1347 kips Peak Coupler Force), (b) 7.2 mph (1276 kips Peak Coupler Force), and (c) 7.5 mph (1375 kips Peak Coupler Force).....16

Figure 13. Example of Window Selection.....17

List of Figures (cont.)

Figure 14. PSD Results as a Function of Length of Signal Examined for Accelerometer 6 for the Empty Tank Car Impact at Stick-Slip–The PSD Plot Obtained for a Window of 0.35 Second, Selected as the Representative Response, Shown in Bold.....18

Figure 15. PSD of Vertical Accelerations Measured at Location 6 for Empty Tank Car Impacts with Spring Load Transfer Mechanisms with Peak Coupler Forces of (a) 375 kips, (b) 444 kips, and (c) 542 kips.....19

Figure 16. PSD of Longitudinal Accelerations Measured at Location 6 for Empty Tank Car Impacts with Spring Load Transfer Mechanisms with Peak Coupler Forces of (a) 375 kips, (b) 444 kips, and (c) 542 kips.....20

Figure 17. PSD of Vertical Accelerations Measured at Location 6 for Empty Tank Car Impacts with Stick-Slip Load Transfer Mechanisms with Peak Coupler Forces of (a) 582 kips, (b) 594 kips, and (c) 619 kips.....21

Figure 18. PSD of Longitudinal Accelerations Measured at Location 6 for Empty Tank Cars Impacts with Stick-Slip Load Transfer Mechanisms with Peak Coupler Forces of (a) 582 kips, (b) 594 kips, and (c) 619 kips.....22

Figure 19. PSD of Vertical Accelerations Measured at Location 6 for Empty Tank Car Impacts with Solid Load Transfer Mechanisms with Peak Coupler Forces of (a) 970 kips, (b) 1004 kips, and (c) 1052 kips.....23

Figure 20. PSD of Longitudinal Accelerations Measured at Location 6 for Empty Tank Car Impacts with Solid Load Transfer Mechanisms with Peak Coupler Forces of (a) 970 kips, (b) 1004 kips, and (c) 1052 kips.....24

Figure 21. PSD of Vertical Accelerations Measured at Location 6 for Full Tank Car Impacts with Spring Load Transfer Mechanisms with Peak Coupler Forces of (a) 468 kips, (b) 496 kips, and (c) 500 kips.....25

Figure 22. PSD of Longitudinal Accelerations Measured at Location 6 for Full Tank Car Impacts with Spring Load Transfer Mechanisms with Peak Coupler Forces of (a) 468 kips, (b) 496 kips, and (c) 500 kips.....26

List of Figures (Cont.)

Figure 23. PSD of Vertical Accelerations Measured at Location 6 for Full Tank Car Impacts with Stick-Slip Load Transfer Mechanisms with Peak Coupler Forces of (a) 479 kips, (b) 486 kips, and (c) 495 kips 27

Figure 24. PSD of Longitudinal Accelerations Measured at Location 6 for Full Tank Car Impacts with Stick-Slip Load Transfer Mechanisms with Peak Coupler Forces of (a) 479 kips, (b) 486 kips, and (c) 495 kips 28

Figure 25. PSD of Vertical Accelerations Measured at Location 6 for Full Tank Car Impacts with Solid Load Transfer Mechanisms with Peak Coupler Forces of (a) 1276 kips, (b) 1347 kips, and (c) 1375 kips 29

Figure 26. PSD of Longitudinal Accelerations Measured at Location 6 for Full Tank Car Impacts with Solid Load Transfer Mechanisms with Peak Coupler Forces of (a) 1276 kips, (b) 1347 kips, and (c) 1375 kips 30

Figure 27. Schematic of the Cylinder Used to Determine the Natural Frequencies of the Tank Car 31

Figure 28. Examples of Mode Shapes for the Natural Frequencies of a Simply Supported Cylinder without Axial Constraint for (a) Bending, (b) Axial, (c) Radial, and (d) Radial-Axial 31

Figure 29. PSD of Vertical Acceleration from Location 6 for Three Solid Impacts of an Empty Tank Car Are Superimposed–Natural Frequencies of a Simply Supported Cylinder for Mode Shapes with a Vertical Component Are Indicated by the Solid Vertical Line (j = 1) and Dashed Vertical Lines (j = 2 through 5) 34

Figure 30. PSD of Longitudinal Acceleration from Location 6 for Three Solid Impacts of an Empty Tank Car Are Superimposed–Natural Frequencies of a Simply Supported Cylinder for Mode Shapes with a Longitudinal Component Are Indicated by the Solid Vertical Line (j = 1) and Dashed Vertical Lines (j = 2 through 5) 35

Figure 31. Vertical Displacement at Location 5 for an Empty Tank Car Impact at 8.0 mph 36

Figure 32. Vertical Displacement at Location 6 for an Empty Tank Car Impact at 8.0 mph 37

Figure 33. Longitudinal Displacement at Location 5 for an Empty Tank Car Impact at 8.0 mph 38

List of Tables

Table 1. Parameters Used in Equations 32
Table 2. Calculated Natural Frequencies for a Simply Supported Cylinder 33

Executive Summary

Under in-service conditions, a railroad tank car is subjected to cyclic loads that can lead to structural damage. Under most conditions, the damage accumulates slowly through fatigue crack growth mechanisms. Fatigue crack damage resulting from normal service conditions is managed in tank cars through a program of periodic inspections. The inspections identify stub sills and tanks with cracks, resulting in either repair of the cracks or retirement of cars found with cracks. In rare cases, however, a tank car can be subjected to an extreme force that leads to a sudden fracture. It is believed that many of the largest coupler-force events encountered by tank cars are induced by rail yard impacts.

A study of the technical requirements for a system to remotely monitor coupler forces on tank cars operating in revenue service was performed [1]. Based on the study of the technical requirements, an accelerometer-based system was recommended as a means to monitor coupler forces resulting from yard impacts. The first step toward developing such a system was performing a series of full-scale impact tests [2]. These tests involved impacting a tank car into a stationary consist of hopper cars. The tests consisted of a series of empty tank car impacts at nominal impact velocities of 2, 4, 6, and 8 miles per hour (mph) and a series of full tank car impacts at nominal impact velocities of 2, 4, 6, and 7 mph. For each empty tank car impact at 8 mph, 3 to 5 inches of movement occurred in the anvil string. For the other impacts in this series, the anvil cars essentially remained stationary. Strains, accelerations, and longitudinal coupler force were recorded as a function of time for each impact. For each impact test of the empty tank car, the coupler on the tank car was approximately 1.5 inches higher than the coupler on the impacted hopper car.

The purpose of this report is to investigate the response of accelerometers mounted at various locations on a tank car that was subjected to coupler impacts. This work was performed as part of the Tank Car Structural Integrity Program sponsored by the Office of Research and Development of the Federal Railroad Administration (FRA). The research team considered the effects of tank car lading, peak coupler force, dominant draft gear mechanism, and accelerometer location on the accelerometer responses. Power spectral density (PSD) analyses were performed on accelerations to quantify the response of the tank car to the impacts. The team compared frequencies identified by the PSD analyses to calculated natural frequencies for a simple thin-walled cylinder.

The dominant draft gear mechanism has a marked effect on the response of the tank car. In general, as speed and energy increase, the draft gear mechanism changes from spring to stick-slip to solid. For spring type impacts for empty tank cars, peak coupler force increased as impact speed increased. For spring type impacts, little difference existed in peak coupler force for full tank car impacts for the range of speeds investigated. Peak coupler force was nearly constant for all stick-slip impacts. The forces were approximately the same for the empty and full tank car impacts, but the impact speeds at which the stick-slip mechanism occurs were lower for the full

cars. For solid impacts, as speed increases, peak coupler force increases. For a given impact speed and a solid load transfer mechanism, full tank car impacts generated higher peak coupler force than empty cars.

The frequencies that were significantly and consistently excited differed between the empty and full tank car impact tests. For the empty tank car impact test results, a frequency near 0 Hz was present in the PSDs of longitudinal acceleration signals. The lack of vibrations and similar magnitude of integrated longitudinal displacements at locations 5 and 6 suggest that this is a rigid body vibration. A frequency of 13 Hz was present in the PSDs of the vertical acceleration signals, coinciding with the first radial-axial mode of a simply supported cylinder. The difference in magnitude of integrated vertical displacements at locations 5 and 6 suggest that this is a structural, not a rigid body vibration. In addition, frequencies of approximately 100 Hz were present in the vertical acceleration signals from impacts with a stick-slip coupler mechanism. The 100 Hz peak coincides with a frequency observed in the force-time traces for impacts with stick-slip draft gear mechanisms and was likely induced by the periodic nature of the coupler-force versus time relationship of the stick-slip coupler mechanism. Additional peaks greater than 250 Hz were present, but these occurred above most of the structural frequencies estimated by a simple model of a cylinder. In the full tank car impact tests, two distinct peaks, at approximately 5 Hz and 26 Hz, were present in the vertical acceleration response. A frequency at 0 Hz and a range of frequencies above 300 Hz were present in the PSDs of longitudinal acceleration signals.

Additional work with filtering and calculation of stock response spectrum (SRS) are required to develop a model for response of tank car to impact. Results suggest that structural response of a tank car subjected to coupler impact can be characterized by vibration at relatively few frequencies. As a result, the response of accelerometers at locations 5 and 6 might be able to be characterized with only a few degrees of freedom.

1. Introduction

During regular service, a railroad tank car is subjected to cyclic loads that can lead to structural damage. Under most conditions, the damage accumulates slowly through fatigue crack growth mechanisms. Fatigue crack damage resulting from normal service conditions is managed in tank cars through a program of periodic inspections. The inspections identify stub sills and tanks with cracks, resulting in either repair of the cracks or retirement of cars found with cracks. In rare cases, however, a tank car can be subjected to an extreme force that leads to a sudden fracture. The cracked head pad, shown in Figure 1, is the result of an extreme coupler force event. In this case, the fracture remained in the head pad and did not extend into the tank shell. However, if the damage resulting from an extreme case such as this were not noticed, a fatigue failure could occur after very little additional service, regardless of when the last inspection occurred. Therefore, the effect of especially damaging impacts on the reliability of tank cars must be considered carefully.

Figure 1. A Sill Pad on a Tank Car–The Arrow Points to a Crack that Was Caused by High Coupler Forces Resulting from an Over-Speed Impact

It is believed that many of the largest coupler-force events encountered by tank cars are induced by rail yard impacts. To address the frequency of these damaging events, a tank car operating environment task force was formed by the Association of American Railroads (AAR), the Chemical Manufacturers Association (now the American Chemistry Council), and the Railway Progress Institute (Association of American Railroads–Chemical Manufacturers Association–Railway Progress Institute) liaison team. Industry representatives, U.S. regulators, and Canadian regulators participated in this task force. A conclusion of this task force was that sufficient data did not exist to assess the extent of this problem. As a result of this conclusion, a study of the technical requirements for a system to remotely monitor coupler forces on tank cars operating in revenue service was performed [1].

Based on the study of the technical requirements, an accelerometer-based system was recommended as a means to monitor coupler forces resulting from yard impacts. The first step toward developing such a system was to perform a series of full-scale impact tests [2]. These tests involved impacting an empty tank car into a stationary consist. The results of these tests showed a relationship between the SRS [3] of measured accelerations and peak longitudinal coupler force. These tests, however, considered only an unloaded tank car in a single impact configuration. To develop a system that is applicable to in-service conditions, the effect of different impact configurations, tank car design, and lading in the tank car must be accounted for in the relationship between coupler force and dynamic response. The next step toward developing a useful system to monitor coupler forces is to account for lading in the tank car. Therefore, the research team performed a second series of tests where the tank car was full. Whether the car is empty or full, the primary draft gear mechanism and the peak coupler force are observed to affect the response.

2. Experimental Procedure

This report discusses two series of impact tests. The first series of impacts involved an empty tank car, and the second series of impacts involved a full tank car. Each series will be discussed further.

2.1 Test Configuration

Each test discussed in this report consisted of an instrumented tank car rolled into a stationary consist of three full hopper cars, as shown in Figure 2. The brakes of the last hopper car in the consist were applied for all impacts.

The series of empty tank car impacts consisted of nominal impact velocities of 2, 4, 6, and 8 mph. For each impact at 8 mph, 3 to 5 inches of movement occurred in the anvil string. During the other impacts in this series, the anvil cars essentially remained stationary. For each impact test of the empty tank car, the coupler on the tank car was approximately 1.5 inches higher than the coupler on the impacted hopper car.

The series of full tank car impacts consisted of nominal impact velocities of 2, 4, 6, and 7 mph. For each impact test of the full tank car, the coupler on the tank car was approximately at the same height as the coupler on the impacted hopper car. Strains, accelerations, and the longitudinal coupler force were recorded as a function of time for each impact.

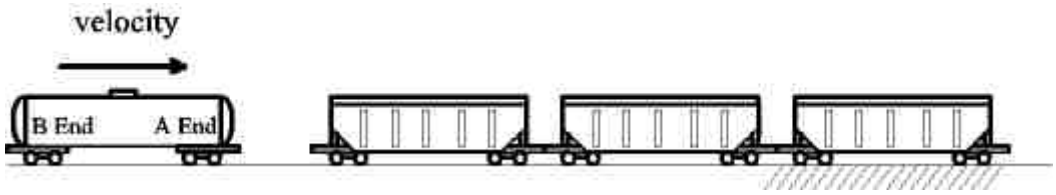

Figure 2. Configuration of Impact Tests–With the Brakes Applied on the Hopper Car at the End of the Consist

2.2 Equipment

A tank car manufactured by American Car and Foundry (ACF) was used for the tests. Figure 3 shows some critical dimensions of this car. The tank design is denoted ACF 4-B-7188, and the underframe design is denoted ACF 4-B-7190 Stub Sill. The tank consists of a steel shell 7/16-inch thick with a 4-inch layer of fiberglass insulation covering the exterior of the shell. A 7/8-inch thick jacket covers the insulation. The car weighs 75.4 kips empty and 263 kips with a full payload of 22,577 gallons of detergent alkylate. The coupler is a 6 1/4 x 8 type E.

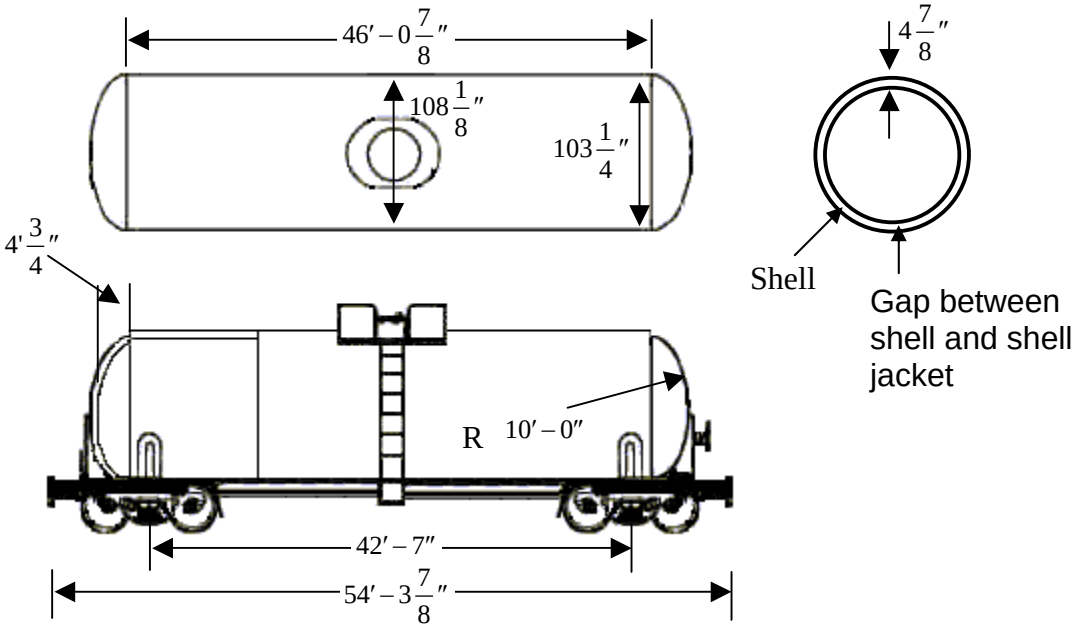

Figure 3. Dimensions of the Tank Car Used in the Impact Tests

A Cardwell Westinghouse Mark 50 all-steel design draft gear was used on both the tank car and the hopper cars that are used as anvil cars. Figure 4 shows a schematic of this draft gear. This gear employs friction wedges plus springs. When first loaded, the draft gear transmits forces through the friction wedges. Under quasi-static loading conditions, as much as 800 to 1000 kips (3600 to 4400 kN) can be developed without breaking the friction bond. Substantially less force, however, can break the friction bond under dynamic loading conditions. After the friction bond is broken, the internal spring-pack results in a nonlinear force-displacement relationship. The stiffness of the spring pack increases as the displacement increases to the full 3.25 inches (82.6 mm) of travel. The load-time trace between the time that the friction bond breaks and the internal spring force develops fully tends to be erratic. As impact speeds increase, this transition tends to become smoother.

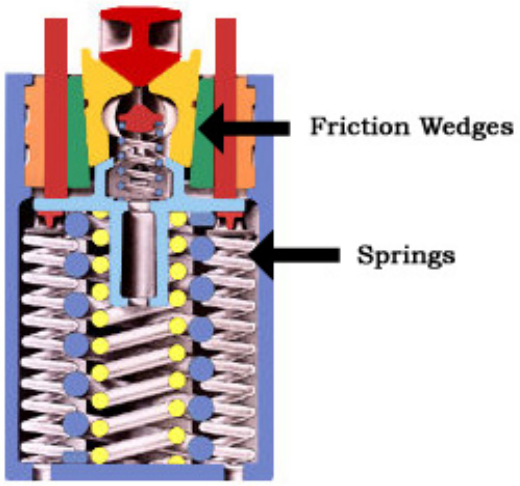

Figure 4. Schematic of Draft Gear Used for Test

2.3 Instrumentation

The tank car was instrumented with 37 accelerometers mounted at 20 locations. Figure 5 shows these locations. At each accelerometer location, except 11, 12, and 17, one accelerometer was oriented in the longitudinal direction, and one accelerometer was oriented in the vertical direction. Locations 11, 12, and 17 had a single accelerometer oriented in the longitudinal direction. The accelerometers mounted near the center and A-end (impacted end) of the car had a capacity of +/- 100 Gs, and those mounted near the B-end of the car had a capacity of +/- 50 Gs. The acceleration data was sampled at 5000 samples/second. These signals were filtered at about 1000 cycles/second. An instrumented coupler was installed at the A-end of the car and used to measure longitudinal coupler force as a function of time during each test.

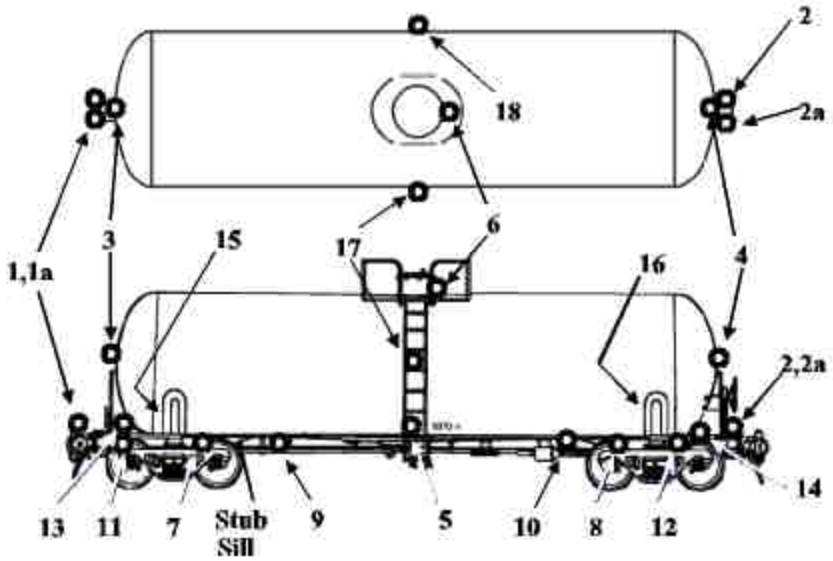

Figure 5. Location of Accelerometers on Tank Car Body

3. Experimental Observations

This section describes draft gear behavior, longitudinal coupler forces, and accelerations measured during the test.

3.1 Draft Gear Behavior

The longitudinal coupler force history resulting from each impact reveals the dominant load transfer mechanism that occurred during that impact. Previous work has shown that changes in the dominant load transfer mechanism resulted in distinct changes in the relationship between SRS values of measured accelerations and peak coupler force [2]. Longitudinal coupler force is plotted against time in Figure 6 for sample tests representing (a) spring, (b) stick-slip, and (c) solid coupler mechanisms for an empty tank car, and in Figure 7 for sample tests representing the same coupler mechanisms for a full tank car. For each impact on the full tank car, additional load peaks follow the primary load peaks. These additional peaks are believed to be induced by the motion of the fluid in the tank car.

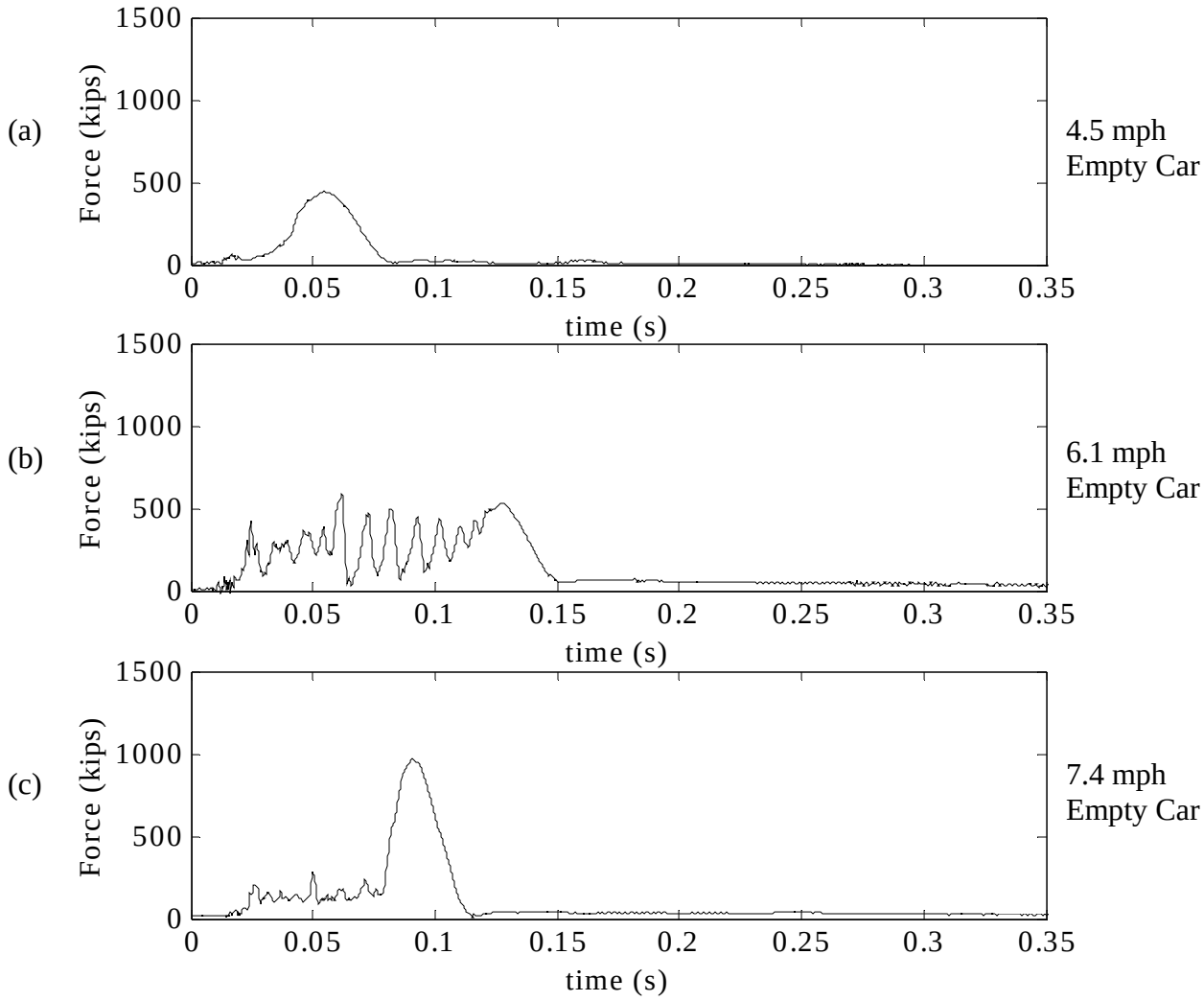

Figure 6. Coupler Force Plotted Against Time for Empty Tank Car Impacts at (a) 4.5 mph, (b) 6.1 mph, and (c) 7.4 mph, Representing Spring, Stick-Slip, and Solid Load Transfer Mechanisms, Respectively

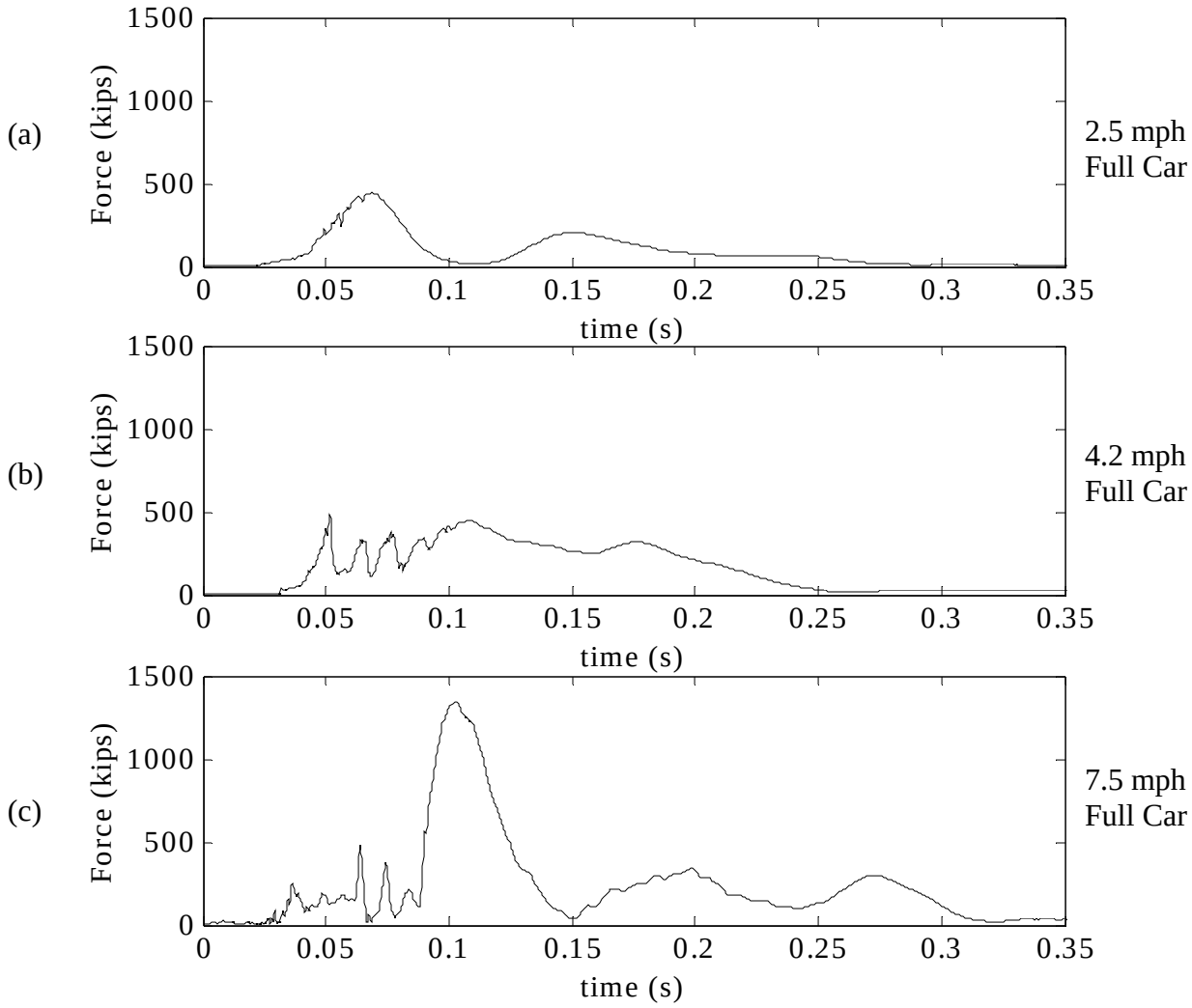

Figure 7. Coupler Force Plotted Against Time for Full Tank Car Impacts at (a) 2.5 mph, (b) 4.2 mph, and (c) 7.5 mph, Representing Spring, Stick-Slip, and Solid Load Transfer Mechanisms, Respectively

3.2 Longitudinal Coupler Forces

The peak longitudinal coupler forces resulting from both sequences of tests are plotted against impact velocity in Figure 8. Open symbols indicate empty car impacts, and solid symbols indicate full tank car impacts. A triangle, a square, and a circle represent spring, stick-slip, and solid draft gear mechanisms, respectively. Three observed trends are:

1. For the empty tank car, as impact speed increases, peak longitudinal coupler force tends to increase.
2. The loaded tank car tends to develop higher coupler forces than the unloaded car, except for impacts where the primary mechanism is stick-slip.

3. For impacts where stick-slip behavior is the dominant mechanism, peak coupler force is relatively insensitive to impact speed.

These observations for spring and solid impacts are consistent with trends predicted by simple lumped mass analyses, which model the couplers as springs. Figure 8 suggests that the complex behavior during stick-slip dominated impacts cannot be modeled as a simple spring.

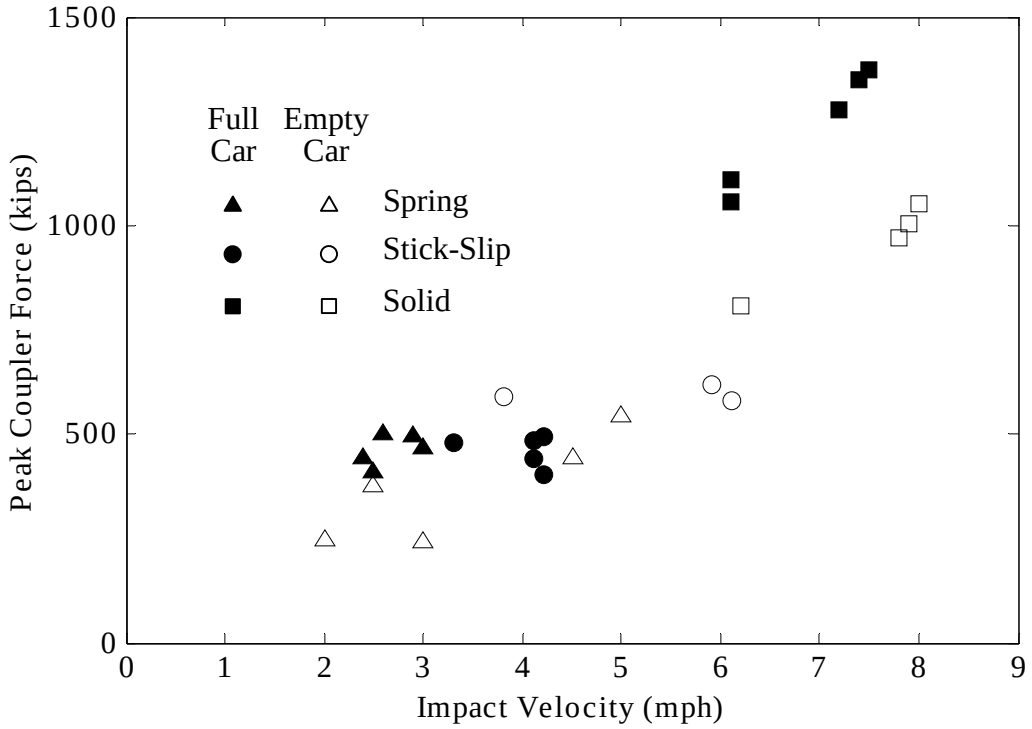

Figure 8. Peak Longitudinal Coupler Forces Plotted Against Impact Velocity for an Empty and Full Tank Car

3.3 Measured Accelerations

For each impact, the responses of all accelerometers were recorded over time. Acceleration was recorded before each impact, so the start time of each impact is assumed to be at the first significant change in the acceleration time history.

As examples, Figure 9 plots the vertical accelerations measured at location 6 resulting from three impacts dominated by the solid load transfer mechanism. Location 6 is near the manway opening on the tank (refer to Figure 5). Figure 10 plots the longitudinal accelerations measured at location 6 resulting from three solid impacts. The resulting peak coupler forces for these impacts are 1052, 970, and 1004 kips for the tests plotted in Figures 9a, 9b, and 9c, and Figures 10a, 10b, and 10c, respectively.

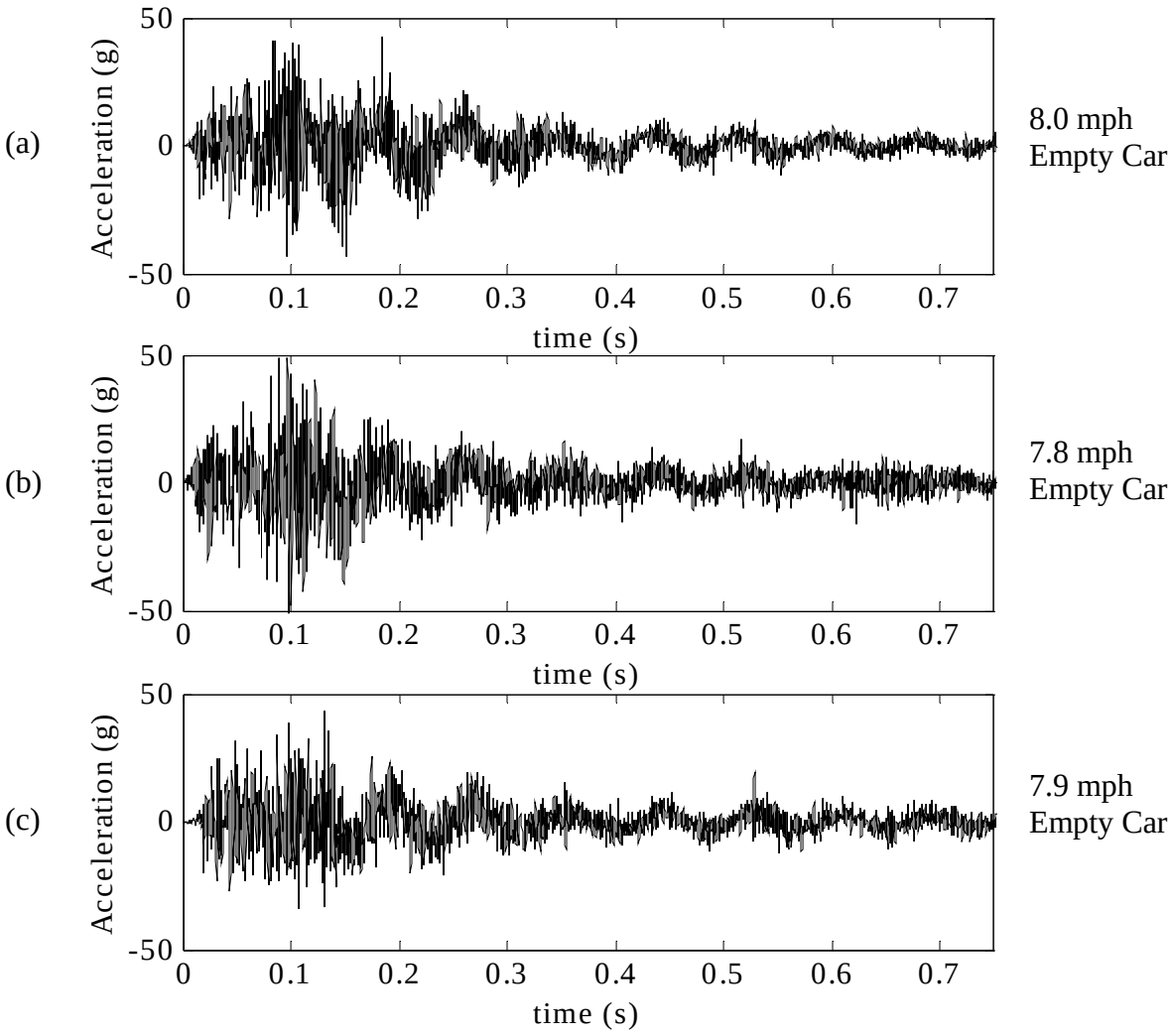

Figure 9. Vertical Accelerations Measured at Location 6 for Three Solid Impacts of an Empty Tank Car at (a) 8.0 mph (1052 kips Peak Coupler Force), (b) 7.8 mph (970 kips Peak Coupler Force), and (c) 7.9 mph (1004 kips Peak Coupler Force)

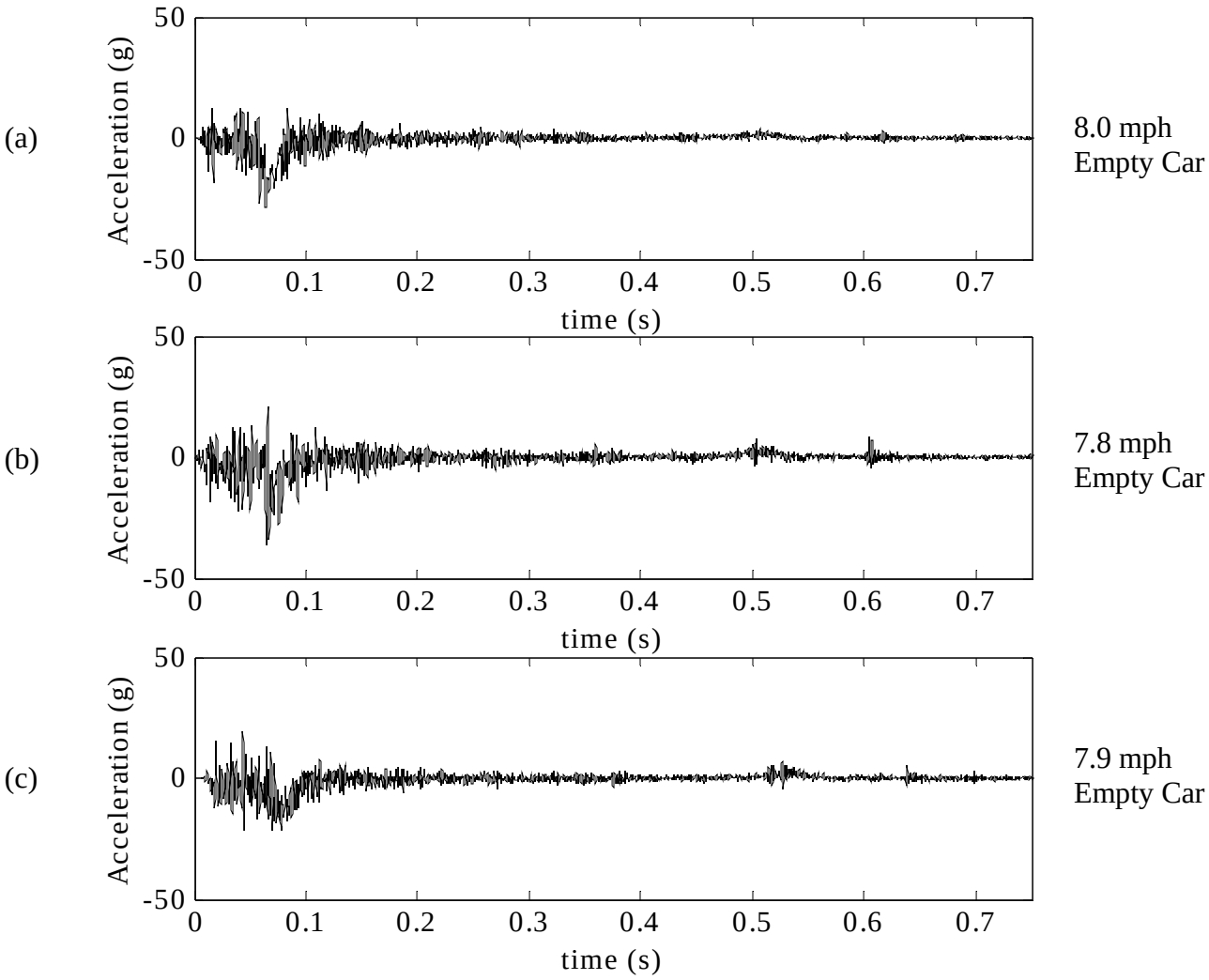

Figure 10. Longitudinal Accelerations Measured at Location 6 for Three Solid Impacts of an Empty Tank Car at (a) 8.0 mph (1052 kips Peak Coupler Force), (b) 7.8 mph (970 kips Peak Coupler Force), and (c) 7.9 mph (1004 kips Peak Coupler Force)

For each of these impacts, the greatest absolute value of vertical acceleration for these impacts occurs approximately 0.06 to 0.10 seconds after the impact starts. This time period coincides with a large spike in the longitudinal force versus time relationship, similar to that observed in Figures 6c and 7c.

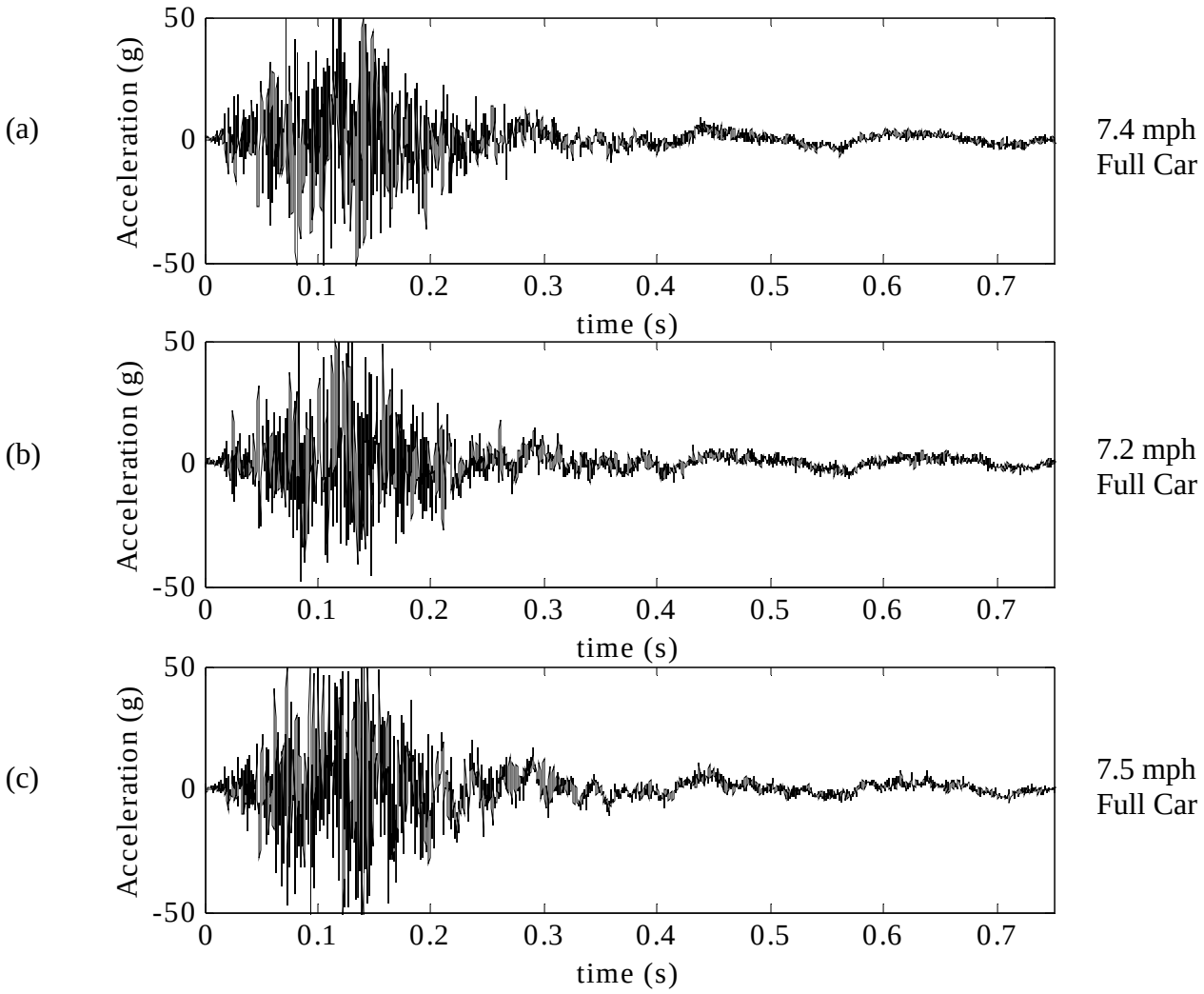

Figure 11. Vertical Accelerations Measured from Location 6 for Three Solid Impacts of a Full Tank Car at (a) 7.4 mph (1347 kips Peak Coupler Force), (b) 7.2 mph (1276 kips Peak Coupler Force), and (c) 7.5 mph (1375 kips Peak Coupler Force)

Figure 11 plots the vertical accelerations measured at location 6, resulting from three full tank car impacts dominated by the solid load transfer mechanism. Figure 12 plots the longitudinal accelerations measured at location 6, resulting from three solid full tank car impacts. The resulting peak coupler forces for these impacts are 1347, 1276, and 1375, respectively.

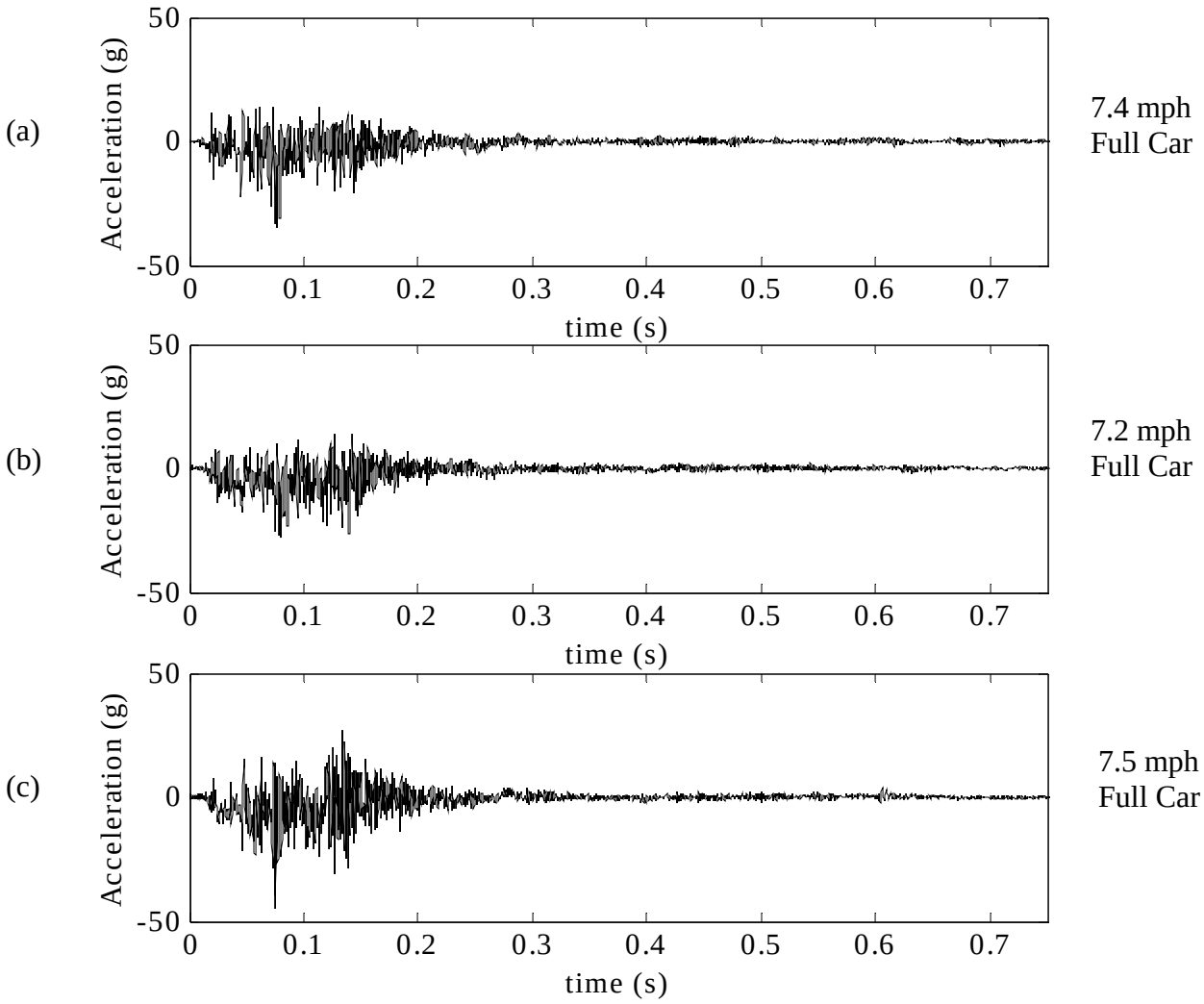

Figure 12. Longitudinal Accelerations Measured from Location 6 for Three Solid Impacts of a Full Tank Car at (a) 7.4 mph (1347 kips Peak Coupler Force), (b) 7.2 mph (1276 kips Peak Coupler Force), and (c) 7.5 mph (1375 kips Peak Coupler Force)

4. Analysis of Results

This section discusses the methodology of the analysis of the recorded acceleration signals.

4.1 Analysis of Measured Accelerations

A PSD analysis was performed on each time history of acceleration to determine the dominant frequencies of the response of the tank cars. Accelerations in both the vertical and longitudinal directions for the empty tank car tests for representative impacts with spring, stick-slip, and solid load transfer mechanisms and for the full car for representative impacts with spring, stick-slip, and solid load transfer mechanisms from all locations were examined.

The results of PSD analyses are dependent on the portion of the signal that is analyzed. To determine the optimum portion of the signal to analyze for the PSD calculations, a consistent method to identify a start time and a constant window size were established for the accelerations signals. Figure 13 shows an example of the process. Double-differentiating the acceleration signal and setting a reasonable threshold value, determined to be $2x10^{+7}$ (g/sec^2), identifies the start time. No sensitivity studies were performed on the start time, but this value resulted in the same start time obtained when using engineering judgment. To investigate the most appropriate value for the window, the window of signal was varied between 0.2 and 1.0 second in increments of 0.05 second. To visualize these results, a plot of PSD analyses, frequency, and the window was developed.

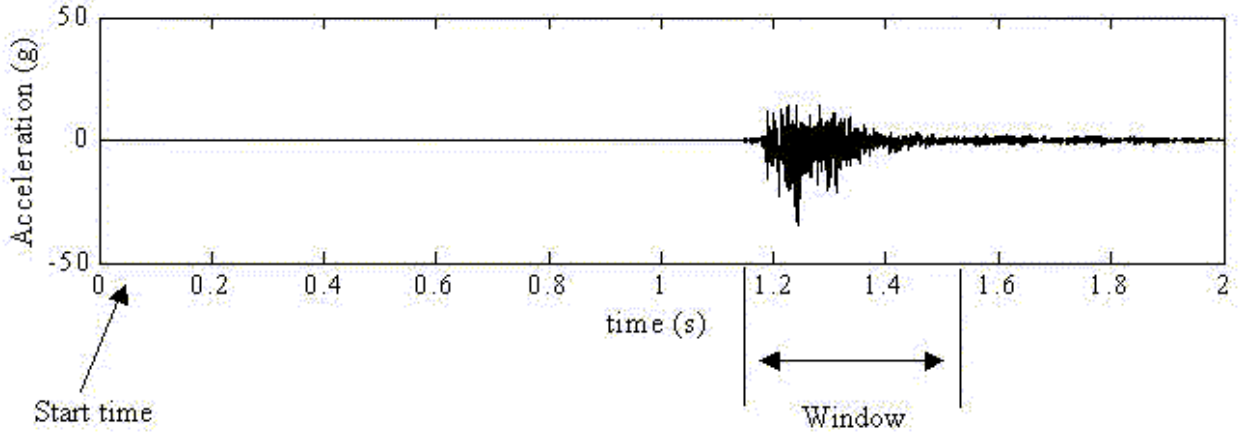

Figure 13. Example of Window Selection

Figure 14 shows a sample 3D plot. For a given window, certain frequencies exhibit PSD peaks. When these peaks are consistent for a range of window values, the peaks appear as fans in the three-dimensional plot that run parallel to the window axis and perpendicular to the frequency axis. It was assumed that the peaks that are consistent throughout a range of windows were the most significant. A window of 0.35 second captures most of the fans and was used for all additional analyses.

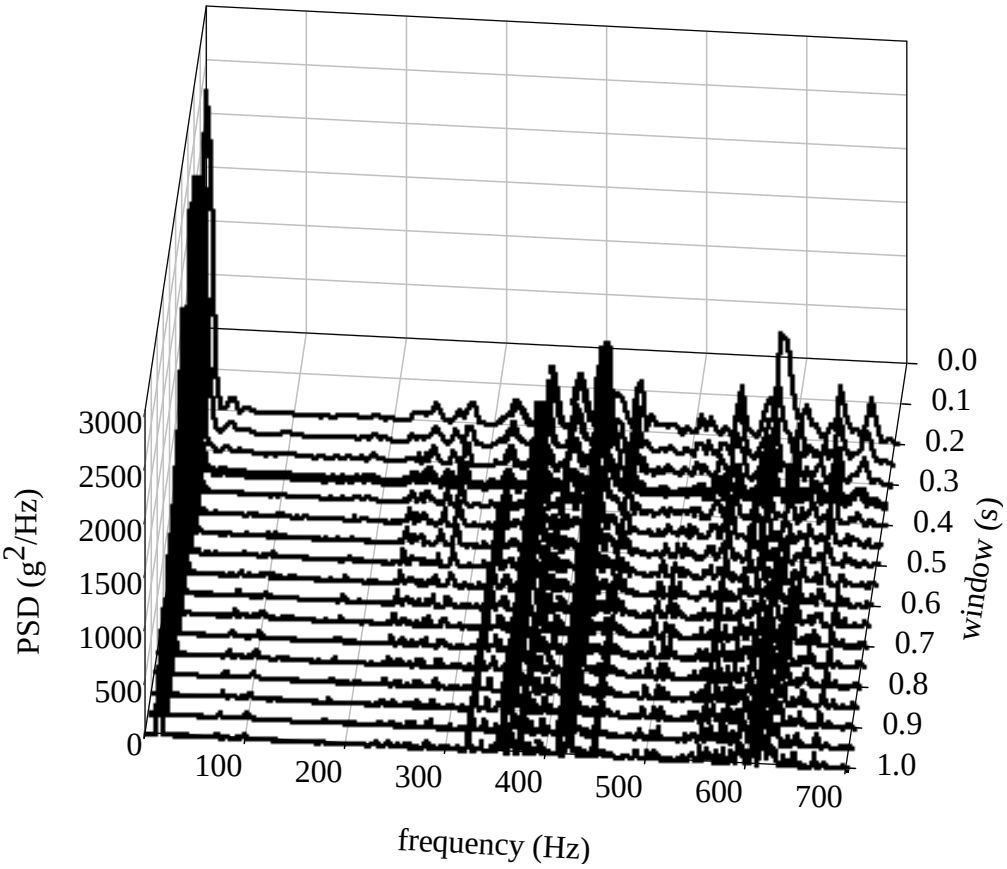

Figure 14. PSD Results as a Function of Length of Signal Examined for Accelerometer 6 for the Empty Tank Car Impact at Stick-Slip–The PSD Plot Obtained for a Window of 0.35 Second, Selected as the Representative Response, Shown in Bold

Figures 15-20 show plots of the PSDs for the vertical and longitudinal acceleration signals from location 6 for one empty tank car impact for each type (spring, stick-slip, and solid). Figures 21-26 show plots of the PSDs for the vertical and longitudinal acceleration signals from location 6 for a loaded tank car impact of each type (spring, stick-slip, and solid).

Accelerations measured at other locations were also analyzed. Results of the PSD analyses on accelerations measured at locations 1, 1A, 2, 2A, 5, 6, 8, 9, 11, 12, 13, 14, 16, 17, and 18 on the empty tank car are shown in Appendix A, Figures A1-A23, and at locations 1, 1A, 5, 6, 9, 10, and 18 on the full tank car are shown in Appendix B, Figures B1-B14.

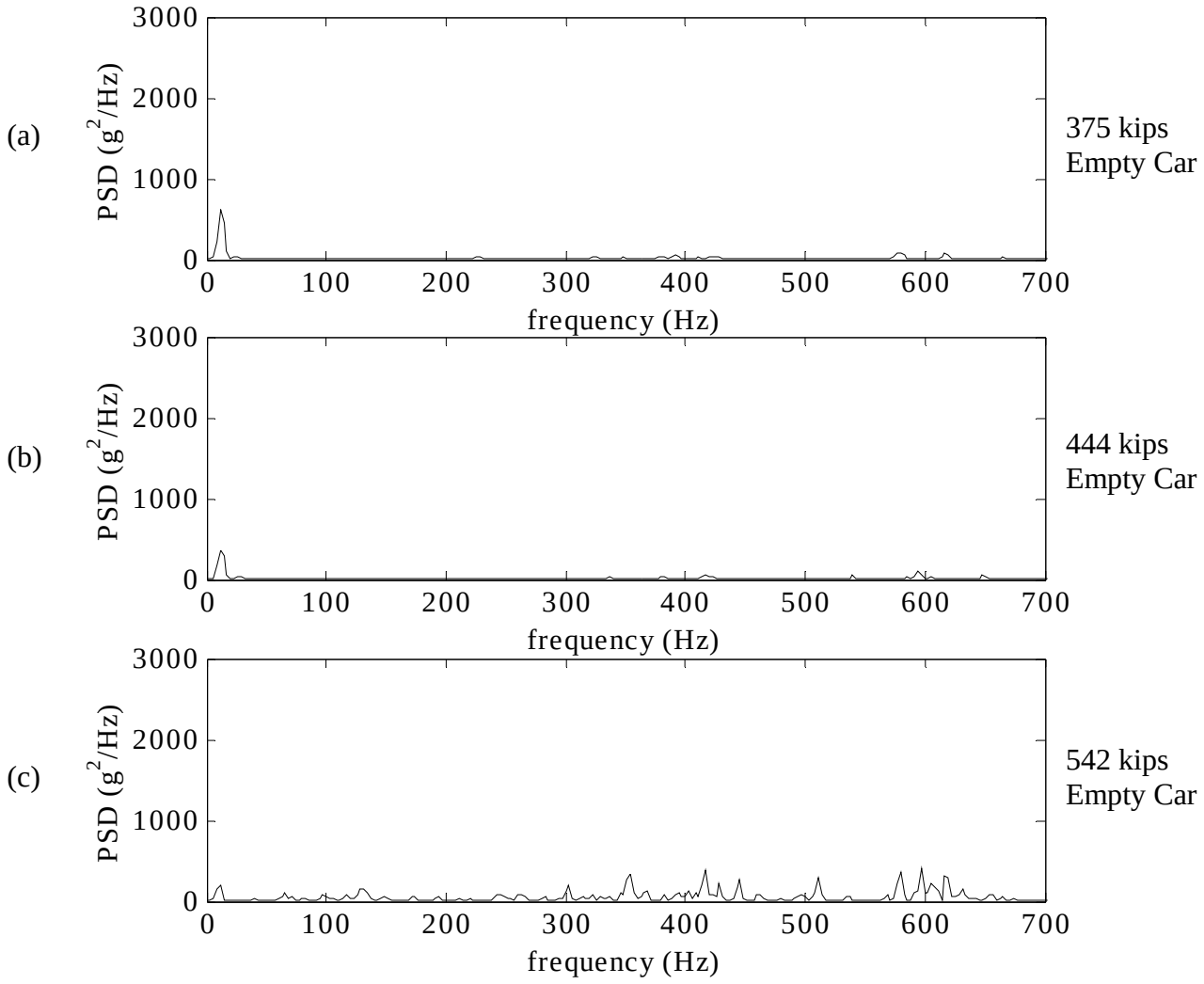

Figure 15. PSD of Vertical Accelerations Measured at Location 6 for Empty Tank Car Impacts with Spring Load Transfer Mechanisms with Peak Coupler Forces of (a) 375 kips, (b) 444 kips, and (c) 542 kips

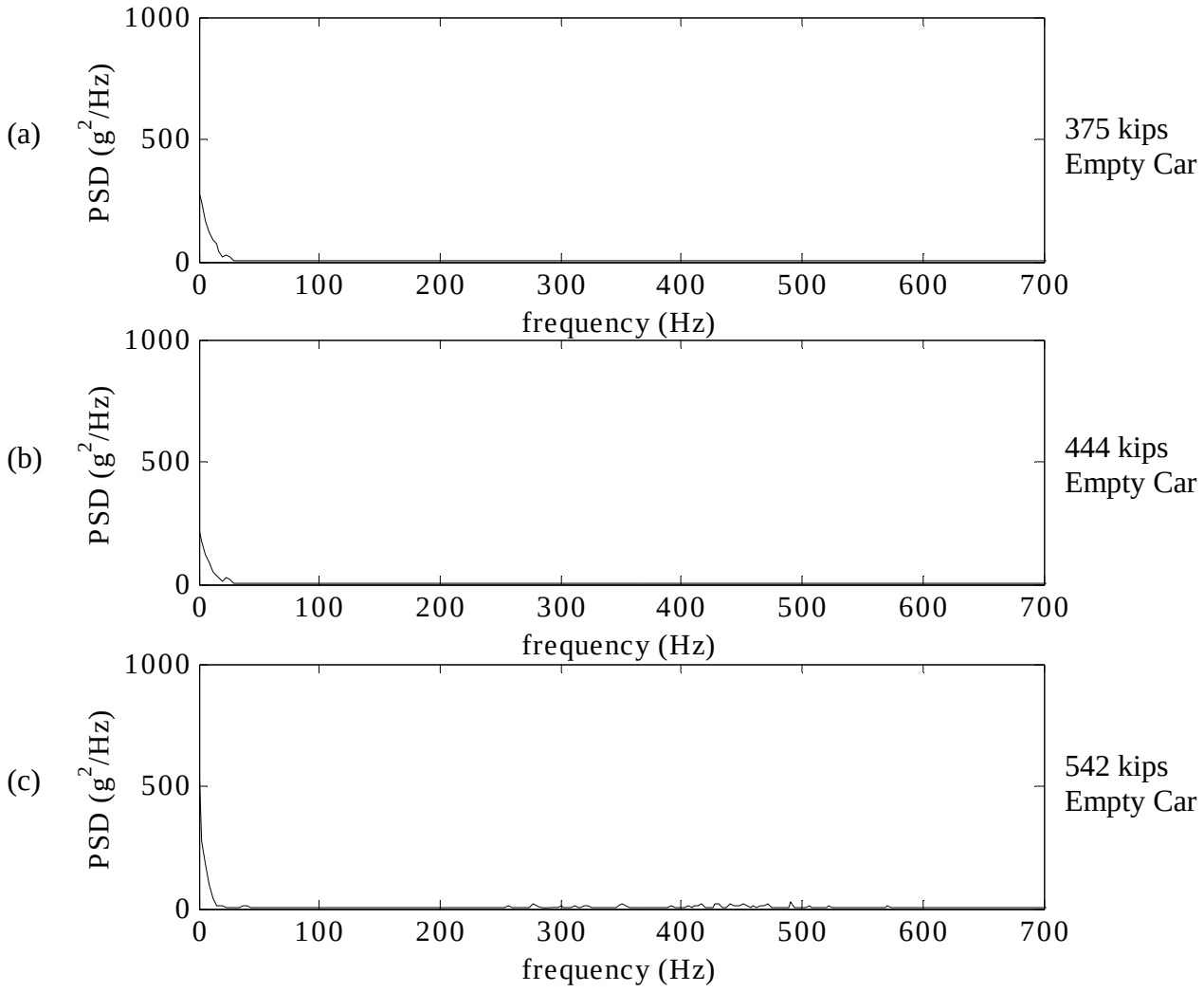

Figure 16. PSD of Longitudinal Accelerations Measured at Location 6 for Empty Tank Car Impacts with Spring Load Transfer Mechanisms with Peak Coupler Forces of (a) 375 kips, (b) 444 kips, and (c) 542 kips

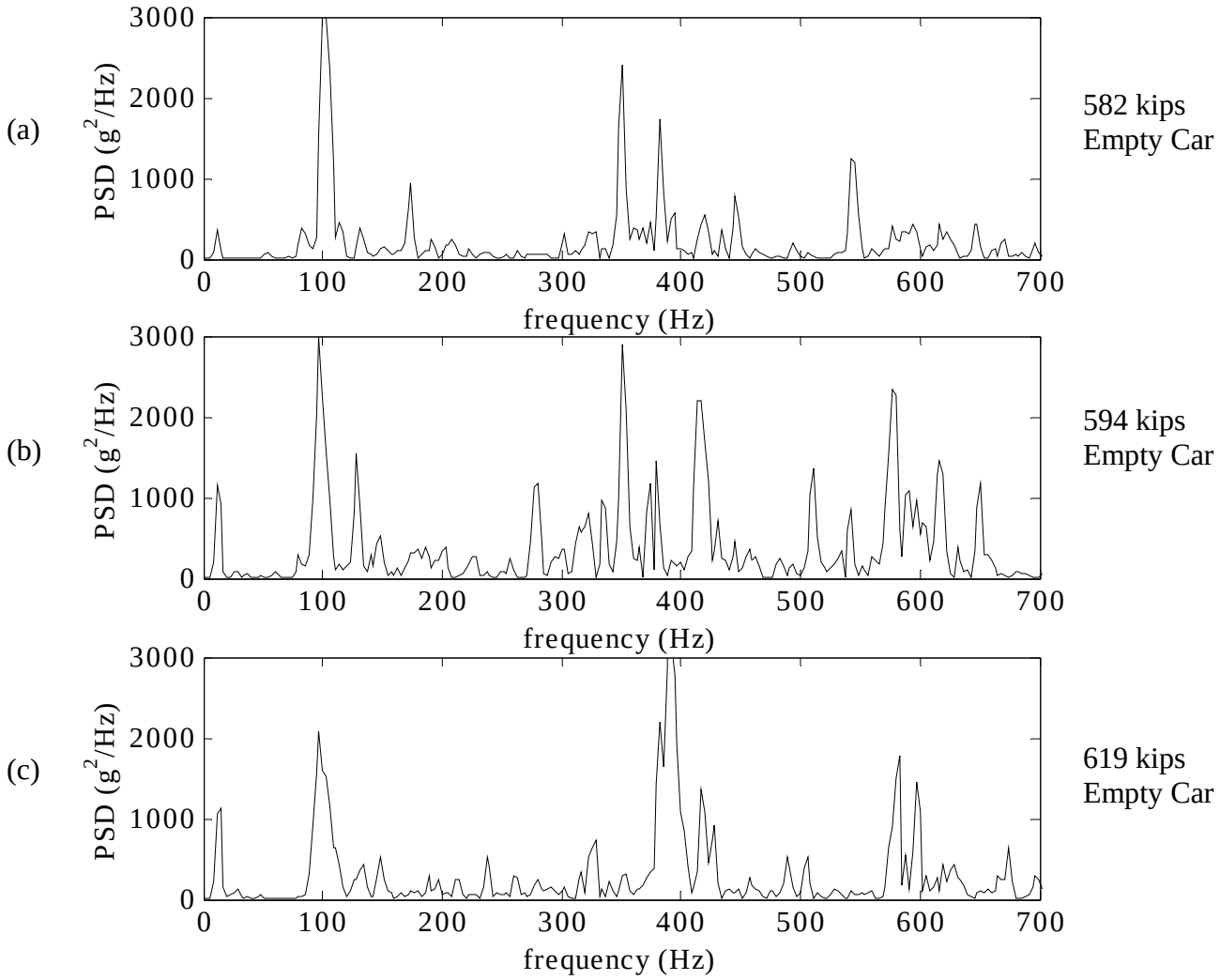

Figure 17. PSD of Vertical Accelerations Measured at Location 6 for Empty Tank Car Impacts with Stick-Slip Load Transfer Mechanisms with Peak Coupler Forces of (a) 582 kips, (b) 594 kips, and (c) 619 kips

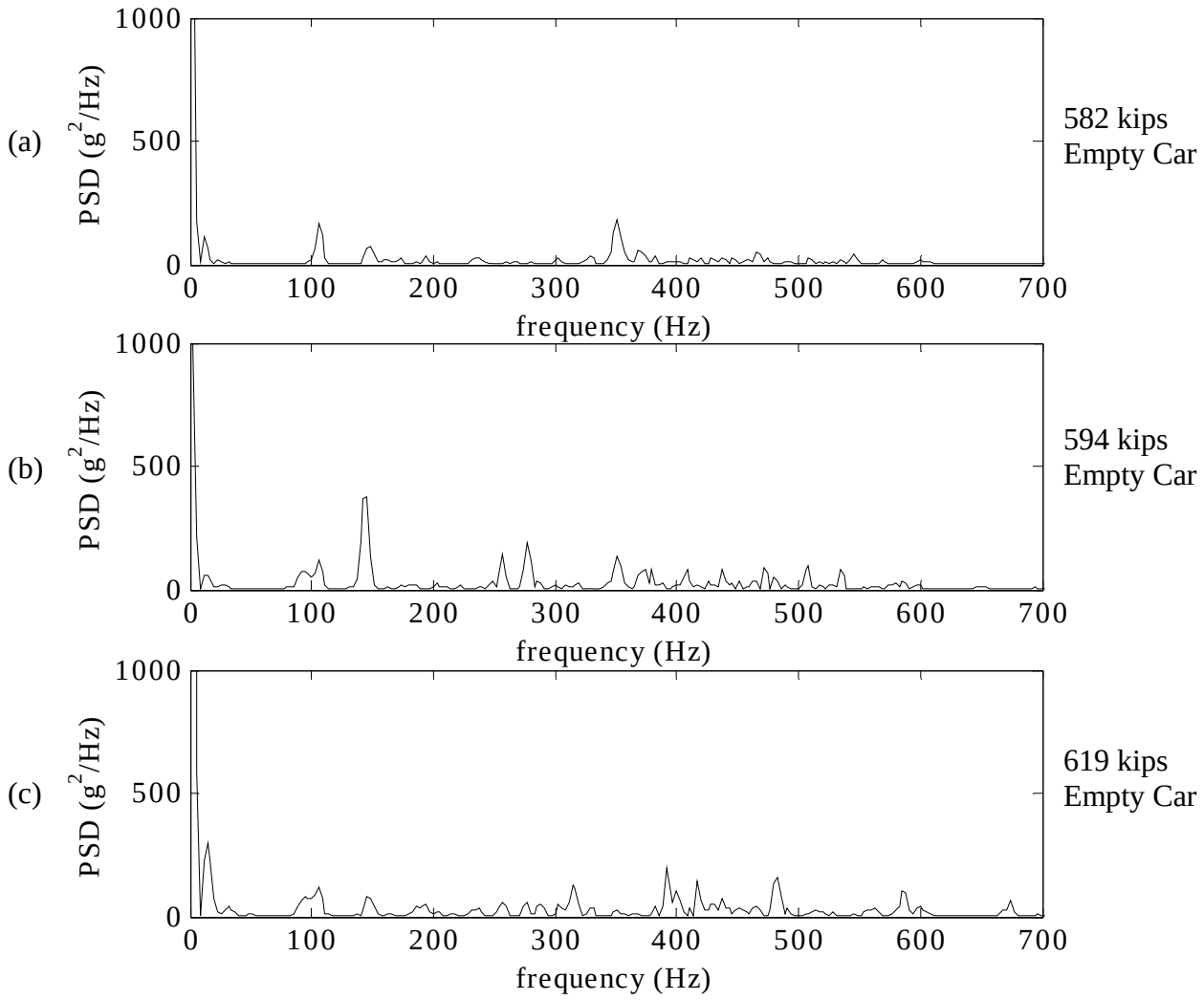

Figure 18. PSD of Longitudinal Accelerations Measured at Location 6 for Empty Tank Car Impacts with Stick-Slip Load Transfer Mechanisms with Peak Coupler Forces of (a) 582 kips, (b) 594 kips, and (c) 619 kips

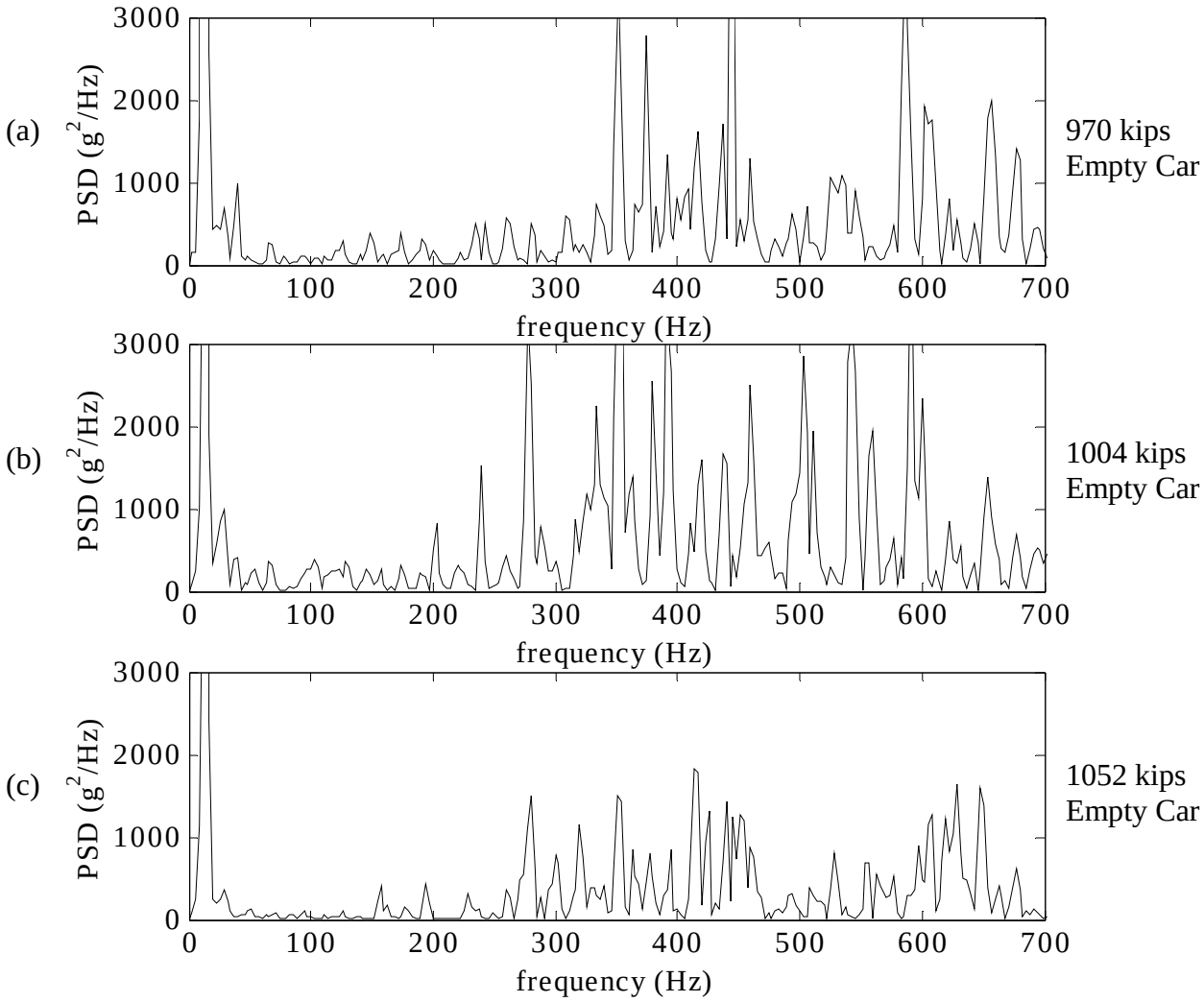

Figure 19. PSD of Vertical Accelerations Measured at Location 6 for Empty Tank Car Impacts with Solid Load Transfer Mechanisms with Peak Coupler Forces of (a) 970 kips, (b) 1004 kips, and (c) 1052 kips

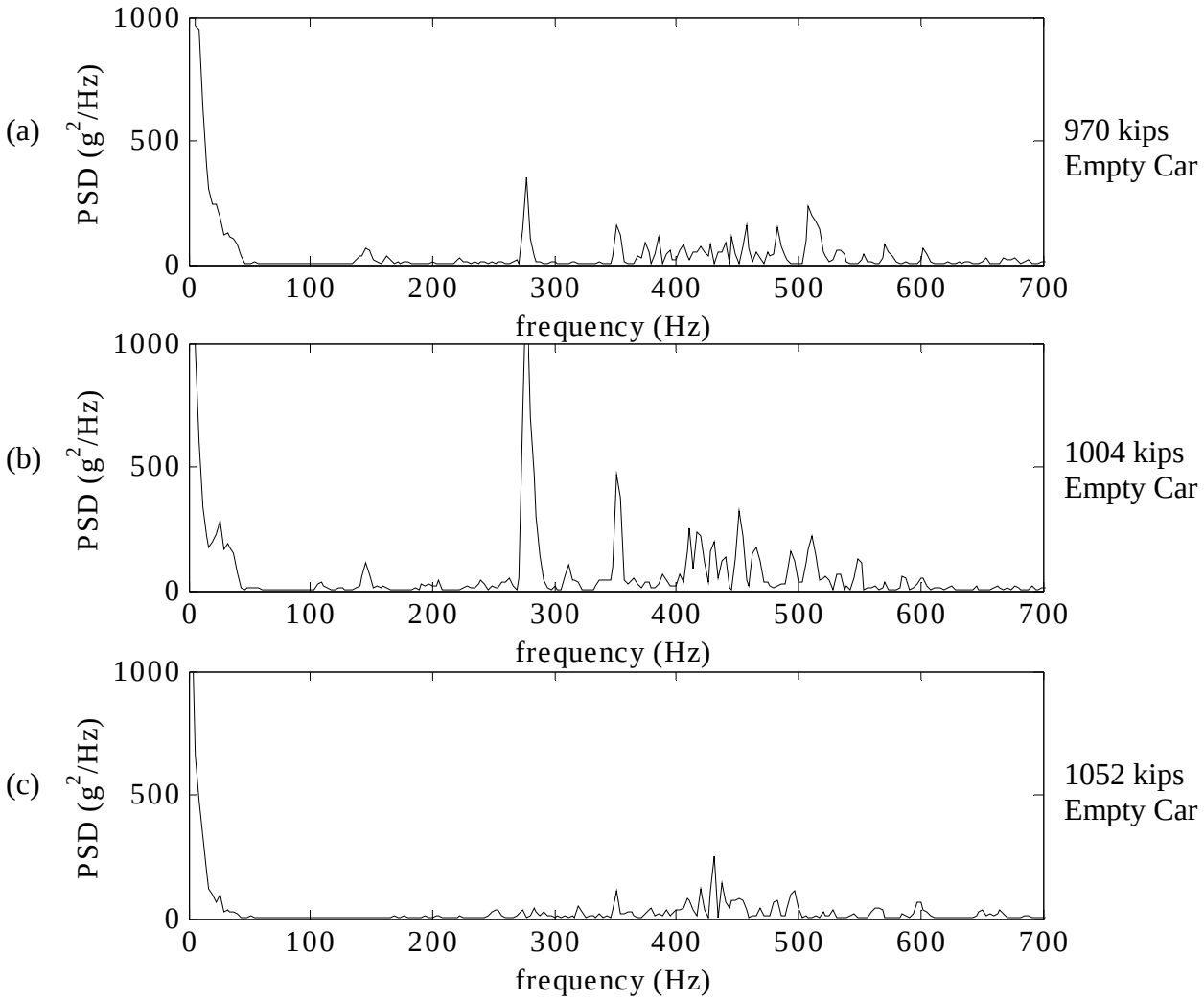

Figure 20. PSD of Longitudinal Accelerations Measured at Location 6 for Empty Tank Car Impacts with Solid Load Transfer Mechanisms with Peak Coupler Forces of (a) 970 kips, (b) 1004 kips, and (c) 1052 kips

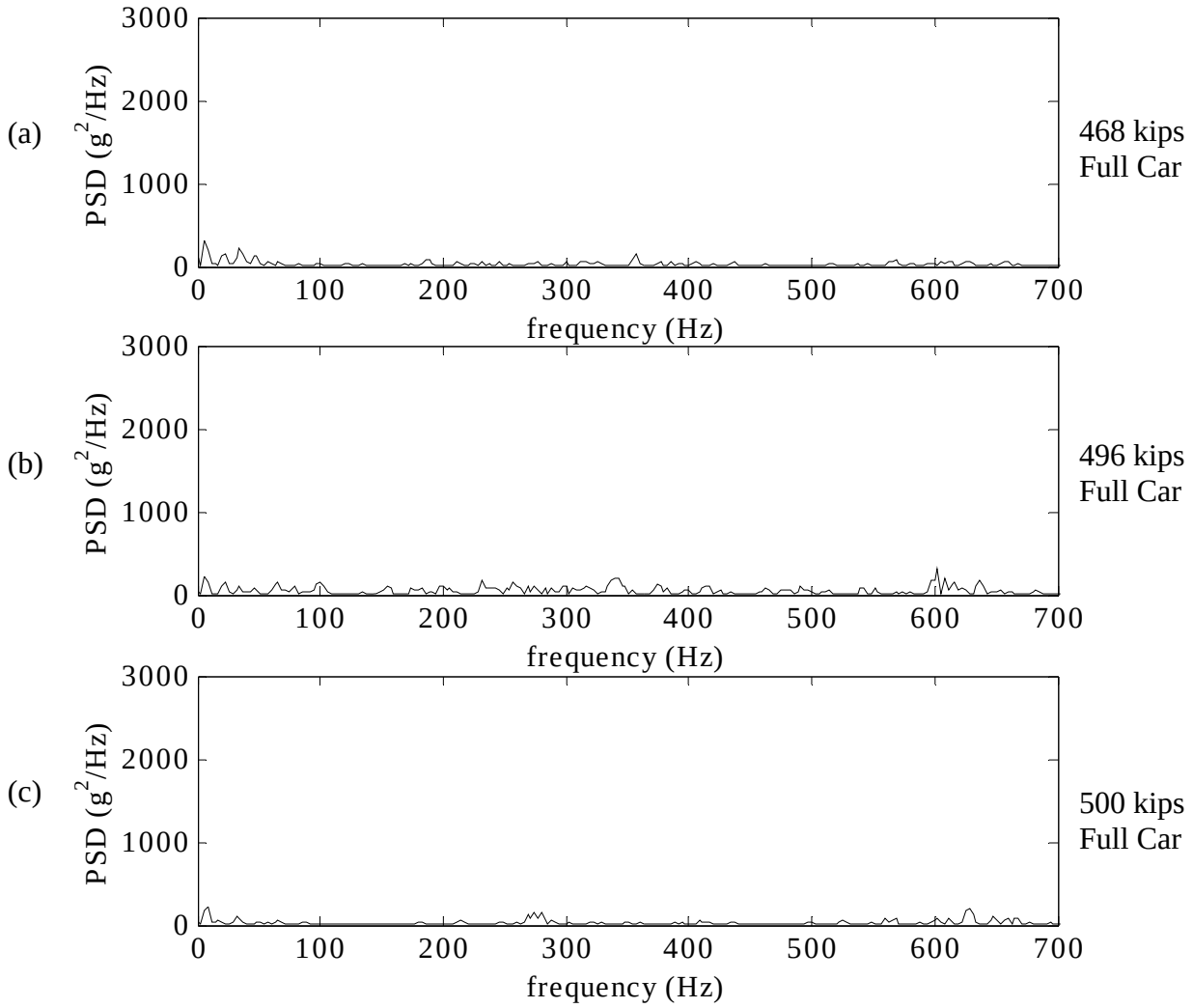

Figure 21. PSD of Vertical Accelerations Measured at Location 6 for Full Tank Car Impacts with Spring Load Transfer Mechanisms with Peak Coupler Forces of (a) 468 kips, (b) 496 kips, and (c) 500 kips

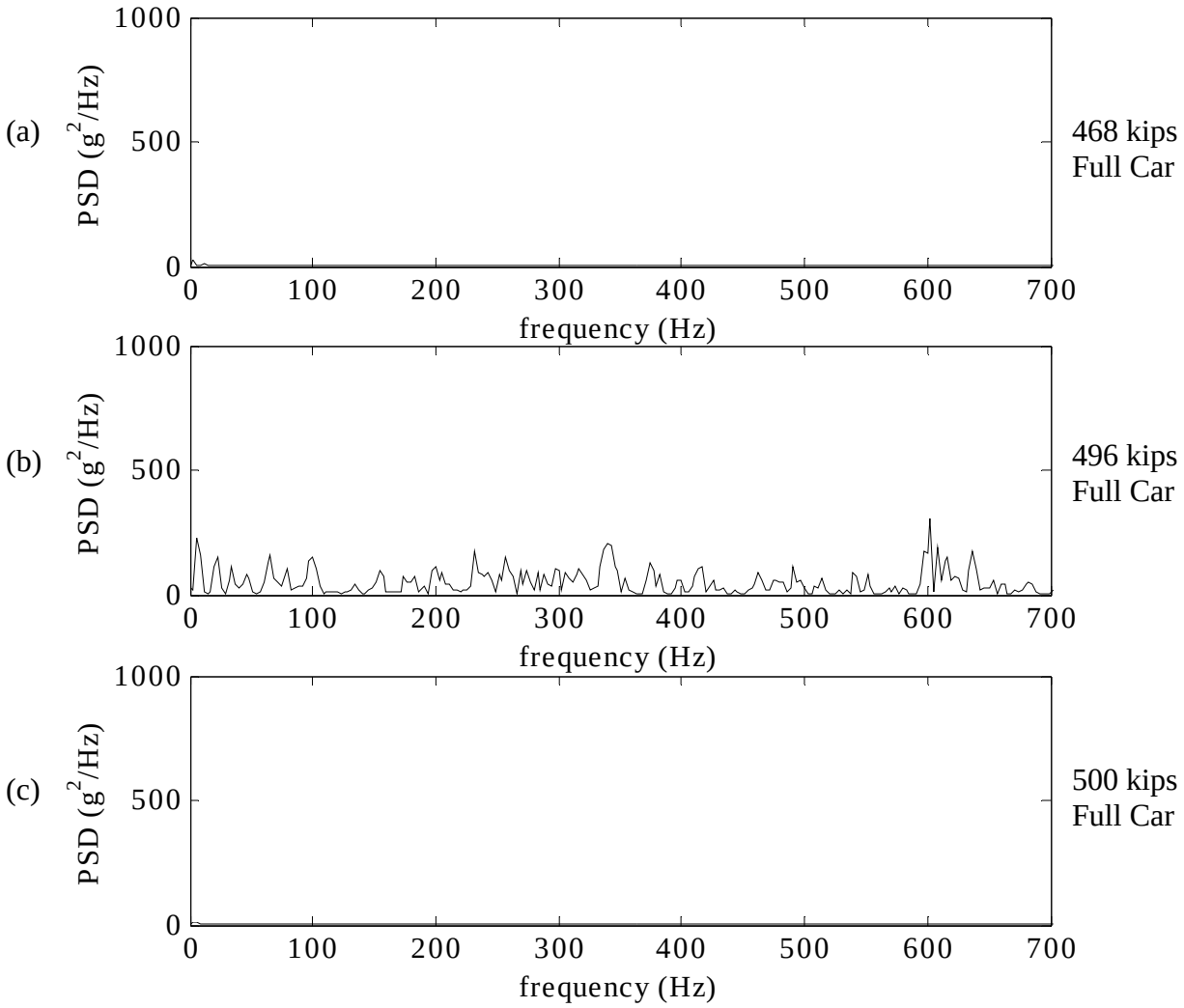

Figure 22. PSD of Longitudinal Accelerations Measured at Location 6 for Full Tank Car Impacts with Spring Load Transfer Mechanisms with Peak Coupler Forces of (a) 468 kips, (b) 496 kips, and (c) 500 kips

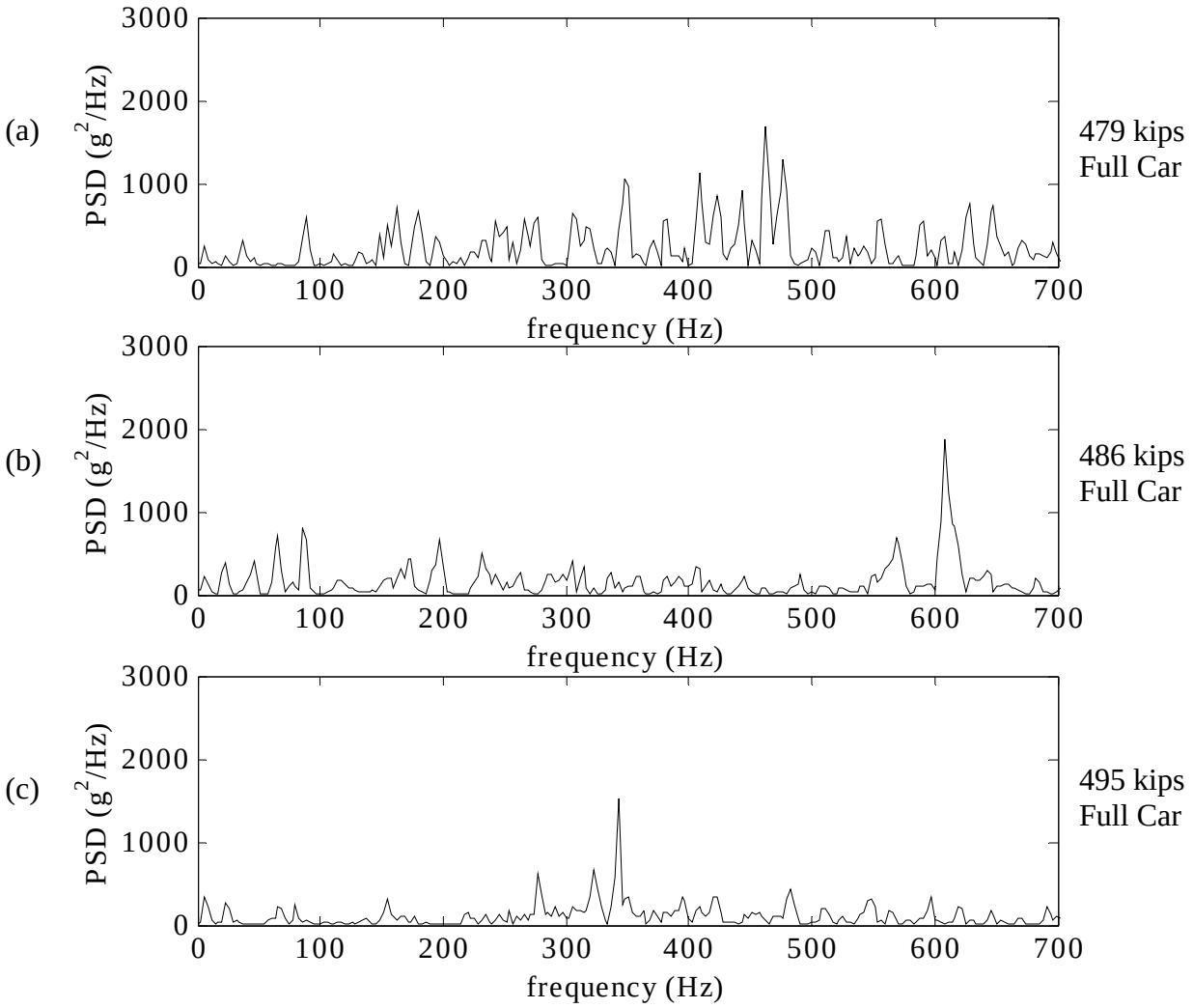

Figure 23. PSD of Vertical Accelerations Measured at Location 6 for Full Tank Car Impacts with Stick-Slip Load Transfer Mechanisms with Peak Coupler Forces of (a) 479 kips, (b) 486 kips, and (c) 495 kips

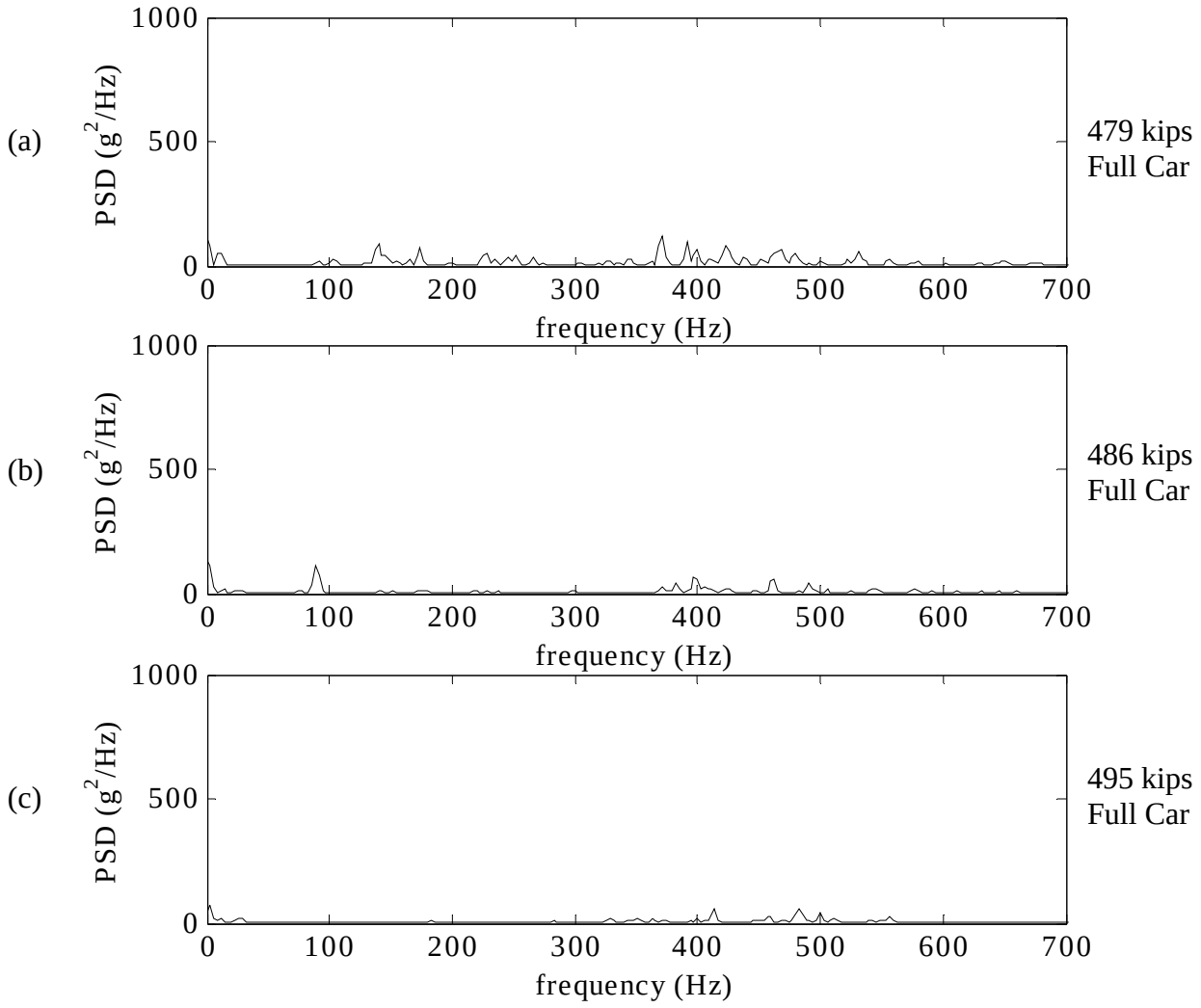

Figure 24. PSD of Longitudinal Accelerations Measured at Location 6 for Full Tank Car Impacts with Stick-Slip Load Transfer Mechanisms with Peak Coupler Forces of (a) 479 kips, (b) 486 kips, and (c) 495 kips

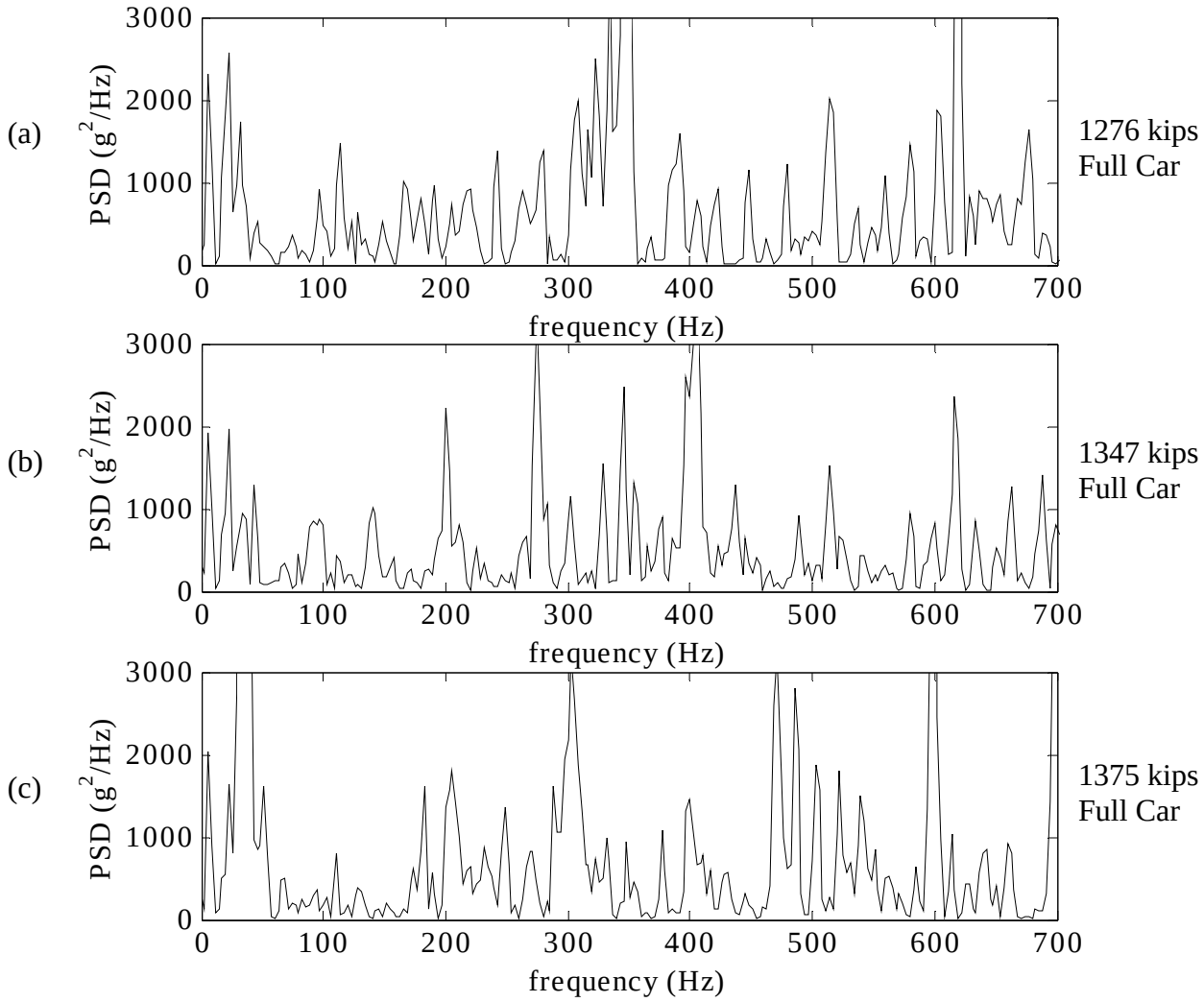

Figure 25. PSD of Vertical Accelerations Measured at Location 6 for Full Tank Car Impacts with Solid Load Transfer Mechanisms with Peak Coupler Forces of (a) 1276 kips, (b) 1347 kips, and (c) 1375 kips

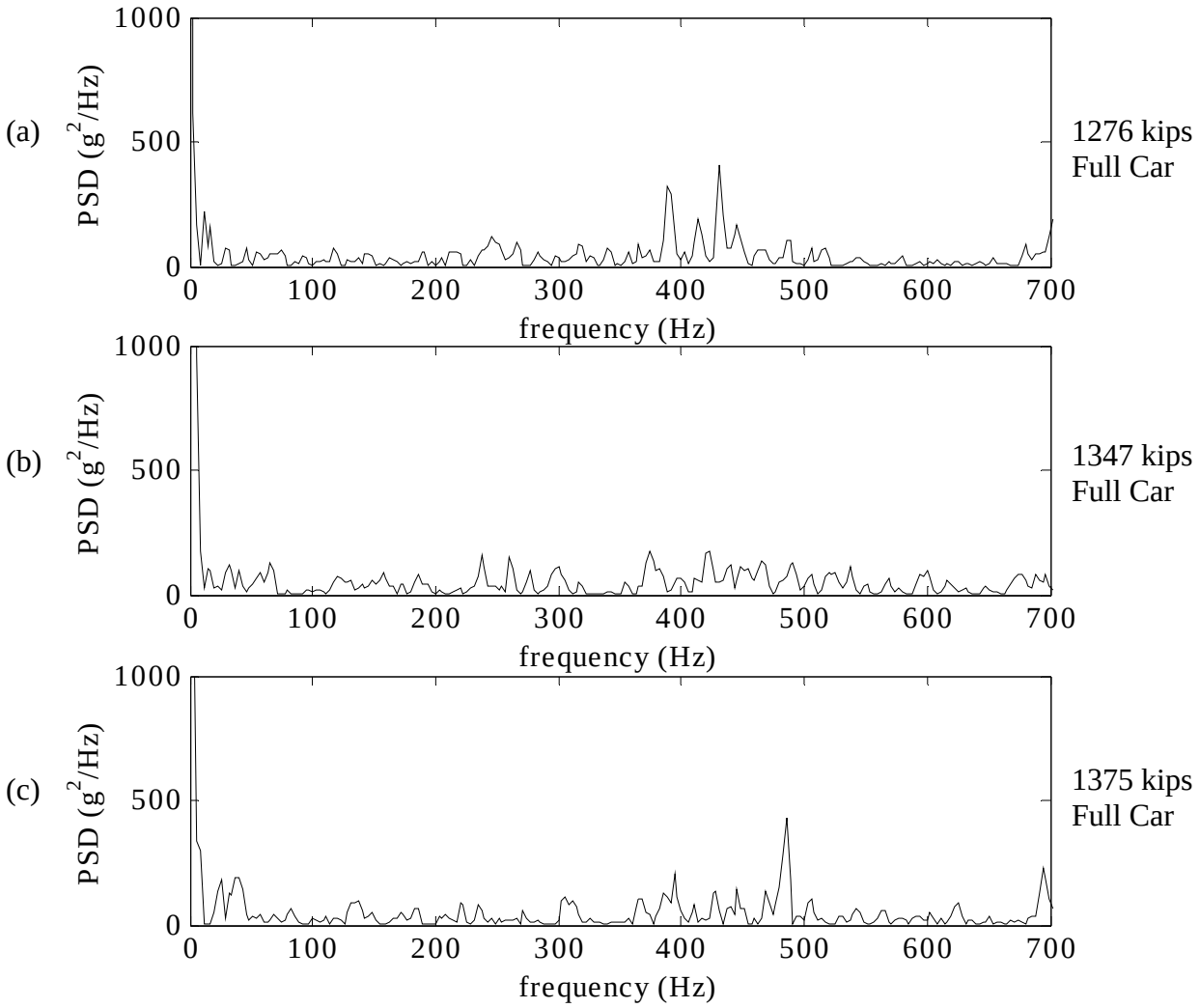

Figure 26. PSD of Longitudinal Accelerations Measured at Location 6 for Full Tank Car Impacts with Solid Load Transfer Mechanisms with Peak Coupler Forces of (a) 1276 kips, (b) 1347 kips, and (c) 1375 kips

4.2 Calculation of Anticipated Natural Frequencies

The natural frequencies of a simple cylinder [5], shown in Figure 27, were calculated using equation (1) to approximate the natural frequencies, $f_{i,j}$, of an empty tank car. These frequencies were then compared to results of the PSD analyses of the recorded acceleration data. Table 1 gives the parameters used for these equations. These values were chosen to represent the (greatly simplified) geometry of the car. The value of Λ was calculated using equations 2-5 for bending, radial, radial-axial, and axial modes, respectively. Mode shapes were calculated using equations 6-9 for bending, radial, radial-axial, and axial modes, respectively. Figure 28 shows examples of the first mode shape for each mode. Table 2 lists the resulting natural frequencies for the first five modes for each mode shape.

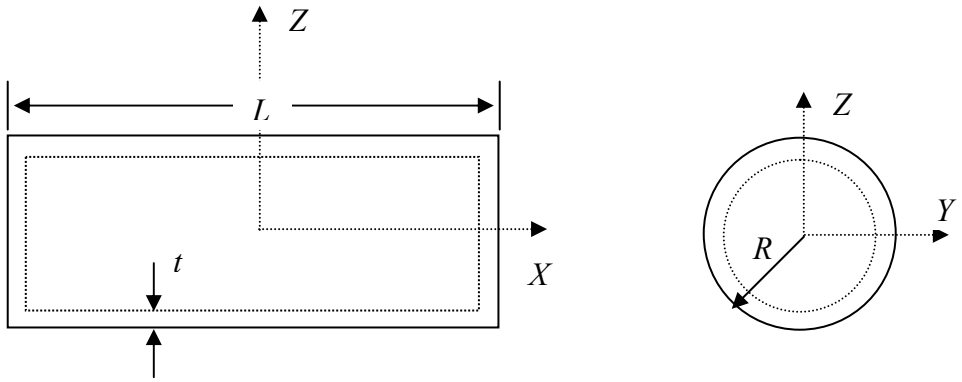

Figure 27. Schematic of the Cylinder Used to Determine the Natural Frequencies of the Tank Car

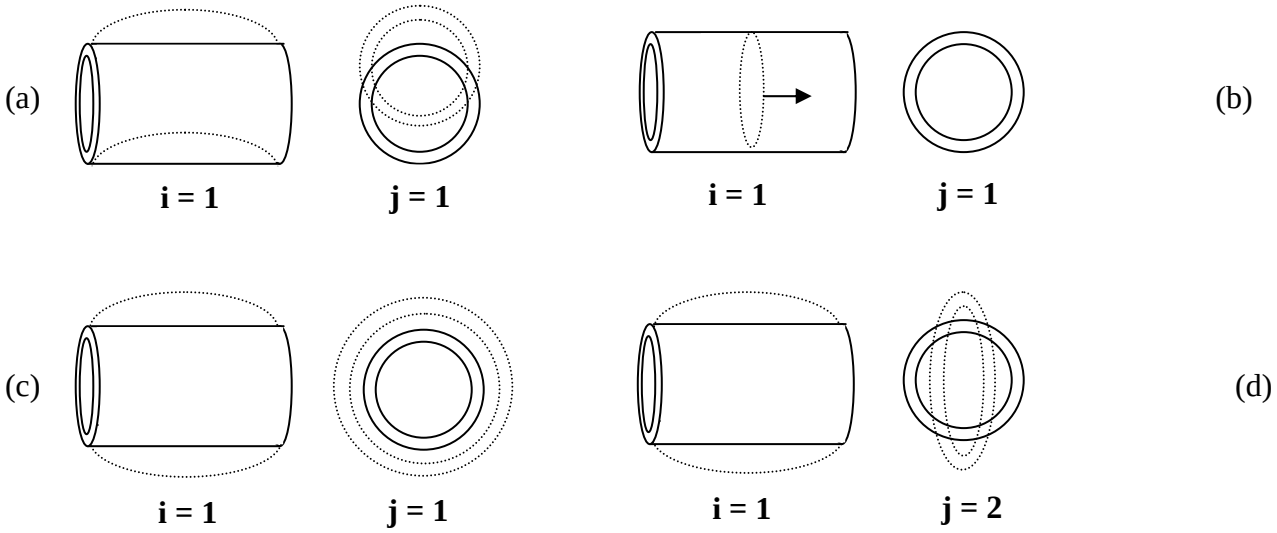

Figure 28. Examples of Mode Shapes for the Natural Frequencies of a Simply Supported Cylinder without Axial Constraint for (a) Bending, (b) Axial, (c) Radial, and (d) Radial-Axial

Table 1. Parameters Used in Equations

R	54.125	inches
u	0.00074	slugs/in^3
ν	0.32	
E	29000000	ksi
L	575.375	inches
t	0.4375	inches

$$f_{i,j} = \left(\frac{\Lambda_{i,j}}{2\cdot\pi\cdot R}\right)\cdot\left[\frac{E}{u\cdot(1-\nu^2)}\right]^{0.5} \tag{1}$$

$$\Lambda_{i,j} = \frac{\left[\left(\frac{j\cdot\pi\cdot R}{L}\right)^4\cdot(1-\nu^2)\cdot\left(\frac{t^2}{12\cdot R^2}\right)\cdot\left[i^2+\left(\frac{j\cdot\pi\cdot R}{L}\right)^2\right]^4\right]^{0.5}}{i^2+\left(\frac{j\cdot\pi\cdot R}{L}\right)^2} \tag{2}$$

$$\Lambda_{i,j} = 1 \tag{3}$$

$$\Lambda_{i,j} = \frac{j^2\cdot\pi^2\cdot(1-\nu^2)^{0.5}}{2^{0.5}}\cdot\frac{R^2}{L^2} \tag{4}$$

$$\Lambda_{i,j} = j\cdot\pi\cdot(1-\nu^2)^{0.5}\cdot\frac{R}{L} \tag{5}$$

$$\begin{pmatrix}\tilde{u}\\ \tilde{v}\\ \tilde{w}\end{pmatrix}_{i,j} = \begin{pmatrix}\cos(\frac{j\cdot\pi\cdot x}{L})\\ 0\\ 0\end{pmatrix} \tag{6}$$

$$\begin{pmatrix} \tilde{u} \\ \tilde{v} \\ \tilde{w} \end{pmatrix}_{i,j} = \begin{pmatrix} 0 \\ 0 \\ \sin(\frac{j \cdot \pi \cdot \mathrm{x}}{L}) \end{pmatrix} \tag{7}$$

$$\begin{pmatrix} \tilde{u} \\ \tilde{v} \\ \tilde{w} \end{pmatrix}_{i,j} = \begin{pmatrix} 0 \\ 0 \\ \sin(\frac{j \cdot \pi \cdot x}{L}) \end{pmatrix} \tag{8}$$

$$\begin{pmatrix} \tilde{u} \\ \tilde{v} \\ \tilde{w} \end{pmatrix}_{i,j} = \begin{pmatrix} A \cdot \cos(i \cdot \vartheta) \cdot \cos(\frac{i \cdot \pi \cdot \mathrm{x}}{L}) \\ B \cdot \cos(i \cdot \vartheta) \cdot \cos(\frac{i \cdot \pi \cdot \mathrm{x}}{L}) \\ C \cdot \cos(i \cdot \vartheta) \cdot \cos(\frac{i \cdot \pi \cdot \mathrm{x}}{L}) \end{pmatrix} \tag{9}$$

Table 2. Calculated Natural Frequencies for a Simply Supported Cylinder

Mode j	Bending (Hz)	Axial (Hz)	Radial (Hz)	Radial-Axial (Hz)
1	36.07	172.61	616.50	13.80
2	144.28	345.23	616.50	47.33
3	324.64	517.84	616.50	96.17
4	577.13	690.45	616.50	151.42
5	901.77	863.07	616.50	206.44

4.3 PSD Results

PSD plots from three solid type impacts are plotted in Figures 29 and 30 for vertical and longitudinal accelerations, respectively. Natural frequencies calculated using a simply supported cylinder have been superimposed over the PSD traces. The solid vertical lines show the primary mode (j = 1), and the dashed vertical line show the remaining modes (j = 2 through 5).

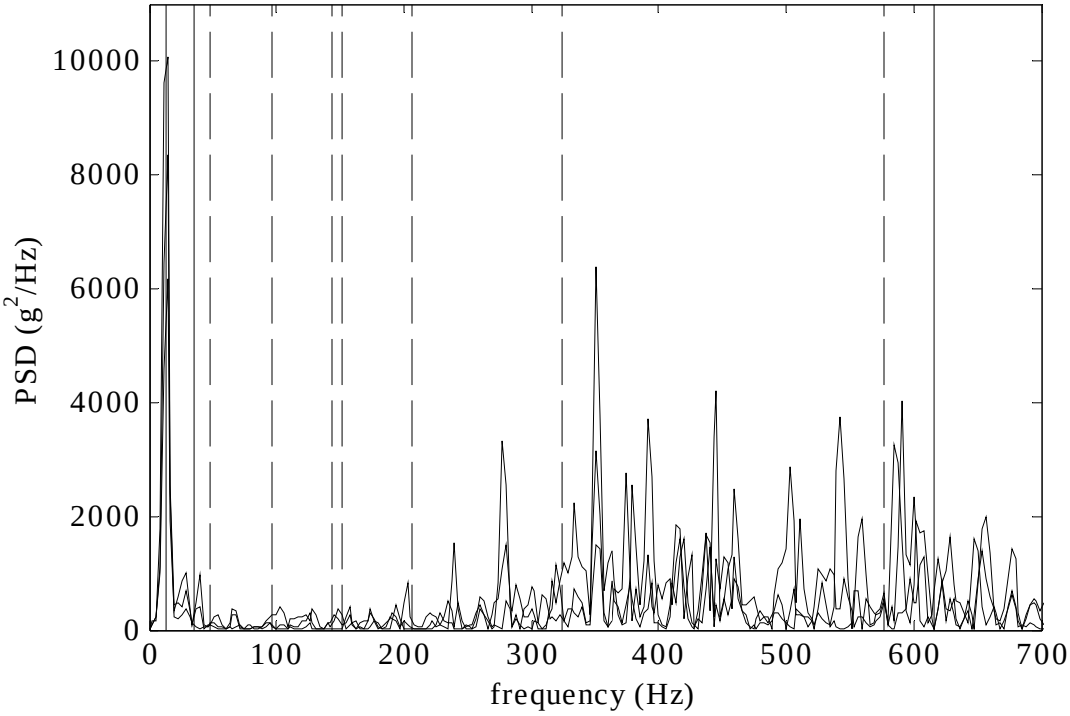

Figure 29. PSD of Vertical Acceleration from Location 6 for Three Solid Impacts of an Empty Tank Car Are Superimposed–Natural Frequencies of a Simply Supported Cylinder for Mode Shapes with a Vertical Component Are Indicated by the Solid Vertical Line (j = 1) and Dashed Vertical Lines (j = 2 through 5)

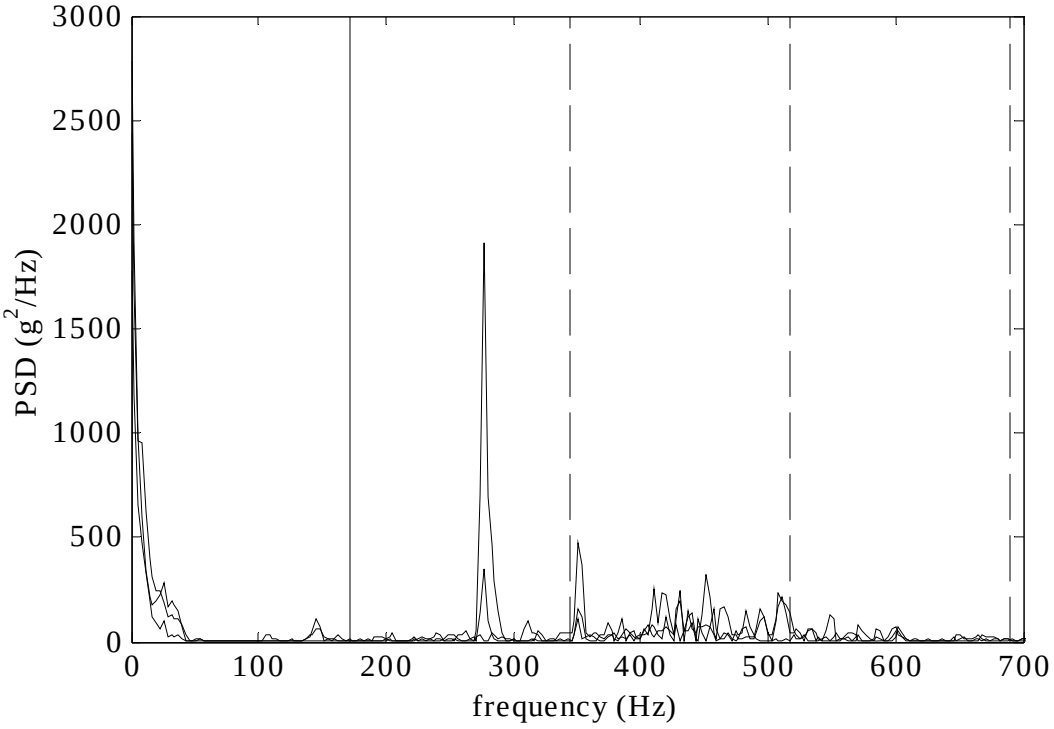

Figure 30. PSD of Longitudinal Acceleration from Location 6 for Three Solid Impacts of an Empty Tank Car Are Superimposed–Natural Frequencies of a Simply Supported Cylinder for Mode Shapes with a Longitudinal Component Are Indicated by the Solid Vertical Line (j = 1) and Dashed Vertical Lines (j = 2 through 5)

4.4 Displacements

Vertical and longitudinal accelerations from a solid type impact were integrated twice to determine displacements at the middle of the tank car for location 5, shown in Figures 31 and 32, and for location 6, shown in Figures 33 and 34. To integrate the acceleration signals, initial and final conditions were assumed. In the vertical direction, initial and final position and velocity were assumed to be zero. In the longitudinal direction, initial displacement was assumed to be zero, and the initial velocity was set to the impact velocity for the test. Final velocity was assumed to be zero. The acceleration signals were adjusted slightly to achieve these conditions by adding or subtracting a constant factor to the acceleration signal. The adjustment was small in magnitude compared to the acceleration signal.

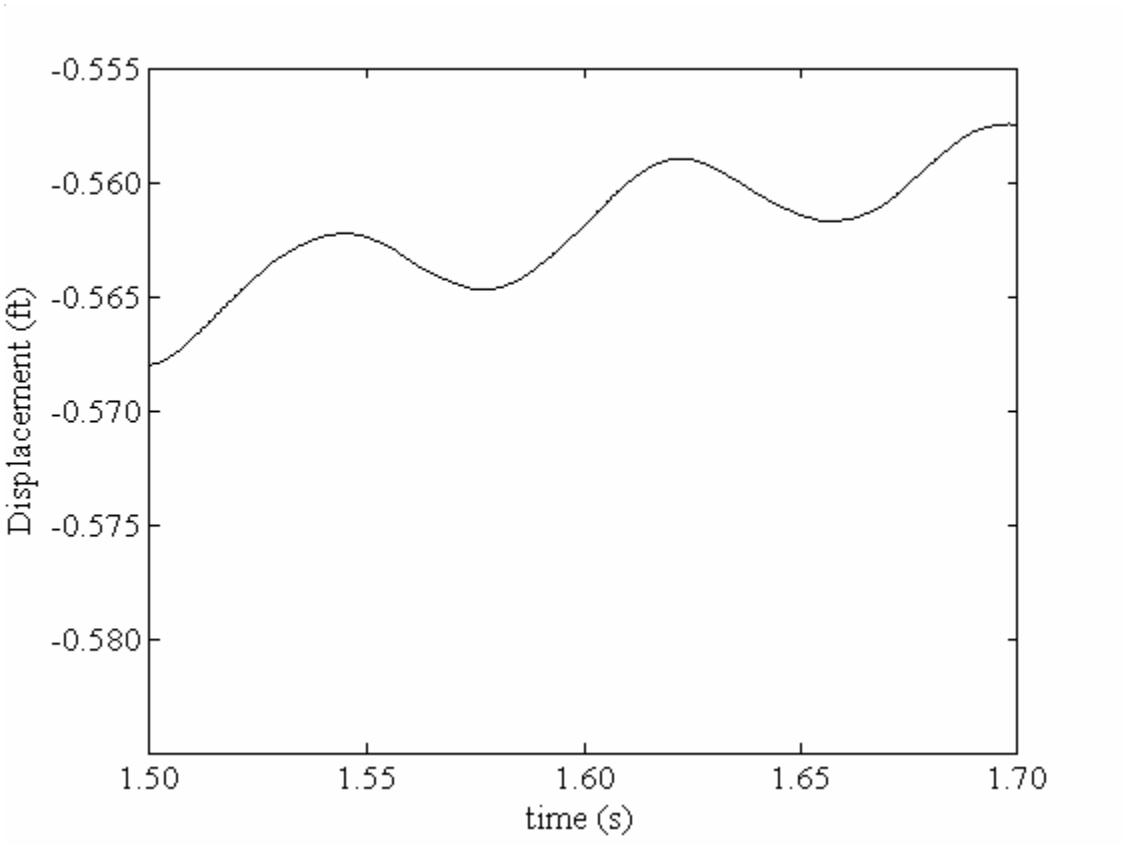

Figure 31. Vertical Displacement at Location 5 for an Empty Tank Car Impact at 8.0 mph

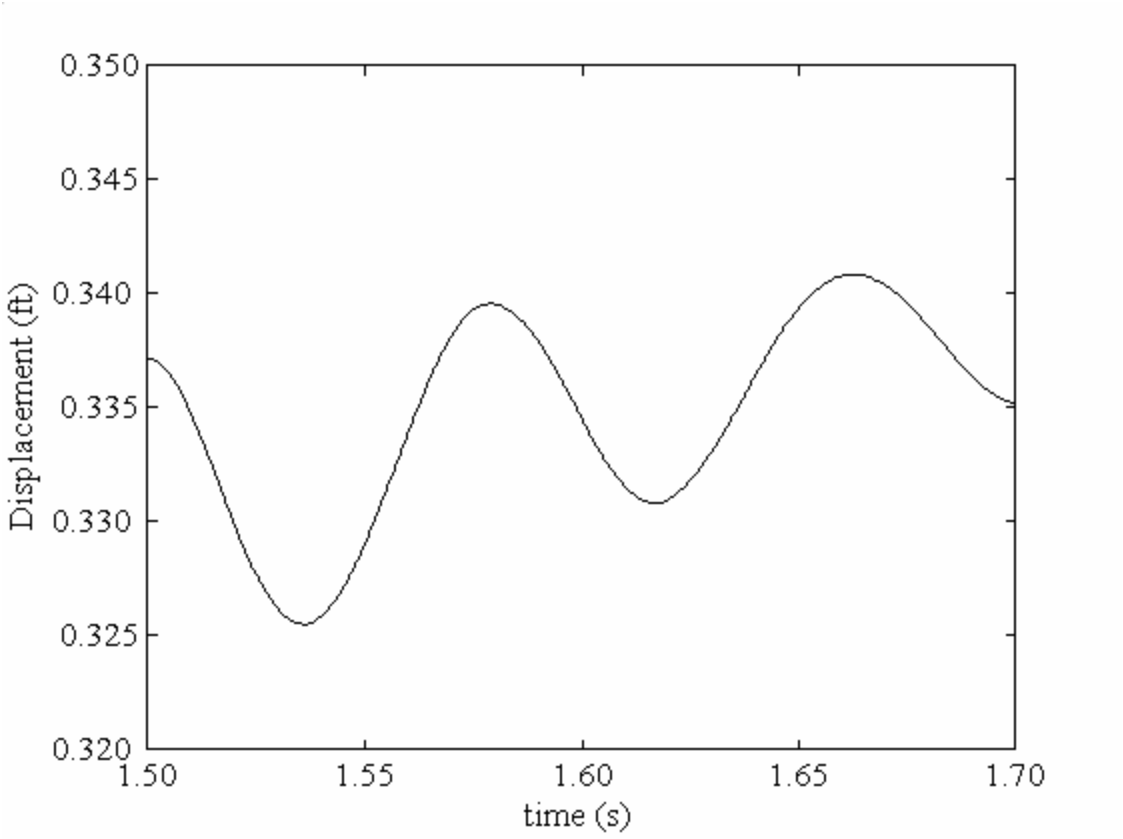

Figure 32. Vertical Displacement at Location 6 for an Empty Tank Car Impact at 8.0 mph

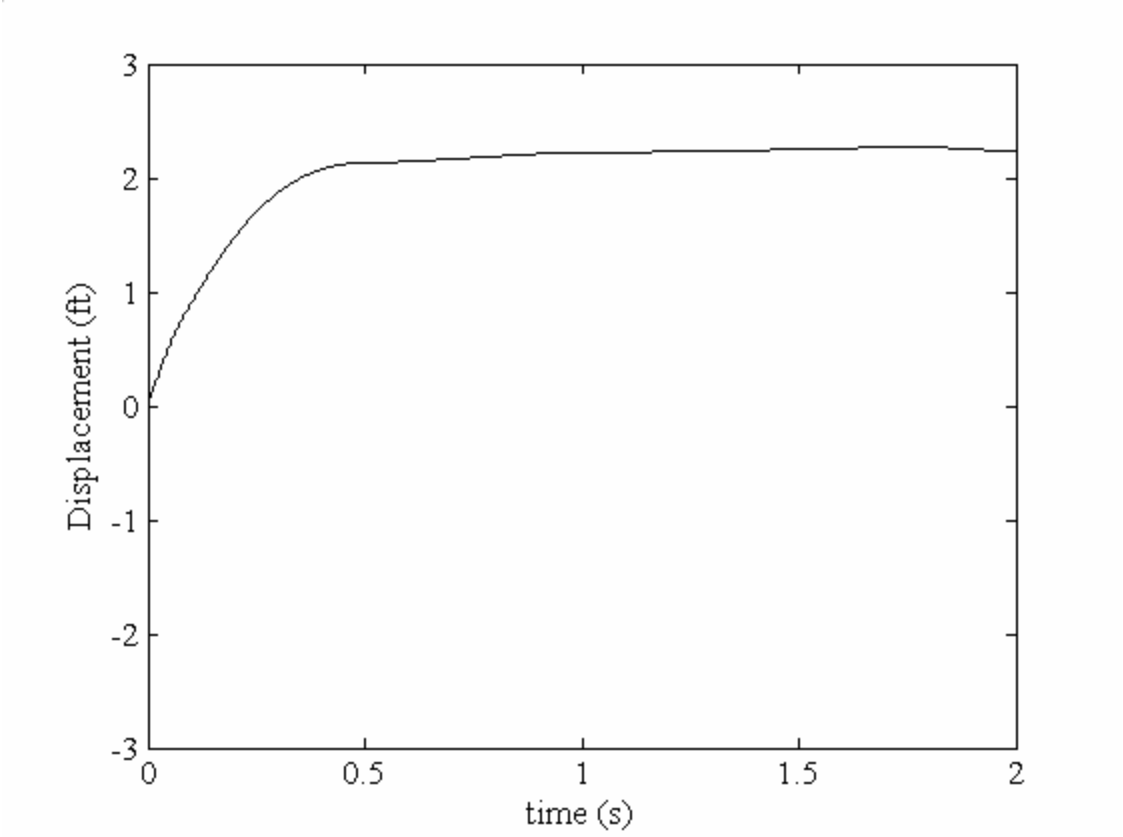

Figure 33. Longitudinal Displacement at Location 5 for an Empty Tank Car Impact at 8.0 mph

5. Discussion

The following sections will discuss the effect of tank car loading, peak coupler force, the dominant draft gear mechanism on the response of the accelerometers, and the results from PSD analyses that were performed on the measured accelerations.

5.1 Draft Gear Mechanism

Three distinct mechanisms by which the draft gear transfers forces to the tank car were observed: spring, stick-slip, and solid. Previous work defined these mechanisms and identified an effect of the draft gear mechanism on the shock response spectrum-peak coupler force relationship [2]. Coupler force versus time plots from impacts characterized by these transfer mechanisms are shown in Figures 6 and 7 for tests on the empty and full tank cars, respectively. The smooth force versus time trace, shown in Figures 6a and 7a, is typical of the spring type load transfer. Under this mechanism, the load is transferred to the friction wedges in the draft gear without the friction wedges slipping. For these impacts, peak coupler force tends to increase with increasing impact speed, up to slipping of the wedges. Once the friction wedges slip, the stick-slip load transfer mechanism occurs. The stick-slip load transfer is characterized by large oscillations, in this case at approximately 100 Hz, in the force versus time history, as shown in Figures 6b and 7b. The stick-slip behavior tends to be not as pronounced in the full tank car impact tests as in the empty tank car tests. The draft gear can travel 3.25 inches under the stick-slip mechanism before developing a solid load transfer mechanism, where the force is transferred directly to the stub sill. Figures 6c and 7c show force versus time traces of impacts dominated by the solid type load transfer mechanism. The solid load transfer mechanism is characterized by small oscillations in the force versus time trace (where the stick-slip mechanism is operative) followed by a single peak with a large force value. The value of the peak force tends to increase with increasing impact speed. The transfer of the impact load directly through the draft gear into the stub sill causes a single large peak in coupler force. The force versus time traces for full tank car impact tests exhibit low frequency oscillations after the peak impact force (at approximately 11 Hz). These oscillations are not present in the force versus time traces for empty tank car impacts and are most likely caused by the sloshing of the lading after the initial impact.

5.2 Coupler Force, Impact Speed, and Draft Gear Mechanism

This study examined the relationship between peak coupler force, impact speed, and primary draft gear mechanism. The peak coupler force from each impact is plotted against impact speed in Figure 8. In general, peak coupler force increases, and the dominant coupler mechanism changes from spring to stick-slip to solid as the impact speed increases. The full tank car impact tests tend to transition from spring to stick-slip at lower speeds than the empty tank car impact tests. For the full car tests, peak coupler force remains relatively constant between 2 mph and 4 mph and does not increase as the dominant coupler mechanism changes from spring to stick-slip. Peak coupler force then increases with increasing impact speed during the impacts where the solid coupler mechanism becomes dominant. A higher peak coupler force was observed in the empty tank car slip-stick impacts than in the full tank car stick-slip impacts. A higher speed was required to induce stick-slip in the empty tank car impacts than for full tank car impacts. The

increase in impact velocity required to transition to stick-slip behavior results from the lower mass of the empty tank. It is likely that this trend would be observed for the solid mechanism as well, but no impacts exist in the range of 4 to 6 mph for the full tank car impact tests to check this hypothesis.

5.3 PSD Analyses

PSD analyses were performed on accelerations that were measured during empty and full car impact tests. The purpose of these analyses was to identify frequencies that were excited by the coupler impacts. For a given impact, the peaks for locations at the A-end (impacted) of the tank car (1, 1A, 3, 7, 11, 13, and 15) have greater power than the peaks for locations at the B-end of the tank car (2, 2A, 4, 8, 10, 14, and 16). Furthermore, the PSD analyses for locations at the A-end of the car exhibit numerous peaks at frequencies above 250 Hz, which were above most of the structural natural frequencies that were deemed most likely to occur and were not consistently excited from test to test. These high frequencies are considered to be noise. This trend was consistent for all coupler mechanisms for both empty and full tank car impacts. In both types of impacts, these frequencies appear in the PSD results from locations at the A-end of the car and locations in the middle of the car but are not significant at the B-end of the car. It was observed that locations at the A-end of the car introduced more noise than locations in the middle of the tank car. As a result, accelerations measured in the middle of the car (locations 5 and 6) were felt to be the best locations to observe structural response. Furthermore, location 5 has additional interaction from stiffener beams and lading (for full car impacts). As a result, location 6 was chosen for careful consideration.

Accelerations measured at location 6 were examined for three solid impacts for empty and full tank car tests. Vertical and longitudinal accelerations measured at location 6 are plotted against time for empty tank car impacts in Figures 9 and 10, respectively. Vertical and longitudinal accelerations measured at location 6 are plotted against time for full tank car impacts in Figures 11 and 12, respectively. The accelerations from the three empty tank car impact tests are similar qualitatively. Peak accelerations differ slightly between the acceleration signals, but all of the acceleration signals have an underlying sinusoidal oscillation through the signal following the initial portion before the impact. The accelerations from the three full tank car impact tests are similar qualitatively and quantitatively. The vertical accelerations from the full tank car test damp out considerably quicker than the vertical accelerations from the empty tank cars tests damp out. This is possibly due to the lading in the full tank car.

PSD results from location 6, for empty and full tank car impacts with spring, stick-slip, and solid draft gear mechanisms, were examined to determine any frequencies that were repeatedly excited by the tank car impacts. The PSD results from the empty tank car impacts, shown in Figures 18-21, exhibit dominant peaks near 0 Hz in the longitudinal direction and 13 Hz in the vertical direction. The PSD results from the full tank car test, shown in Figures 22-26, exhibit dominant peaks near 0 Hz in the longitudinal direction and at both 5 Hz and 23 Hz in the vertical direction. A frequency of 100 Hz was also apparent in the vertical direction in the empty tank car impacts with a stick-slip coupler mechanism. This peak also occurs for full tank car impact, but these are not as significant during the full tank car impacts. These peaks correspond to 100 Hz oscillations in the coupler force versus time traces observed for impacts with a stick-slip draft gear mechanism.

5.4 The Relationship of PSD Results to Natural Frequencies

Figure 29 shows a plot of the PSD results for the vertical accelerations from location 6, for three empty car impacts with a solid coupler mechanism characteristic. The solid vertical lines show the first mode of the calculated natural frequencies for various types of vibrations. The dashed vertical lines show the second through fifth modes. The first mode of the radial-axial mode, 13 Hz, corresponds with a significant peak in the PSD. Figure 30 shows a plot of the PSD results of longitudinal accelerations from location 6, for three empty car impacts with solid coupler mechanism characteristics. The solid vertical line shows the first mode of the calculated natural frequencies. The dashed vertical lines show the second through fifth modes. The peak at 0 Hz represents rigid body motion.

Vertical and longitudinal accelerations recorded from locations 5 and 6 from an empty tank car impact with a solid draft gear mechanism were integrated to examine the displacement versus time history during the impact. Displacements integrated from vertical accelerations at locations 5 and 6 are plotted against time in Figures 31 and 32, respectively. A frequency of approximately 13 Hz (coinciding with PSD results) is present in the oscillations of the vertical displacements at locations 5 and 6. For a given vibration cycle, vertical displacement at location 6 has approximately twice as the amplitude as vertical displacements at location 5. If these displacements were the result of rigid body movement, the amplitude would be the same at both locations. Therefore, these results suggest the 13 Hz vibration results from structural, not rigid body, vibration. Displacements integrated from longitudinal accelerations at location 5 are plotted against time in Figure 33. Although some small oscillations are present, the resulting displacements are dominated by a single translation on the order of 2 feet. This, coupled with a strong PSD response at 0 Hz, suggests that the longitudinal accelerations result largely from rigid body displacements.

6. Summary and Conclusions

The purpose of this report was to investigate the response of accelerometers mounted at various locations on a tank car that was subjected to coupler impacts. The effects of tank car loading, peak coupler force, and dominant draft gear mechanism on the accelerometer responses were considered. PSD analyses were performed on accelerations to quantify the response of the tank car to the impacts. Frequencies identified by the PSD analyses were compared to calculated natural frequencies for a simple thin-walled cylinder.

The dominant draft gear mechanism has a marked effect on the response of the tank car. In general, as speed and energy increase, the draft gear mechanism changes from spring to stick-slip to solid. For spring-type impacts on empty tank cars, peak coupler force increased as impact speed increased. For spring-type impacts, little difference existed in peak coupler force for full tank car impacts for the range of speeds investigated. At very low speeds these coupler forces would presumably be lower. Peak coupler force was nearly constant for all stick-slip impacts. The forces were approximately the same for the empty and full tank car impacts, but the impact speeds at which the stick-slip mechanism occurred were lower for the full cars. For solid impacts, as speed increases peak coupler force increases. For a given impact speed and a solid load transfer mechanism, full tank car impacts generated higher peak coupler force than empty cars.

Accelerations measured at various locations on the tank car were examined for both the empty and full tank car impact tests, with spring, stick-slip, and solid draft gear load transfer mechanisms. For a given impact, the strength of the peaks in the PSDs tends to decrease from the A-end (impact) to the B-end of the tank car. Locations at the A-end of the vehicle introduced significant amount of noise into the PSD plots. Locations at the B-end of the vehicle tend to not produce a strong response to the impact. The middle of the tank car, such as locations 5 and 6, provides a compromise in the amount of noise versus strength of signal from the impacts and the response of the vehicle. Therefore, location 6 was chosen as the primary location to examine.

The frequencies that were significantly and consistently excited differed between the empty and full tank car impact tests. For the empty tank car impact test results, a frequency near 0 Hz was present in the PSDs of longitudinal acceleration signals. The lack of vibrations and similar magnitude of integrated longitudinal displacements at locations 5 and 6 suggests that this is a rigid body vibration. A frequency of 13 Hz was present in the PSDs of the vertical acceleration signals and coincides with the first radial-axial mode of a simply supported cylinder. The difference in magnitude of integrated vertical displacements at locations 5 and 6 suggests that this is a structural, not a rigid body, vibration. In addition, frequencies of approximately 100 Hz were present in the vertical acceleration signals from impacts with a stick-slip coupler mechanism. The 100 Hz peak coincides with a frequency observed in the force-time traces for impacts with stick-slip draft gear mechanisms and was likely induced by the periodic nature of the coupler force versus time relationship of the stick-slip coupler mechanism. Additional peaks greater than 250 Hz were present, but these occurred above most of the structural frequencies estimated by a simple model of a cylinder. In the full tank car impact tests, two distinct peaks, at approximately 5 Hz and 26 Hz, were present in the vertical acceleration response. A frequency

at 0 Hz and a range of frequencies above 300 Hz were present in the PSDs of longitudinal acceleration signals.

Additional work with filtering and calculation of SRS is required to develop a model for response of tank car to impact. Results suggest that structural response of a tank car subjected to coupler impact can be characterized by vibration at relatively few frequencies. As a result, the response of accelerometers at locations 5 and 6 might be able to be characterized with only a few degrees of freedom.

References

1. Smith, K.B., Parker, E.S., Iler, D.J., "Rail Car Service Spectra Generation for Full-Scale Accelerated Fatigue Testing," in *Applications of Automated Technology in Fatigue and Fracture Testing and Analysis, ASTM STP 1411,* A.A. Braun, P.C. McKeighan, M.A. Nicholson and P.R. Lohr, eds. American Society for Testing and Materials, West Conshohocken, PA, 2002.

2. Koch, K.D., Riddell, W.T., Treichel, T.T., Barkan, C P.L., "Structural Response and Coupler Forces During Tank Car Impacts," *43rd Mechanical Working and Steel Processing Conference Proceedings, Vol. XXXIX*, Iron and Steel Society, Warrendale, PA, pp. 837-848, 2001.

3. Thompson, W.T., "Transient Vibration," Theory of Vibrations with Applications, Third Edition, Prentice Hall, New Jersey, 1988, pp. 96-100.

4. Sommerfield, H. (Engineer at Cardwell/Westinghouse Air Brake Company), personal communication, January 2001.

5. Blevins, R.D., Formulas for Natural Frequency and Mode Shape, Krieger Publishing Company, Melbourne, Florida, 1979, pp. 300-305.

Appendix A.
PSD Results of Empty Car Impact Tests

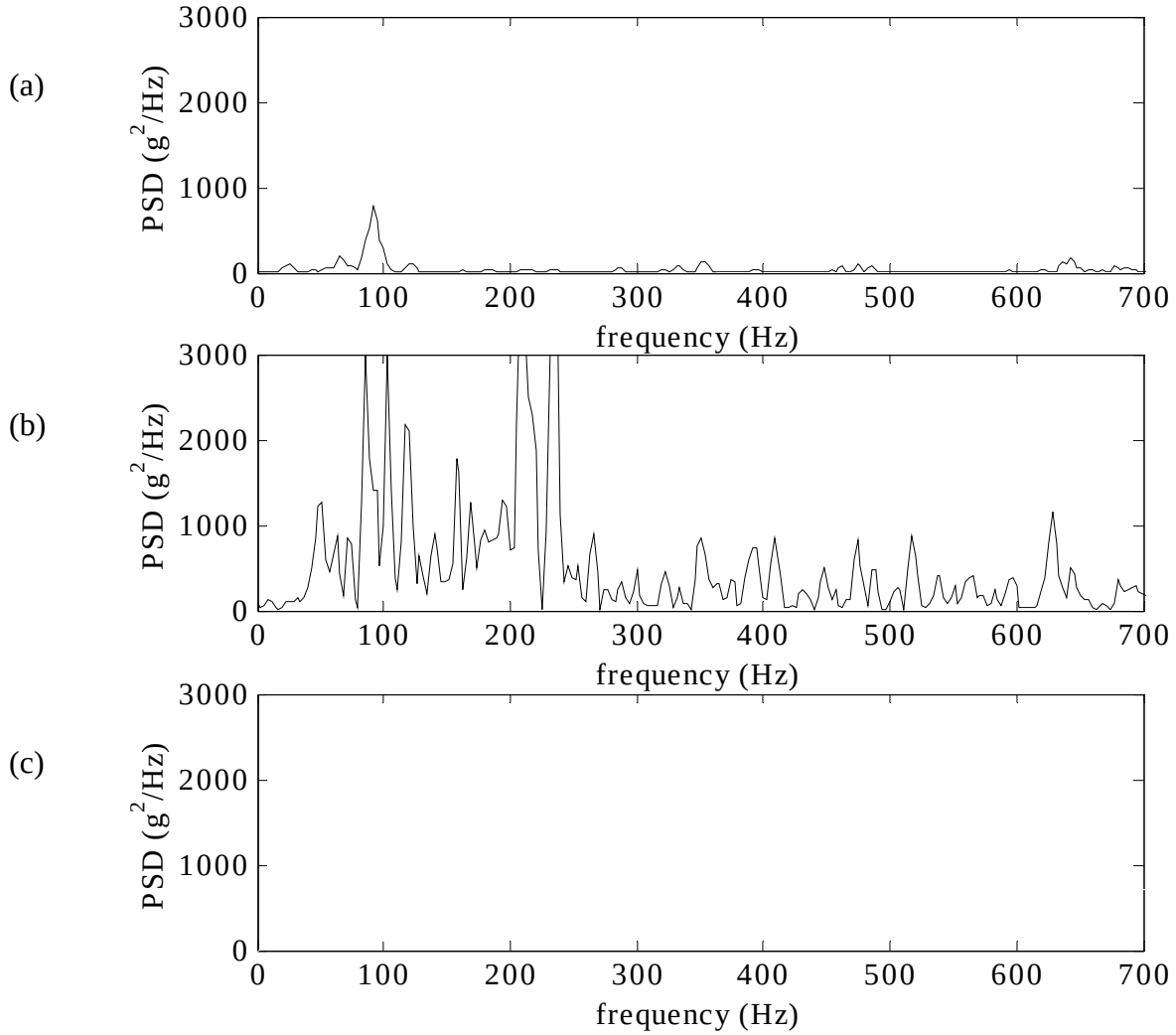

Figure A-1. PSD of Vertical Acceleration from Location 1 for (a) Spring, (b) Stick-Slip, and (c) Solid Load Transfer Mechanisms for the Empty Tank

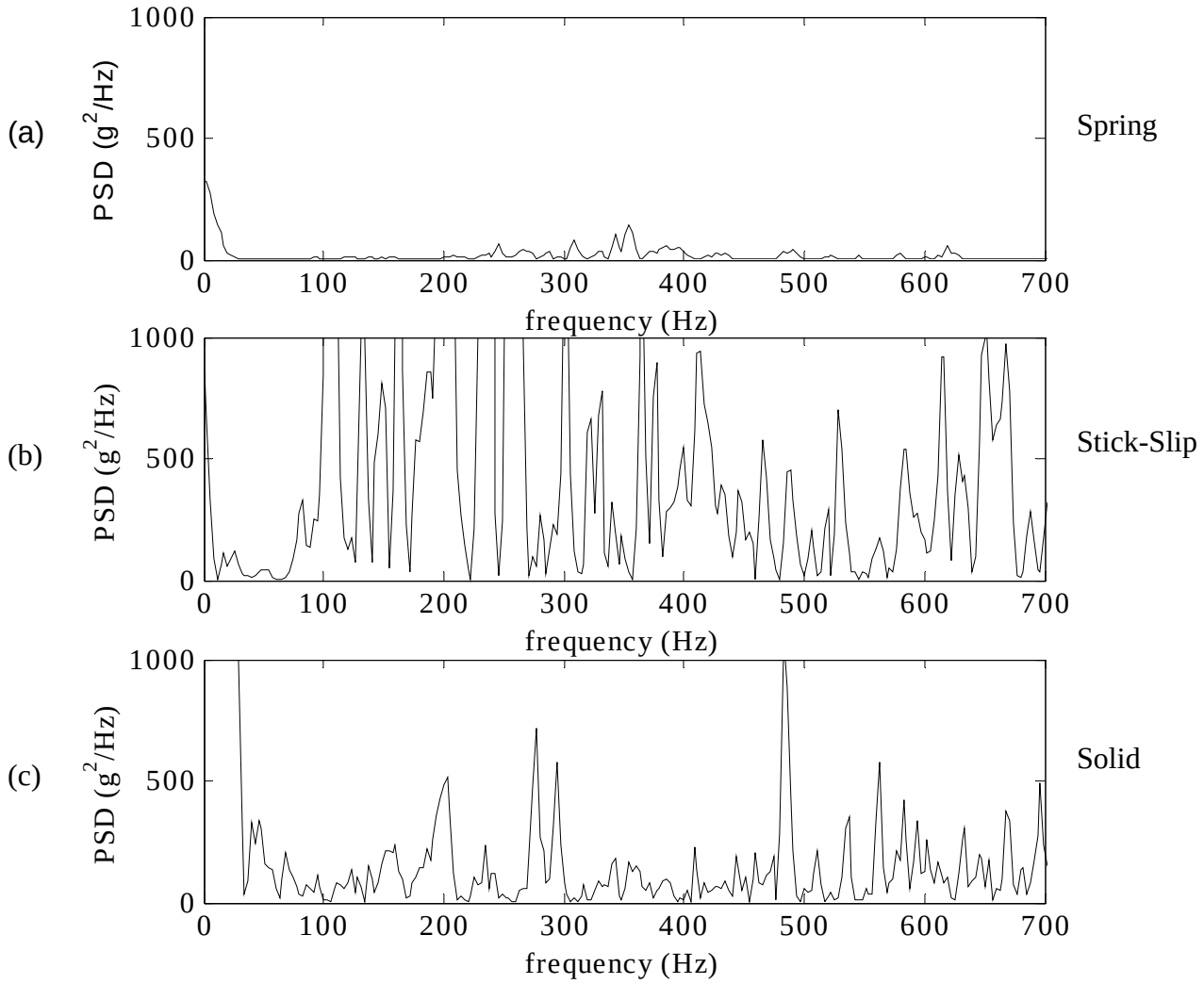

Figure A-2. PSD of Longitudinal Acceleration from Location 1 for (a) Spring, (b) Stick-Slip, and (c) Solid Load Transfer Mechanisms for the Empty Tank Car

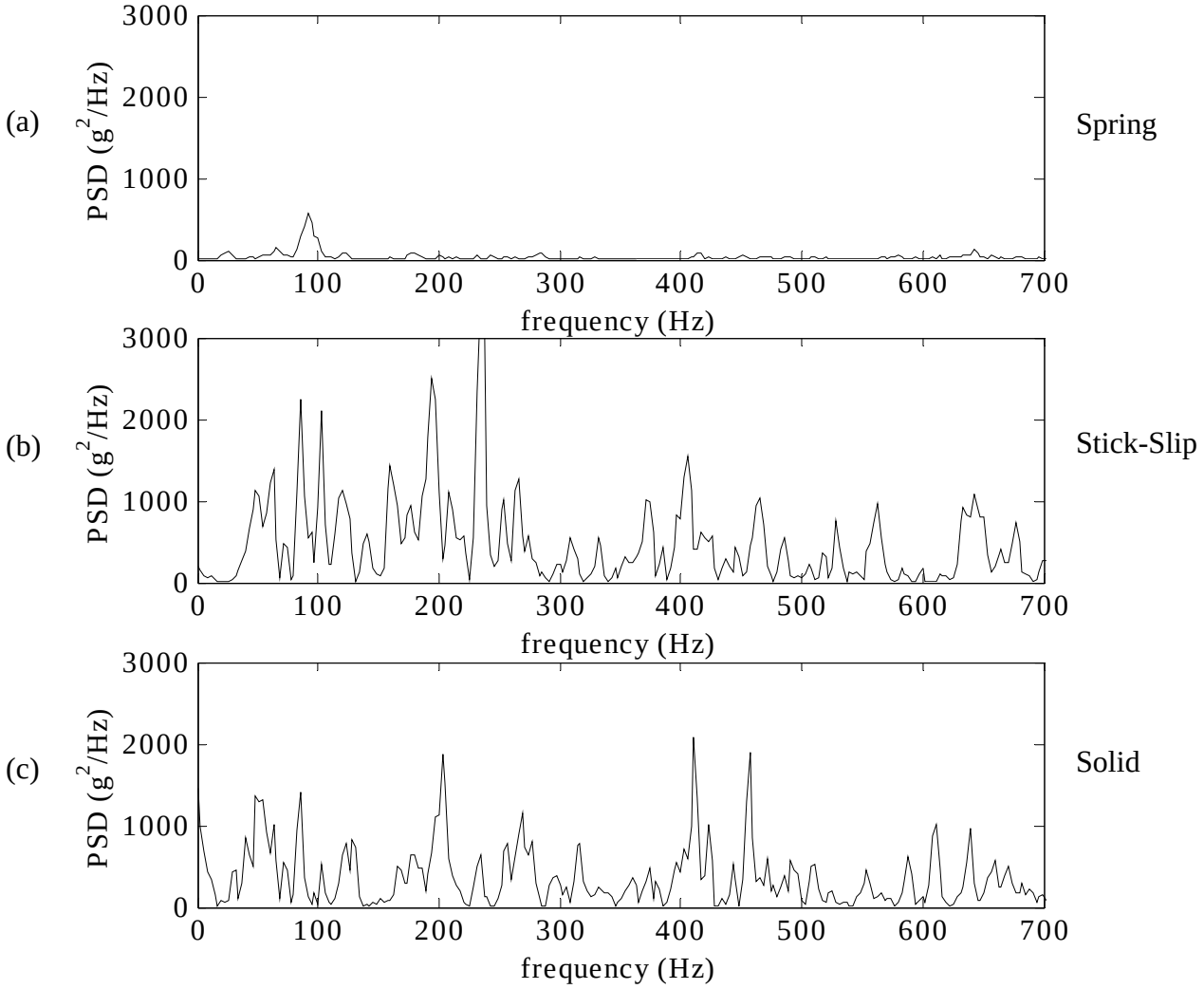

Figure A-3. PSD of Vertical Acceleration from Location 1A for (a) Spring, (b) Stick-Slip, and (c) Solid Load Transfer Mechanisms for the Empty Tank Car

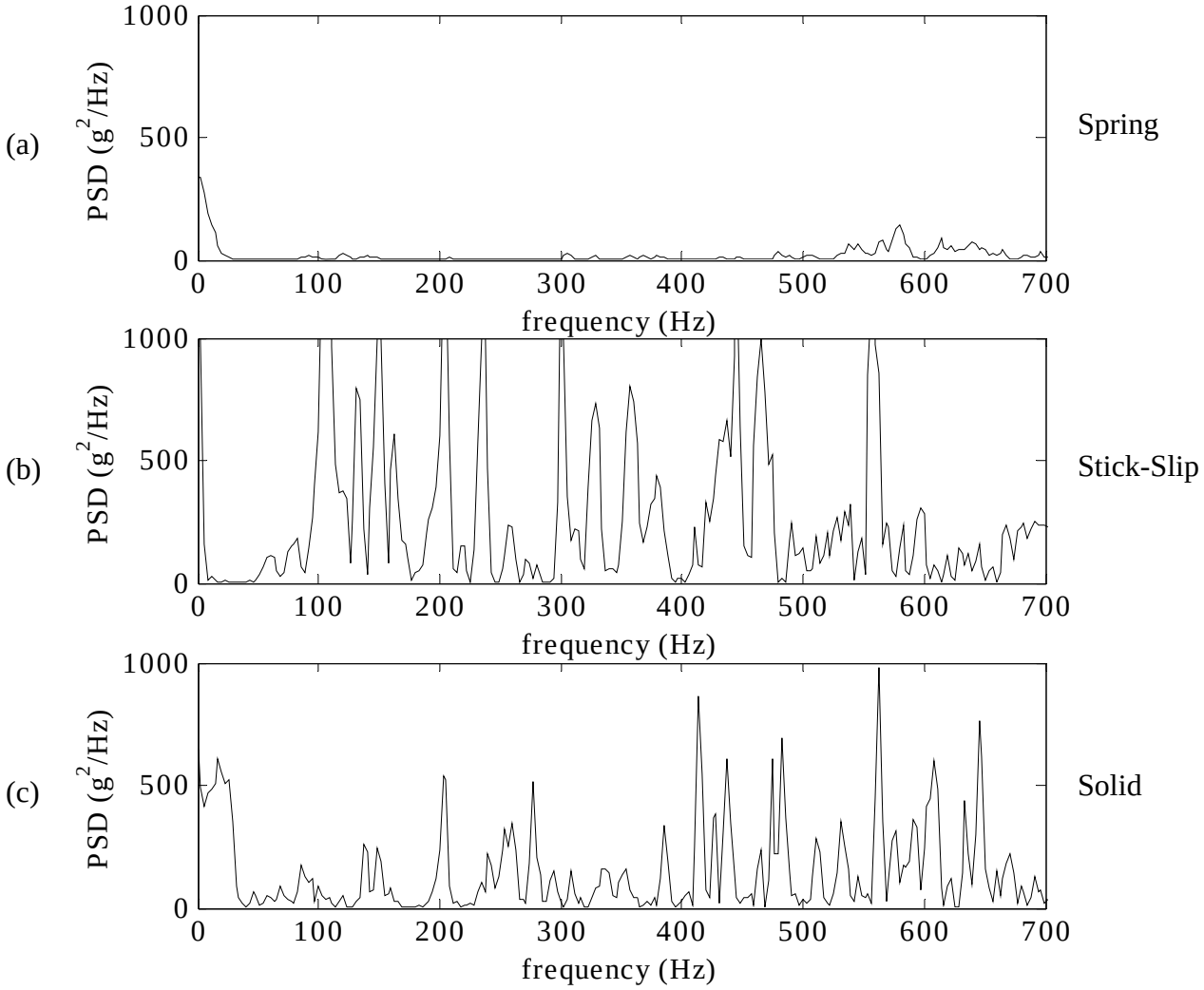

Figure A-4. PSD of Longitudinal Acceleration from Location 1A for (a) Spring, (b) Stick-Slip, and (c) Solid Load Transfer Mechanisms for the Empty Tank Car

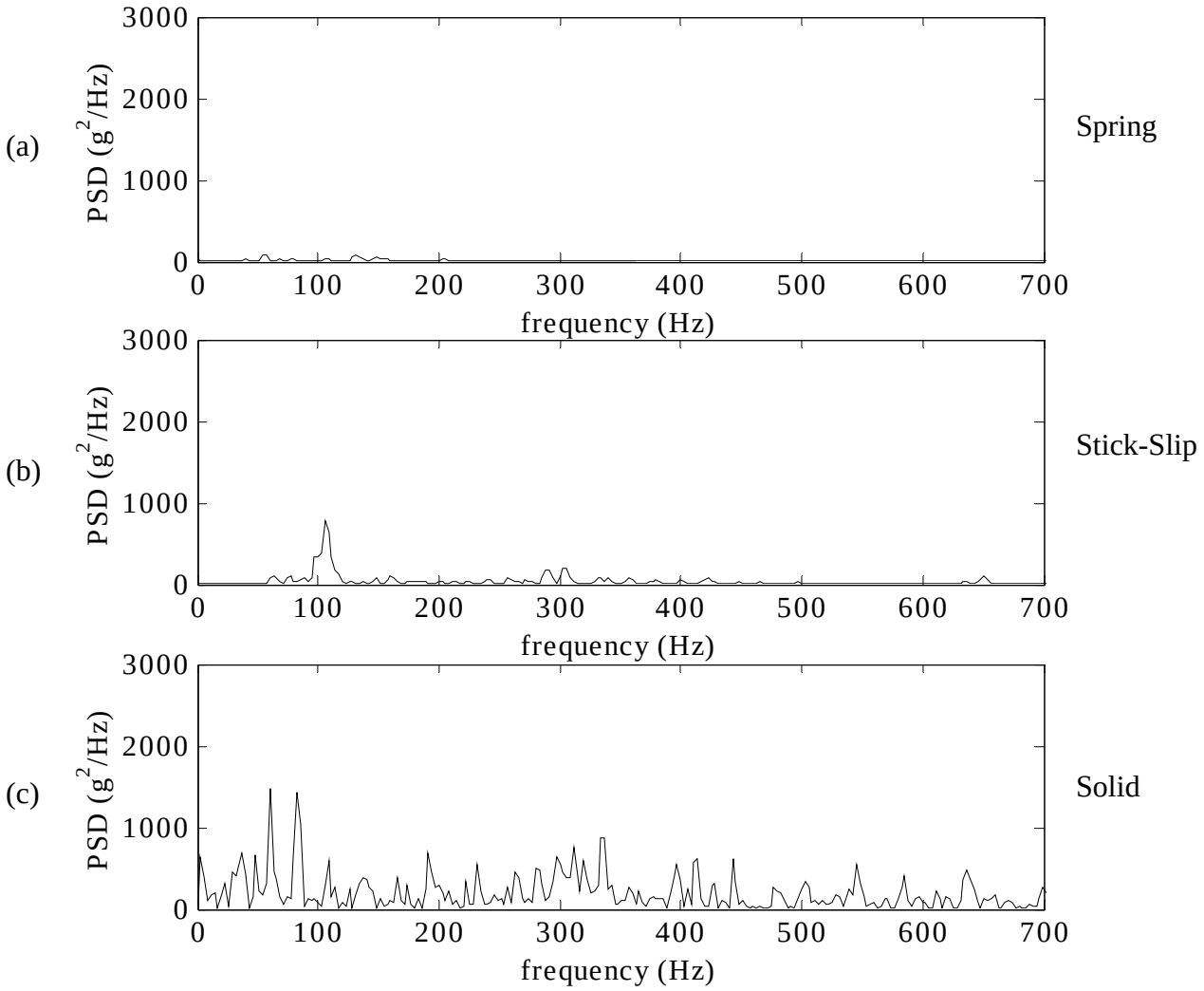

Figure A-5. PSD of Vertical Acceleration from Location 2 for (a) Spring, (b) Stick-Slip, and (c) Solid Load Transfer Mechanisms for the Empty Tank Car

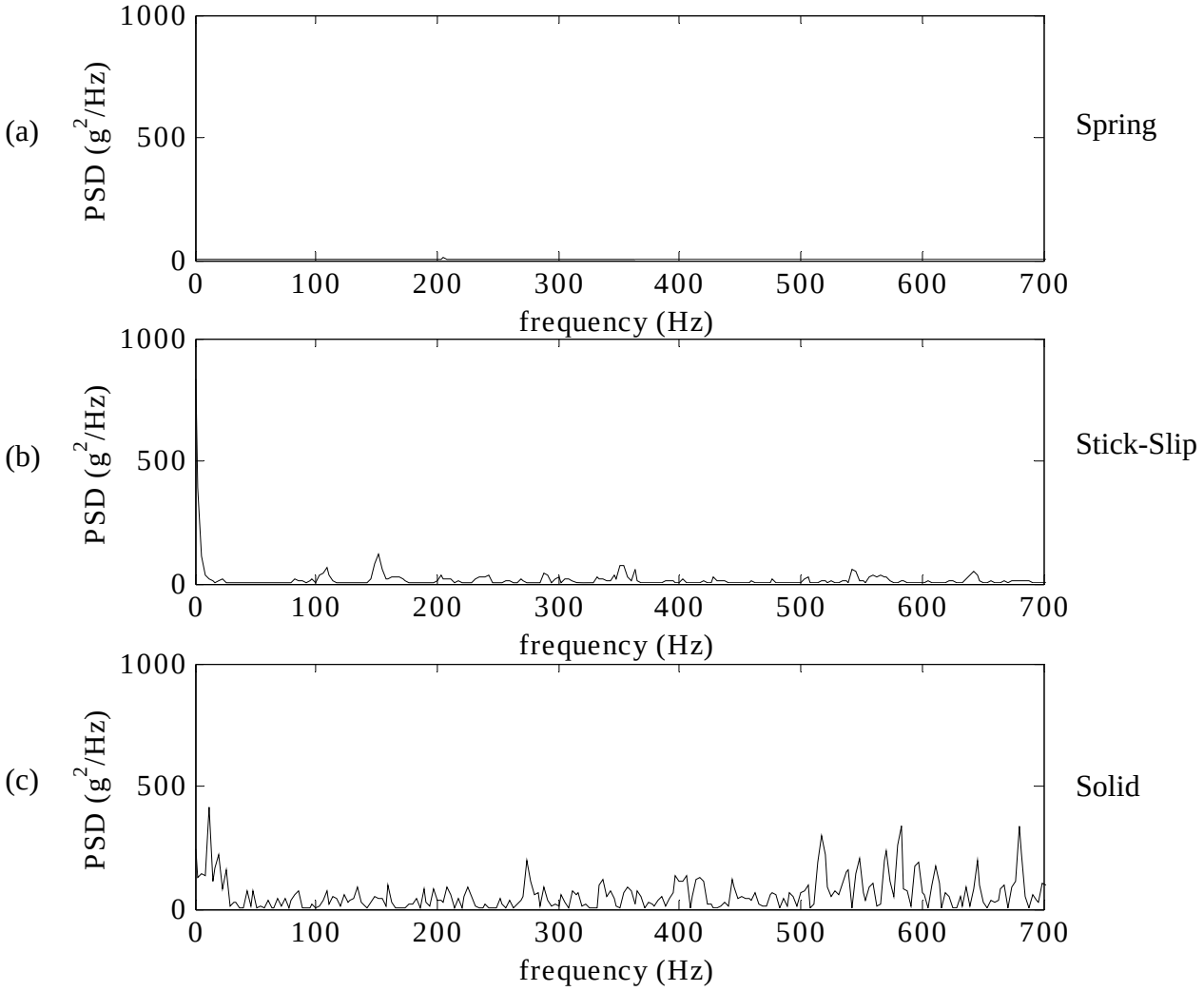

Figure A-6. PSD of Longitudinal Acceleration from Location 3 for (a) Spring, (b) Stick-Slip, and (c) Solid Load Transfer Mechanisms for the Empty Tank Car

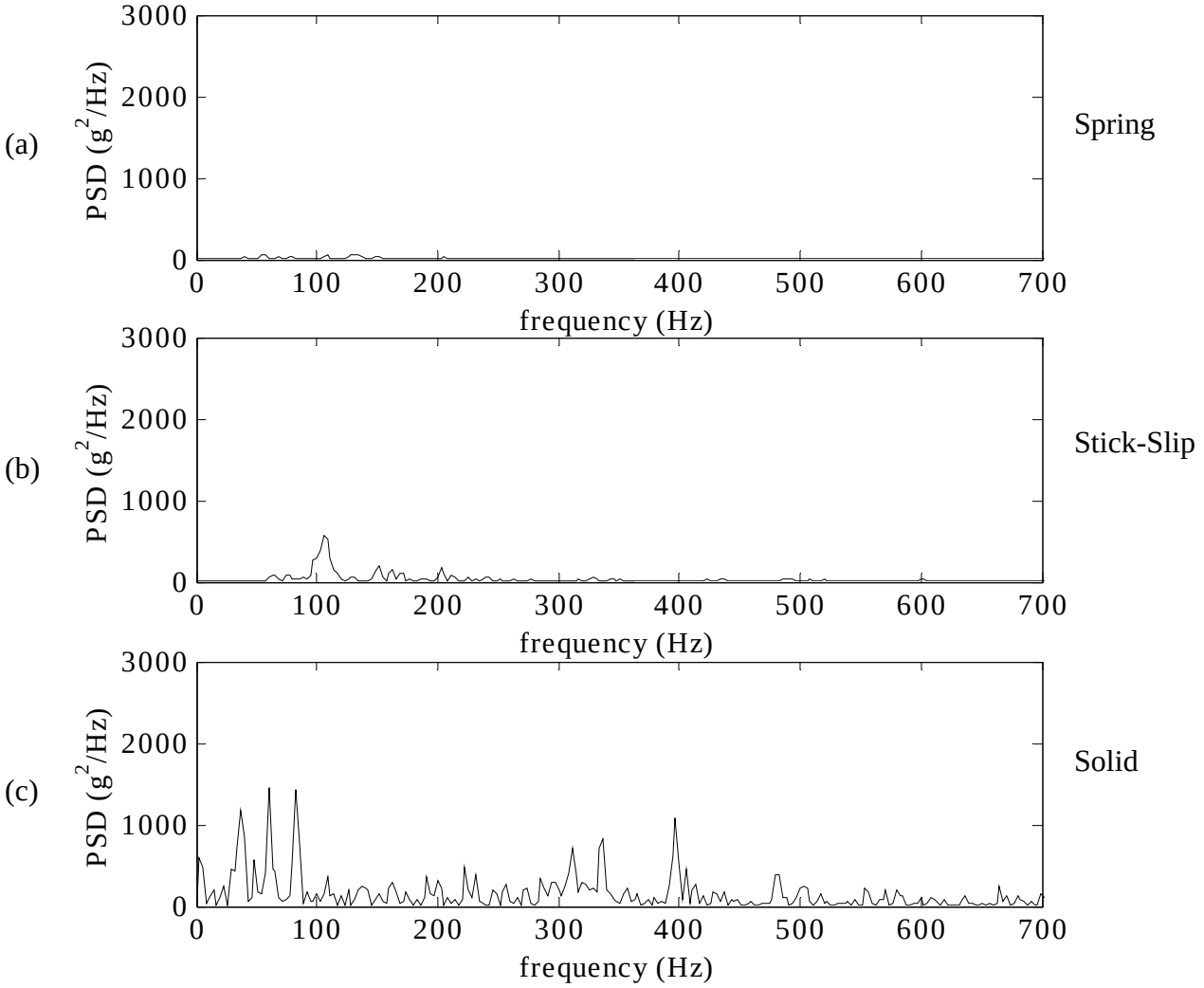

Figure A-7. PSD of Vertical Acceleration from Location 2A for (a) Spring, (b) Stick-Slip, and (c) Solid Load Transfer Mechanisms for the Empty Tank Car

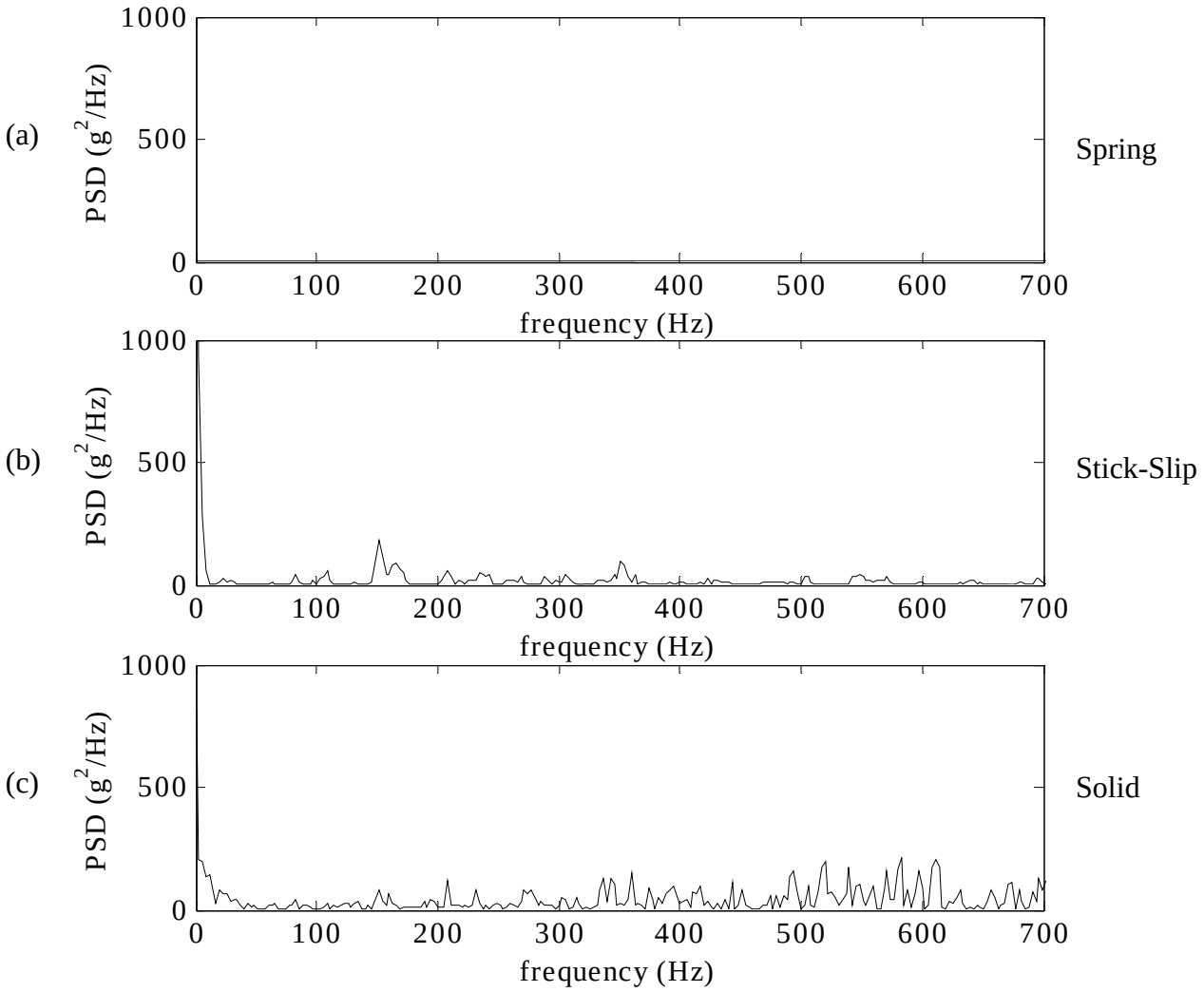

Figure A-8. PSD of Longitudinal Acceleration from Location 2A for (a) Spring, (b) Stick-Slip, and (c) Solid Load Transfer Mechanisms for the Empty Tank Car

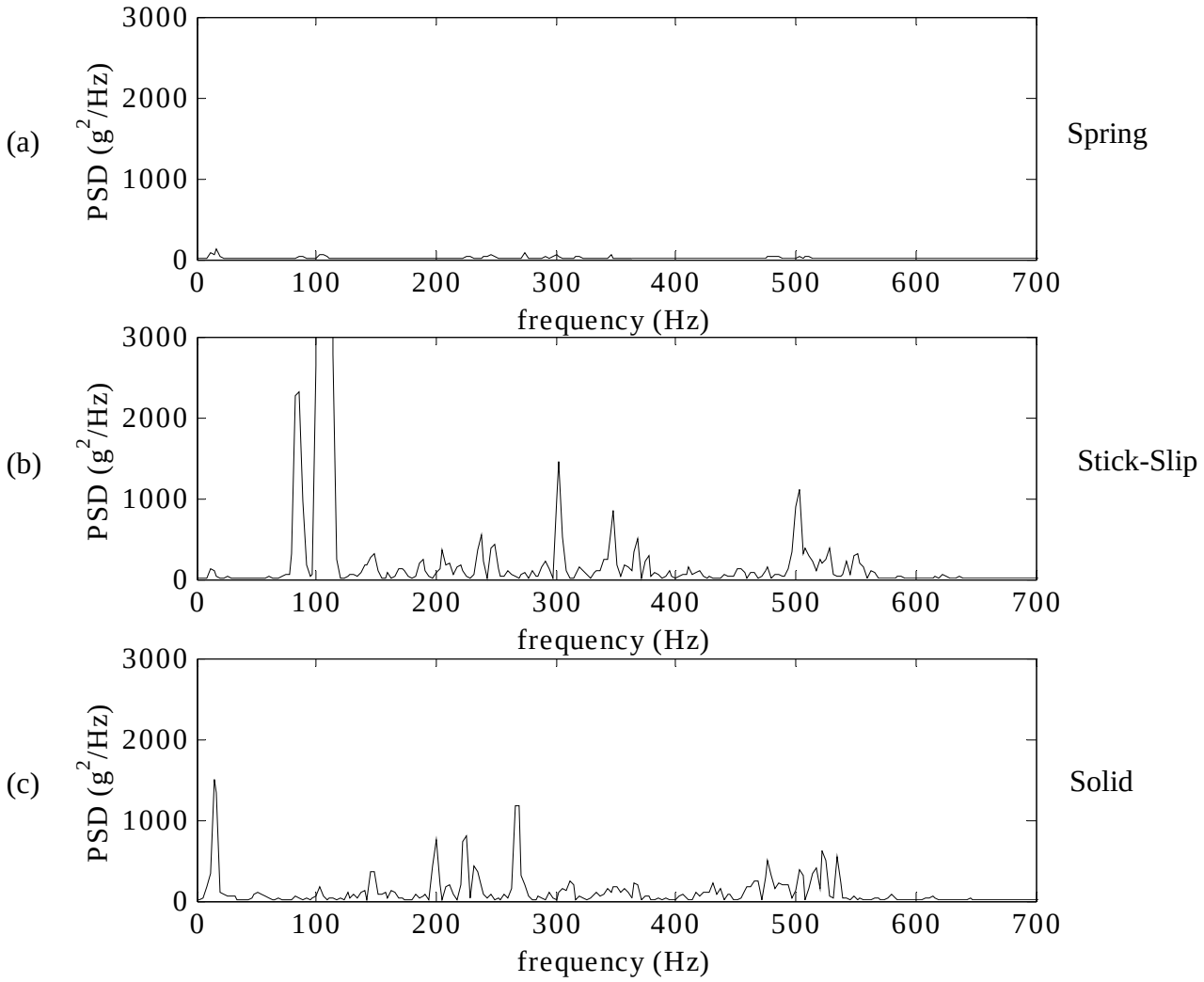

Figure A-9. PSD of Vertical Acceleration from Location 5 for (a) Spring, (b) Stick-Slip, and (c) Solid Load Transfer Mechanisms for the Empty Tank Car

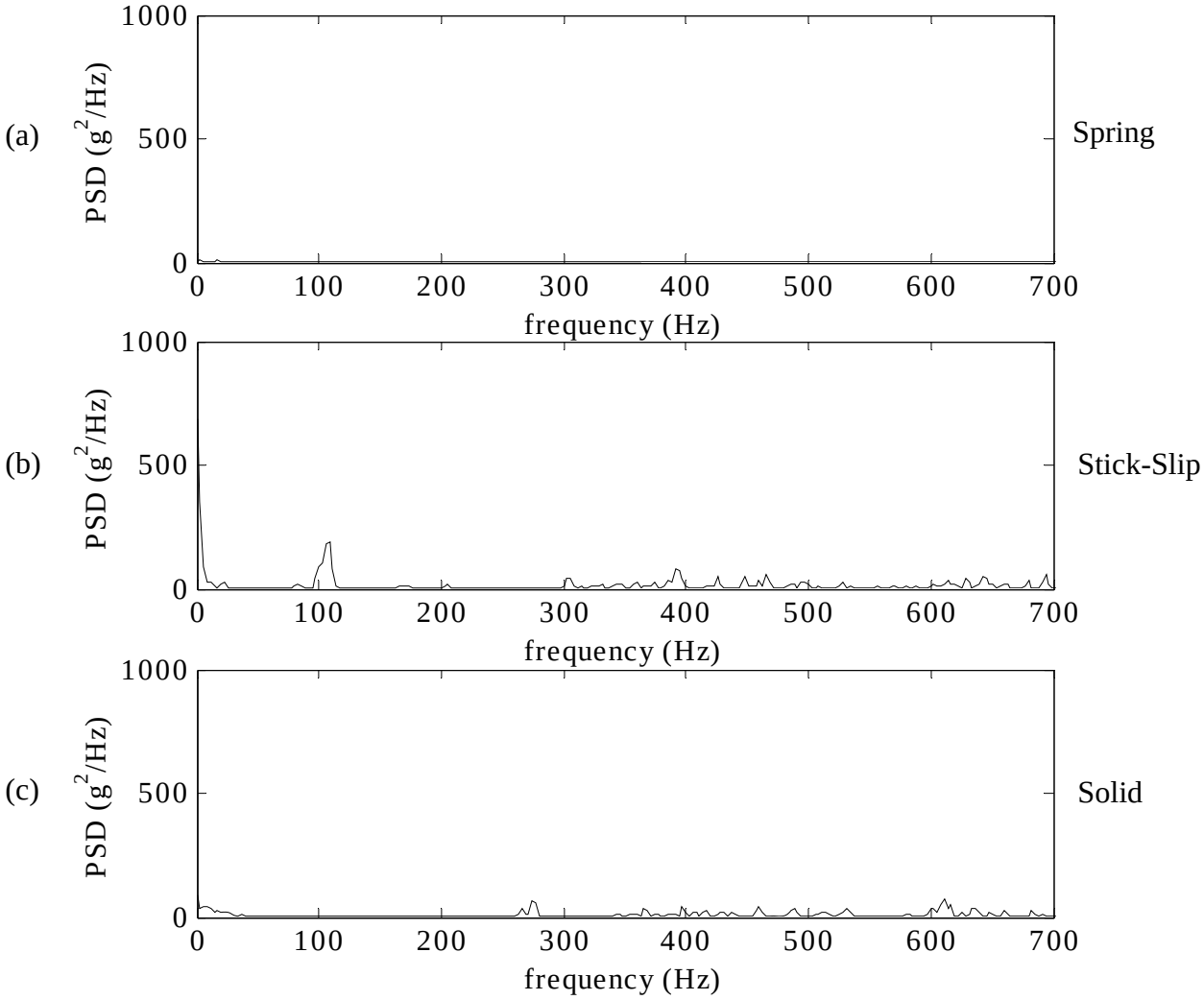

Figure A-10. PSD of Longitudinal Acceleration from Location 5 for (a) Spring, (b) Stick-Slip, and (c) Solid Load Transfer Mechanisms for the Empty Tank Car

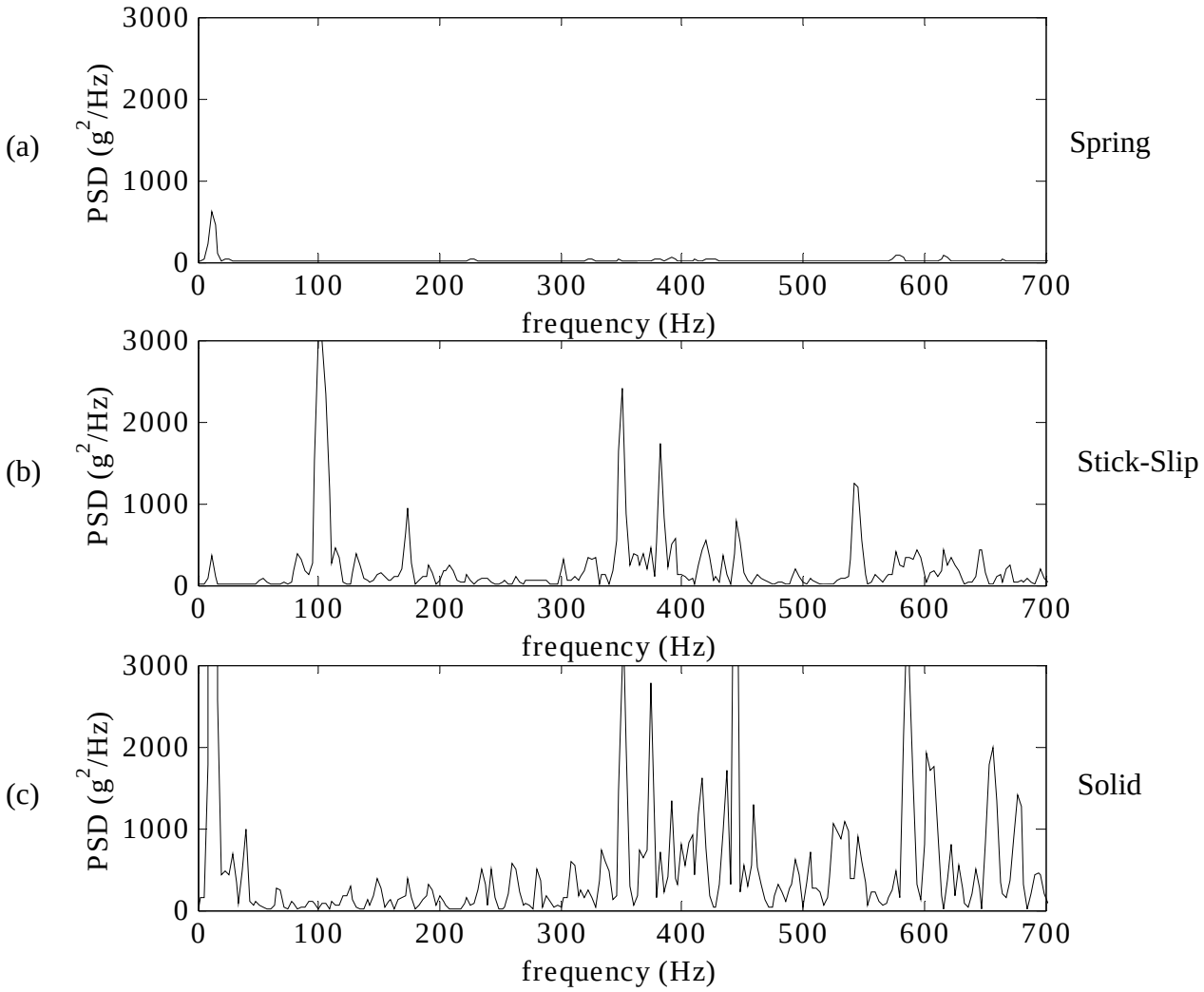

Figure A-11. PSD of Vertical Acceleration from Location 6 for (a) Spring, (b) Stick-Slip, and (c) Solid Load Transfer Mechanisms for the Empty Tank Car

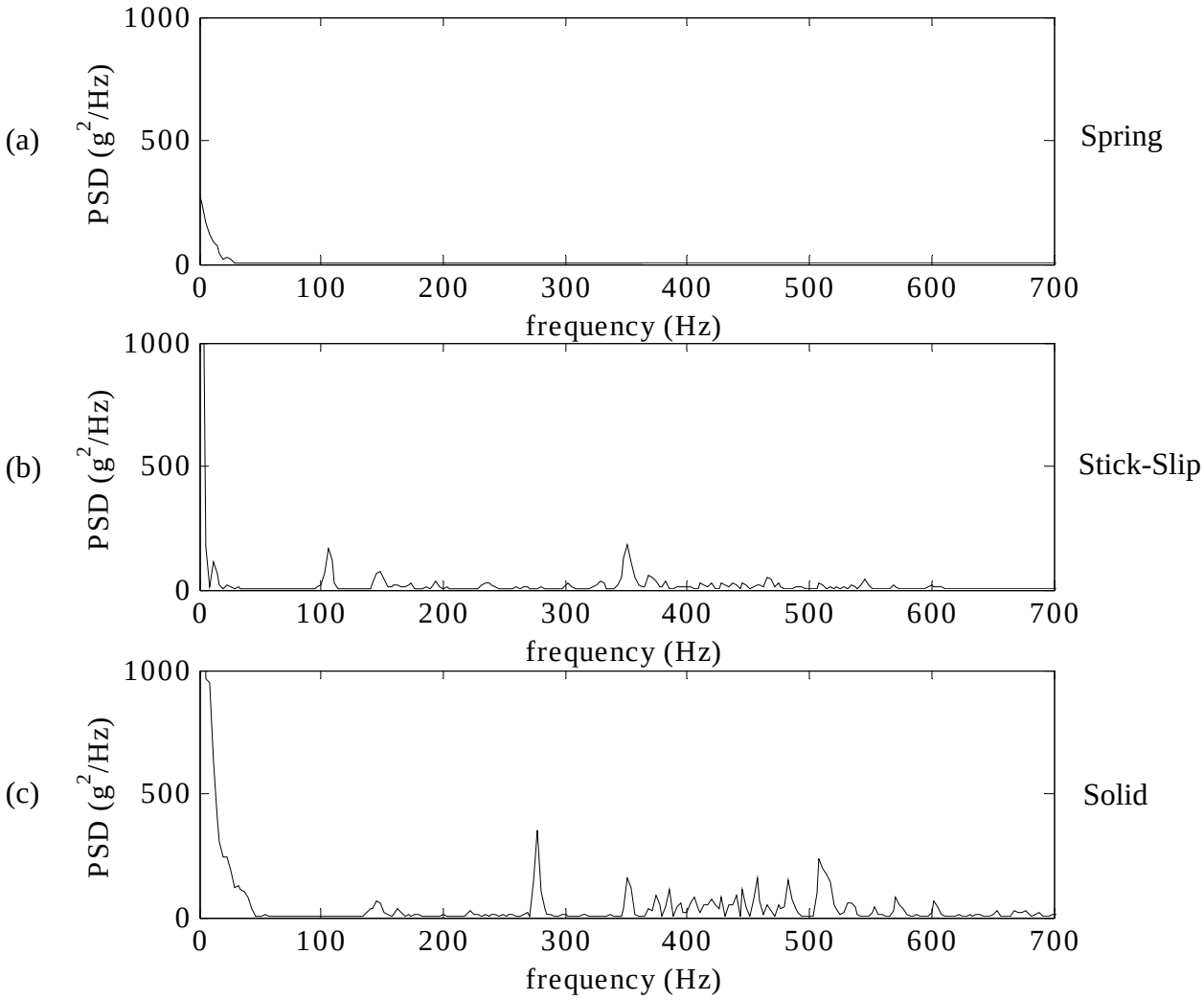

Figure A-12. PSD of Longitudinal Acceleration from Location 6 for (a) Spring, (b) Stick-Slip, and (c) Solid Load Transfer Mechanisms for the Empty Tank Car

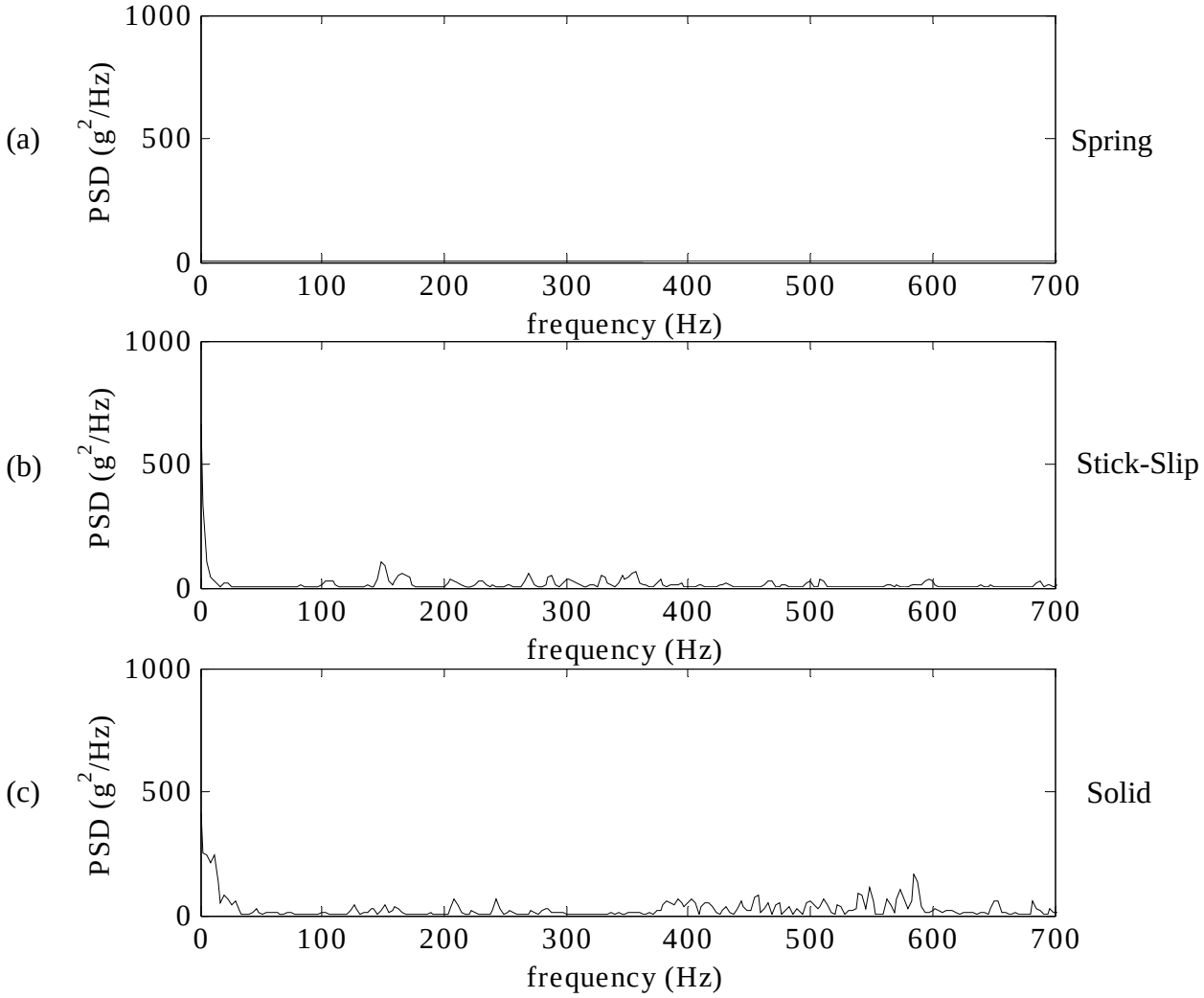

Figure A-13. PSD of Longitudinal Acceleration from Location 8 for (a) Spring, (b) Stick-Slip, and (c) Solid Load Transfer Mechanisms for the Empty Tank Car

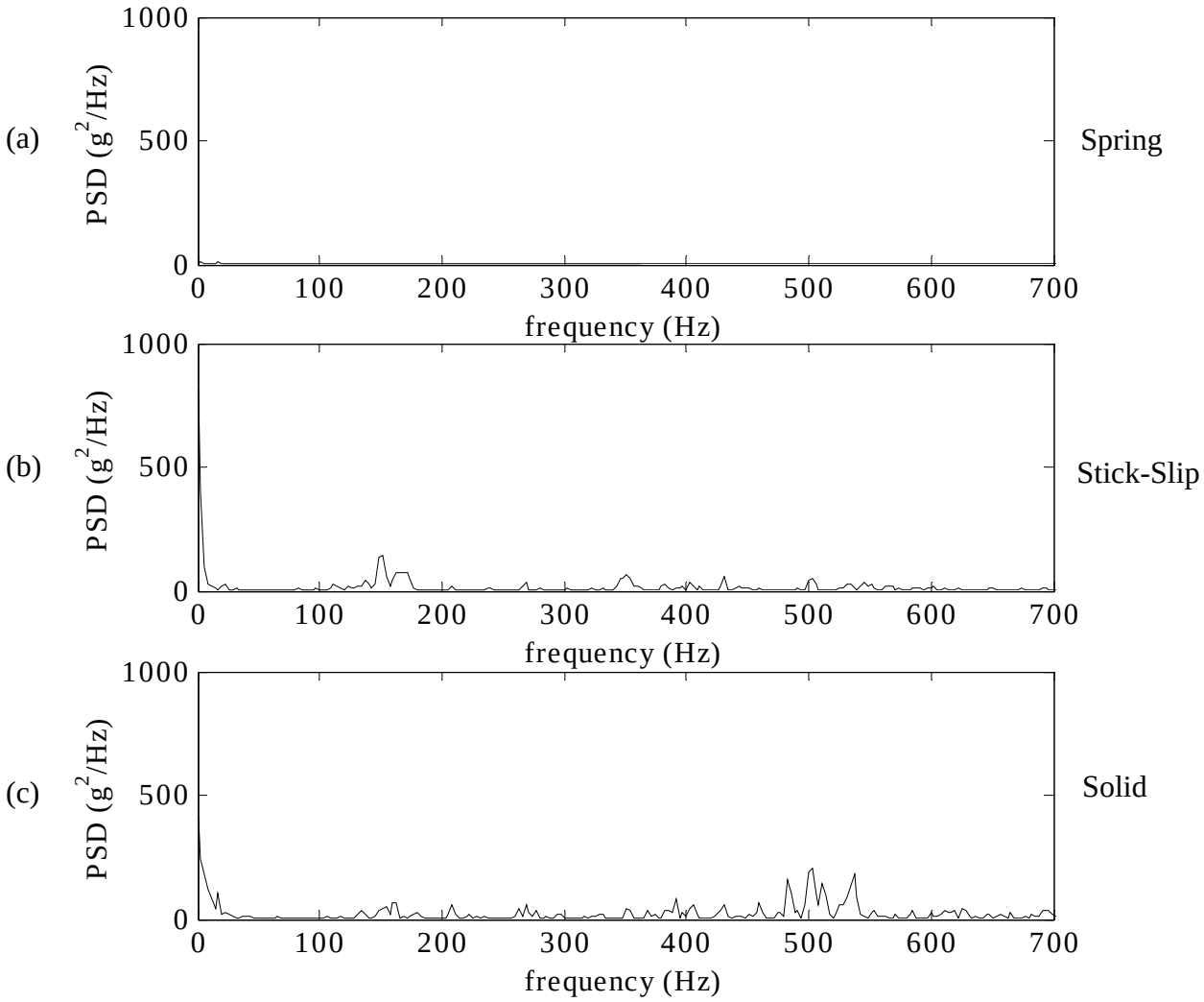

Figure A-14. PSD of Longitudinal Acceleration from Location 9 for (a) Spring, (b) Stick-Slip, and (c) Solid Load Transfer Mechanisms for the Empty Tank Car

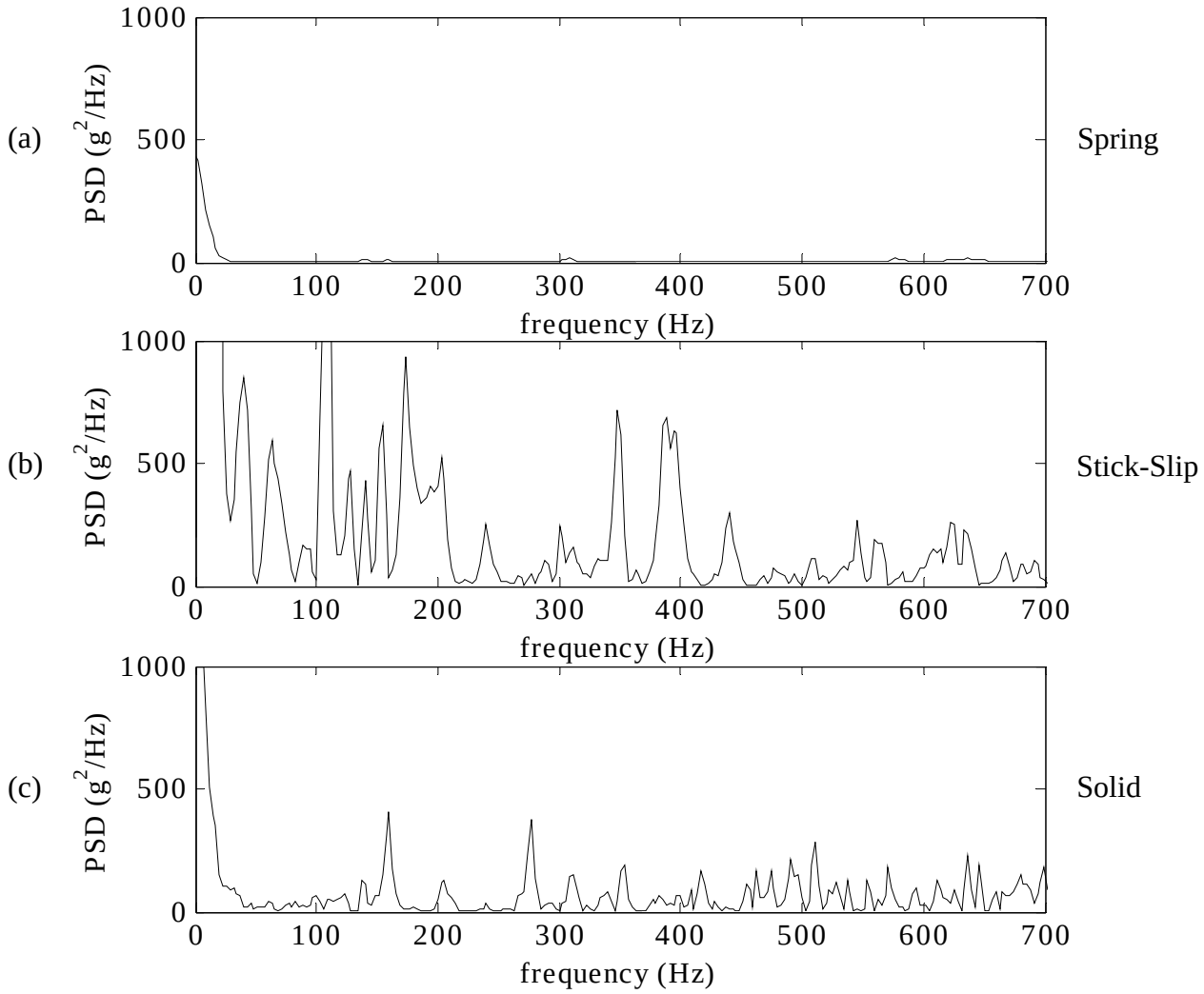

Figure A-15. PSD of Longitudinal Acceleration from Location 11 for (a) Spring, (b) Stick-Slip, and (c) Solid Load Transfer Mechanisms for the Empty Tank Car

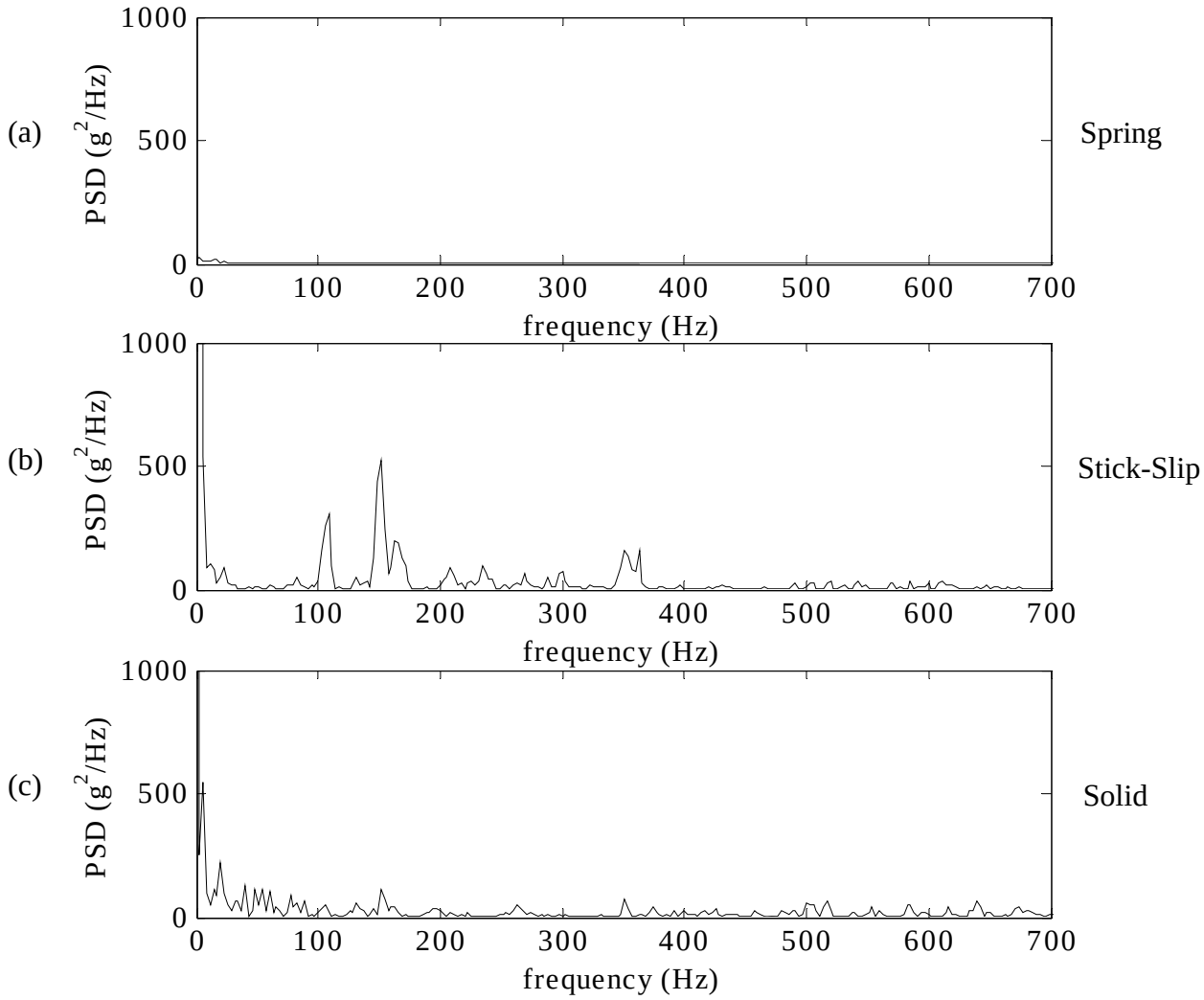

Figure A-16. PSD of Longitudinal Acceleration from Location 12 for (a) Spring, (b) Stick-Slip, and (c) Solid Load Transfer Mechanisms for the Empty Tank Car

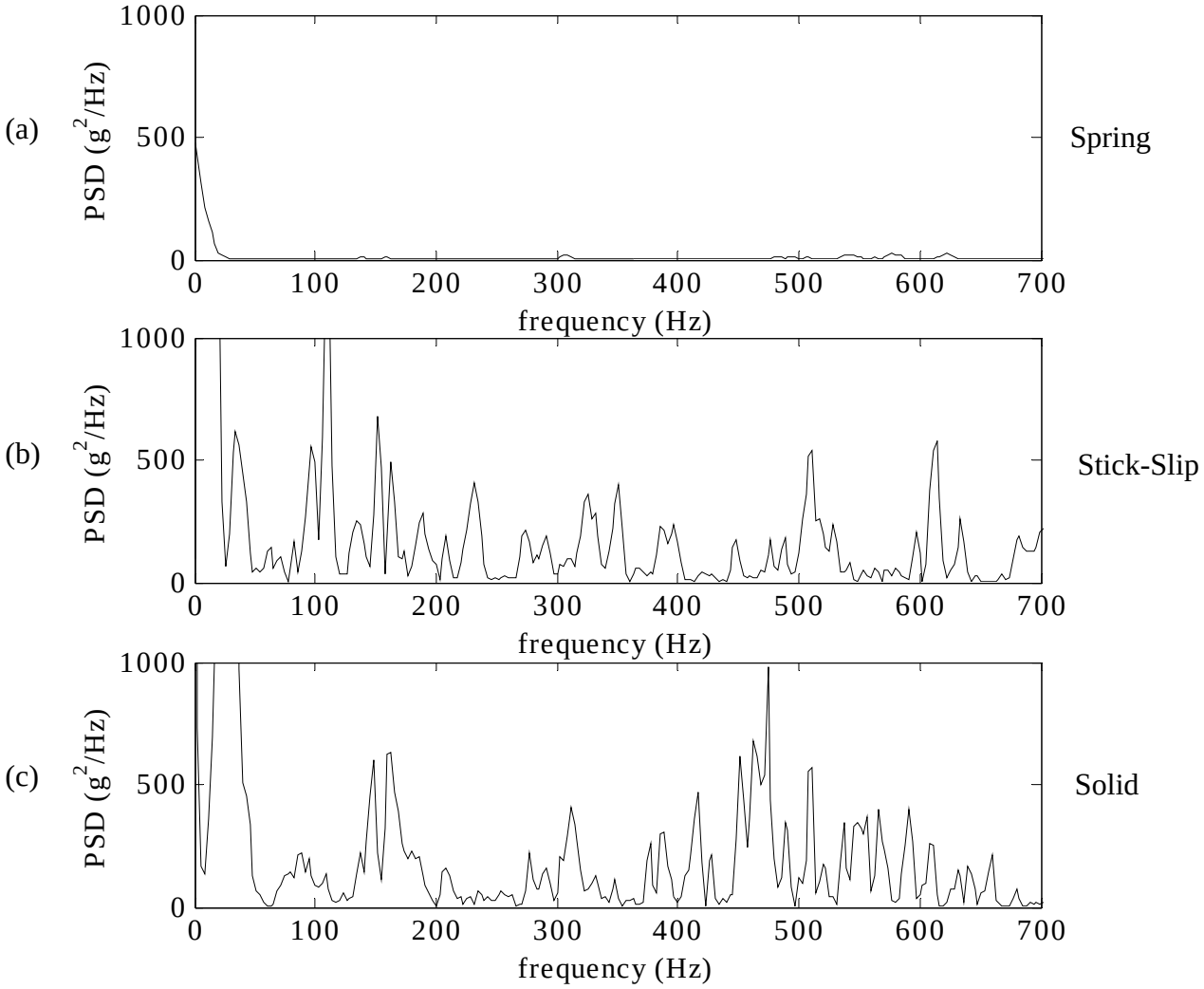

Figure A-17. PSD of Longitudinal Acceleration from Location 13 for (a) Spring, (b) Stick-Slip, and (c) Solid Load Transfer Mechanisms for the Empty Tank Car

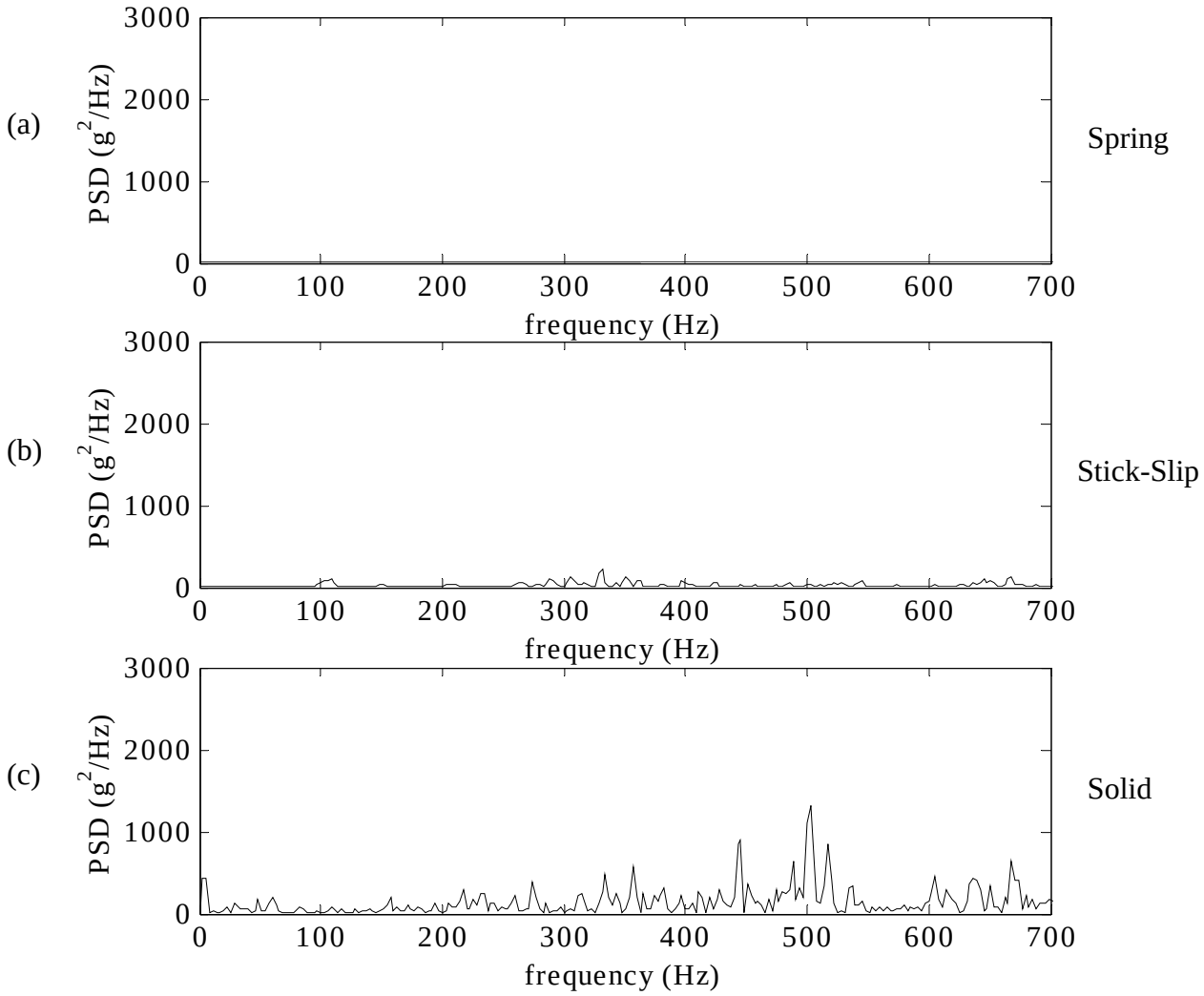

Figure A-18. PSD of Vertical Acceleration from Location 14 for (a) Spring, (b) Stick-Slip, and (c) Solid Load Transfer Mechanisms for the Empty Tank Car

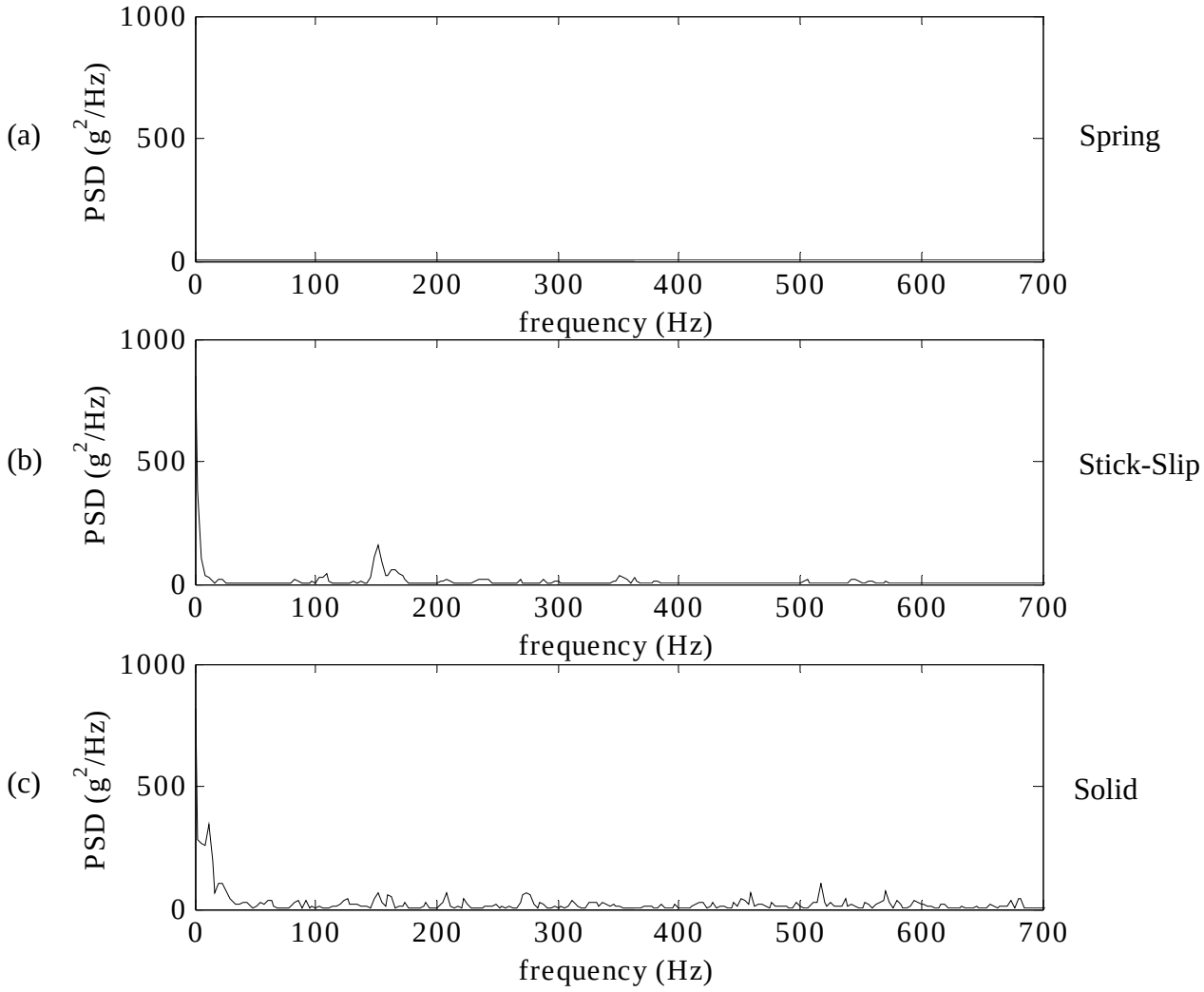

Figure A-19. PSD of Longitudinal Acceleration from Location 14 for (a) Spring, (b) Stick-Slip, and (c) Solid Load Transfer Mechanisms for the Empty Tank Car

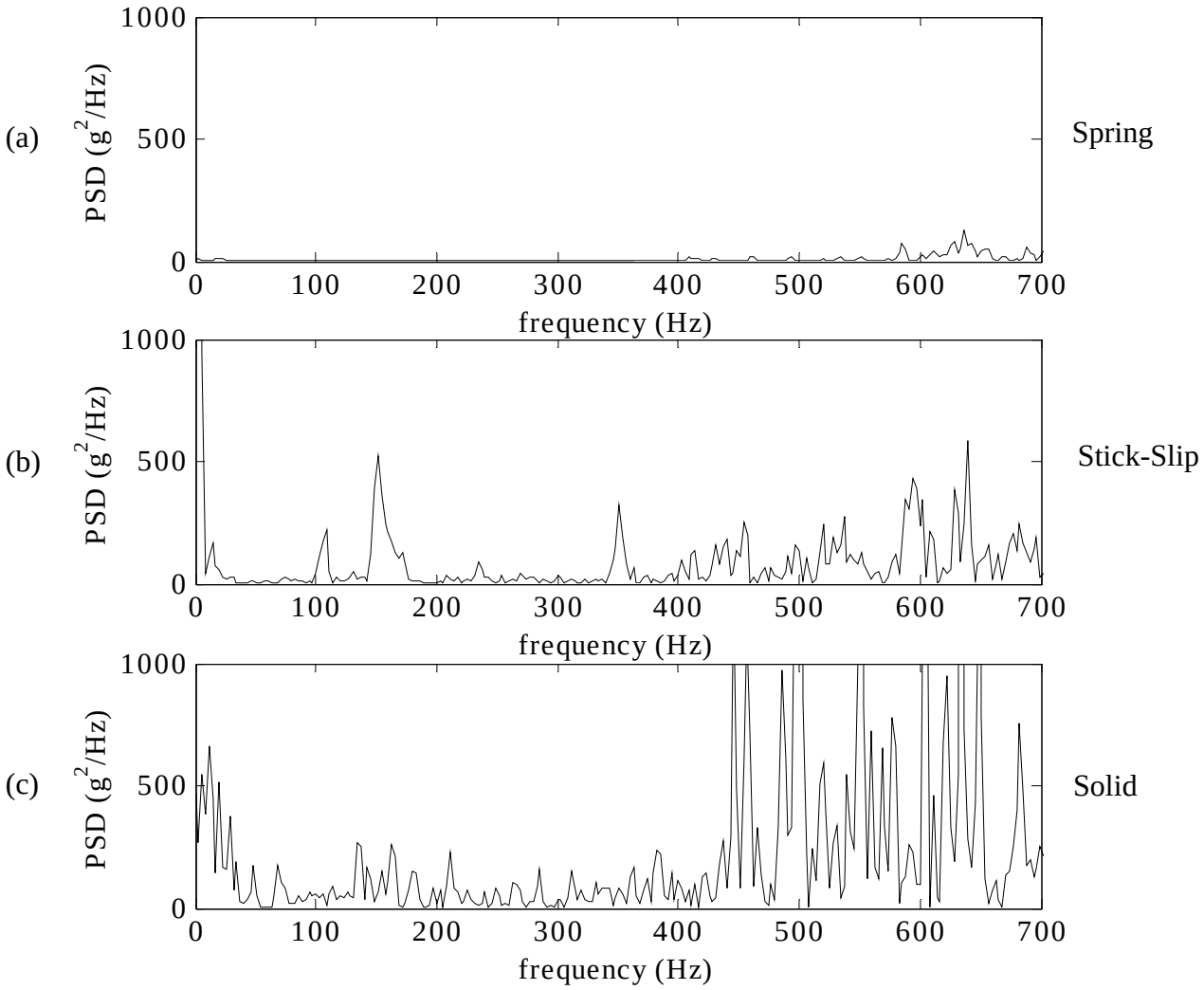

Figure A-20. PSD of Longitudinal Acceleration from Location 16 for (a) Spring, (b) Stick-Slip, and (c) Solid Load Transfer Mechanisms for the Empty Tank Car

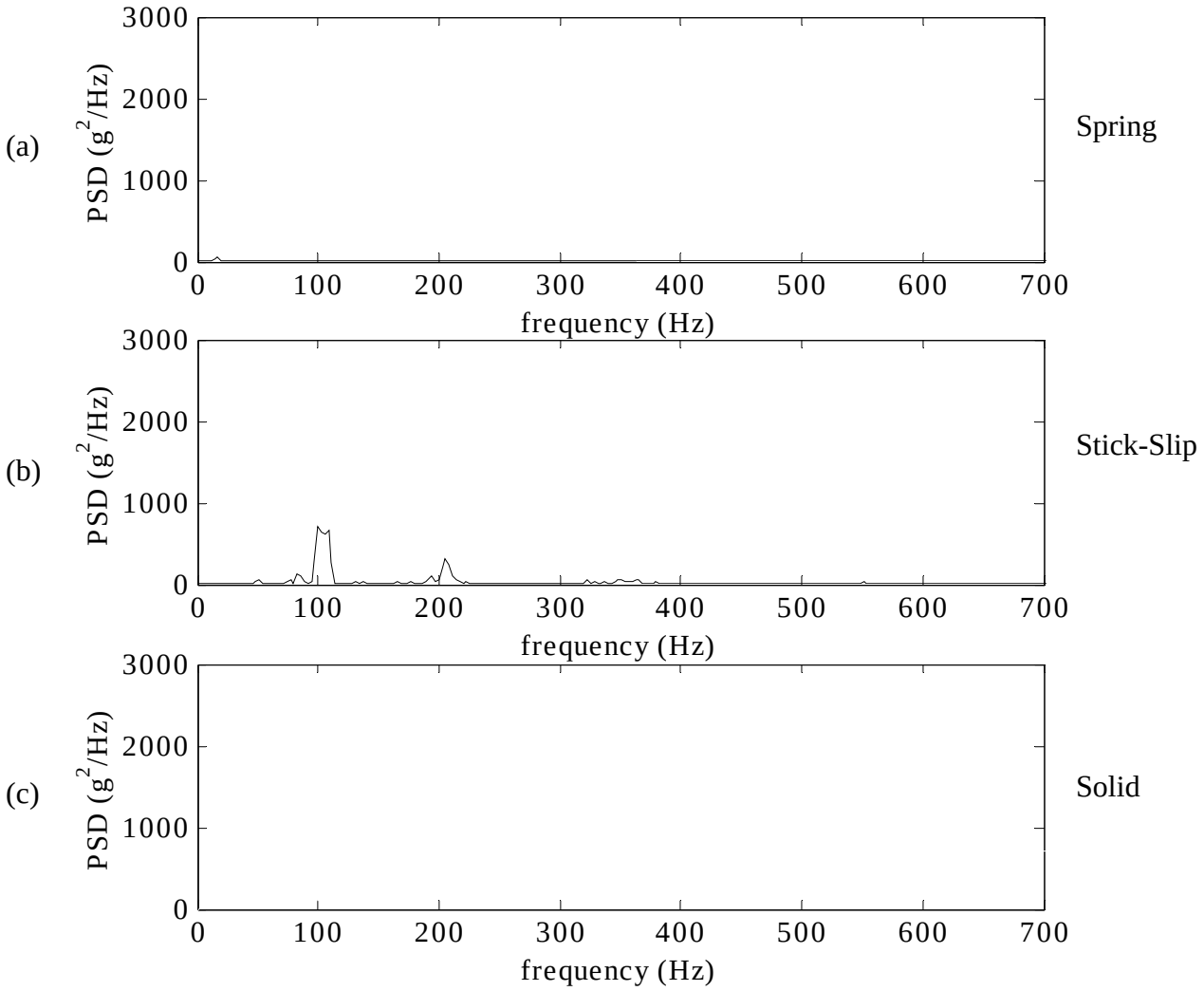

Figure A-21. PSD of Vertical Acceleration from Location 17 for (a) Spring, (b) Stick-Slip, and (c) Solid Load Transfer Mechanisms for the Empty Tank Car

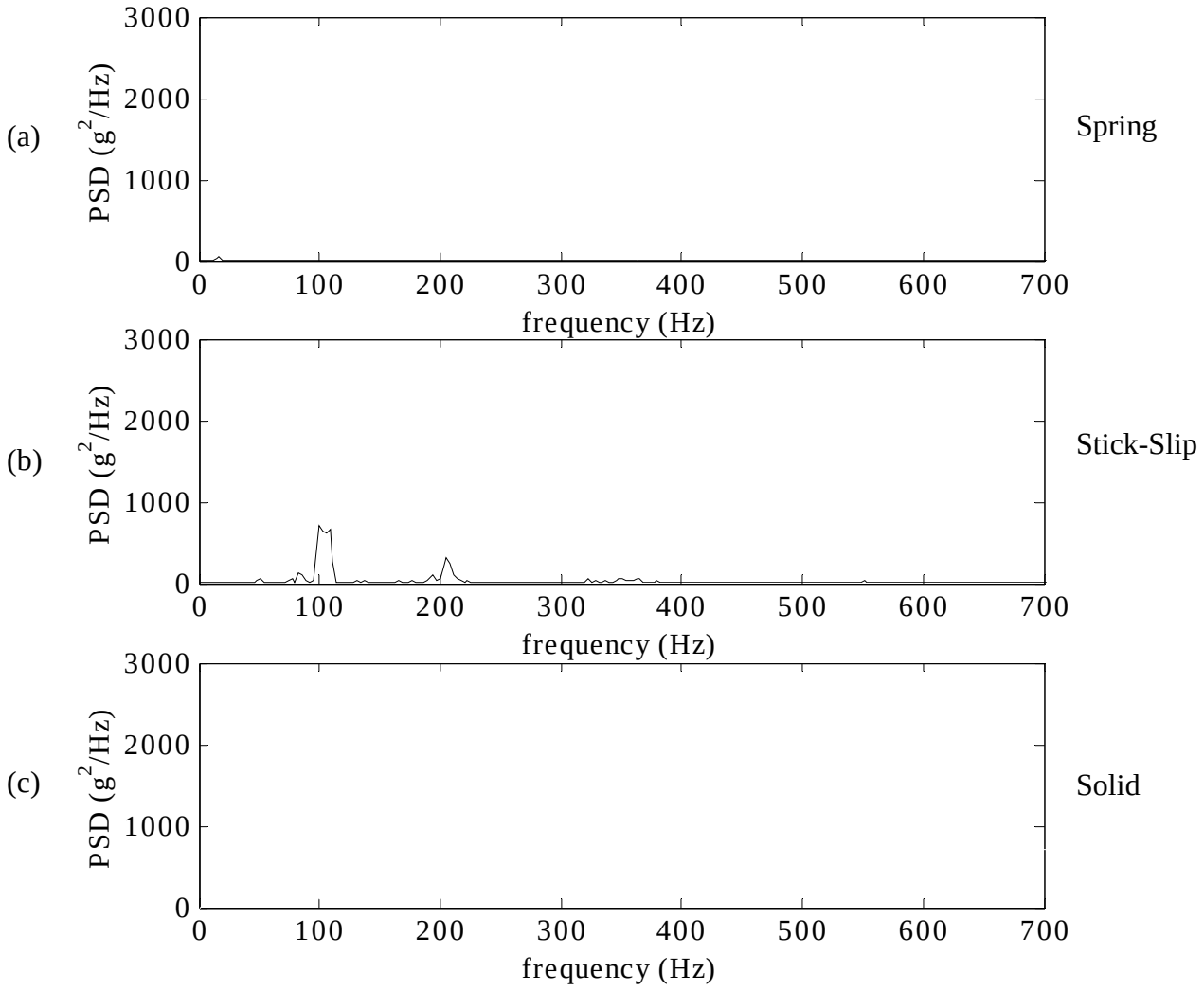

Figure A22. PSD of Vertical Acceleration from Location 18 for (a) Spring, (b) Stick-Slip, and (c) Solid Load Transfer Mechanisms for the Empty Tank Car

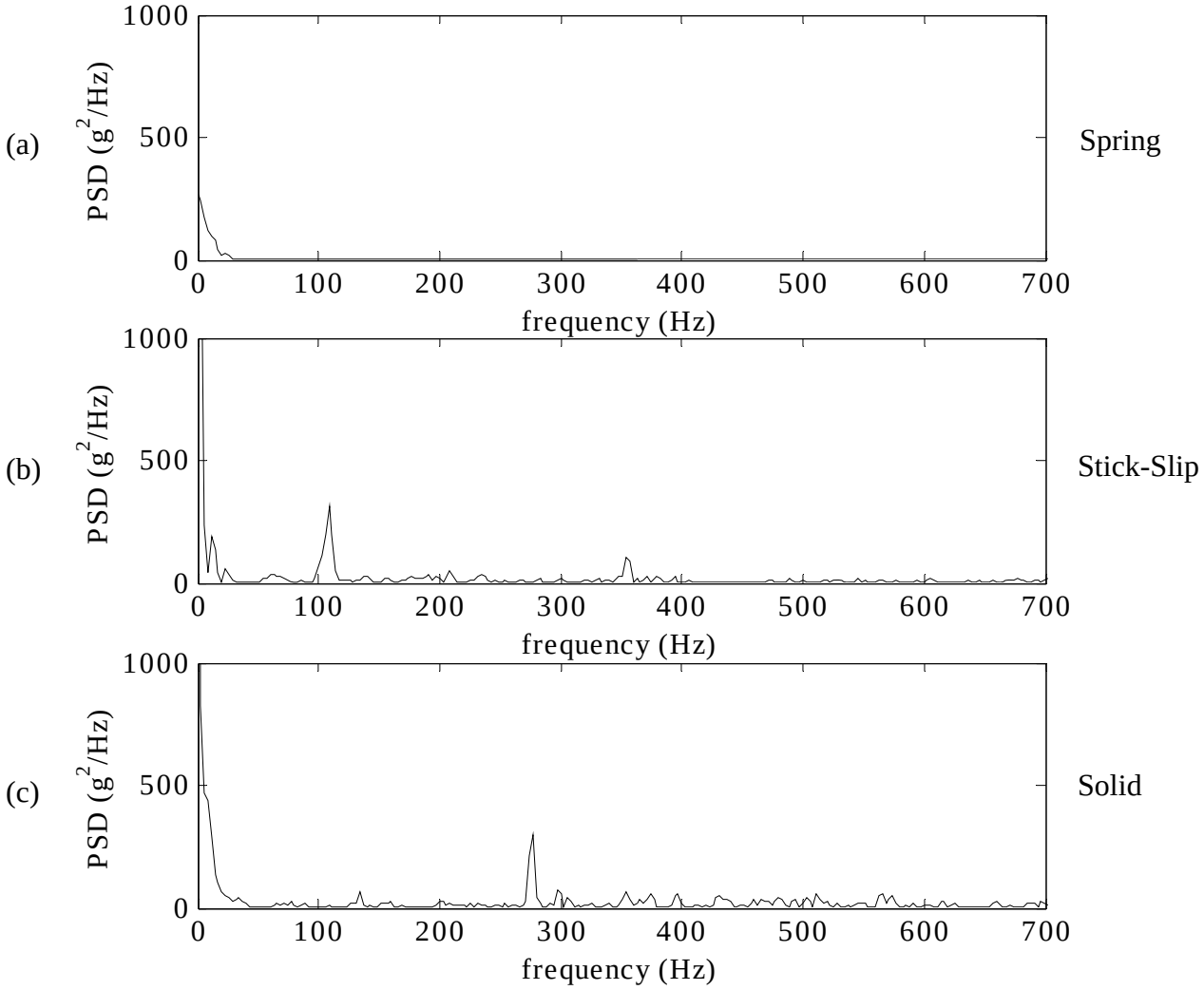

Figure A-23. PSD of Longitudinal Acceleration from Location 18 for (a) Spring, (b) Stick-Slip, and (c) Solid Load Transfer Mechanisms for the Empty Tank Car

Appendix B.
PSD Results of Full Car Impact Tests

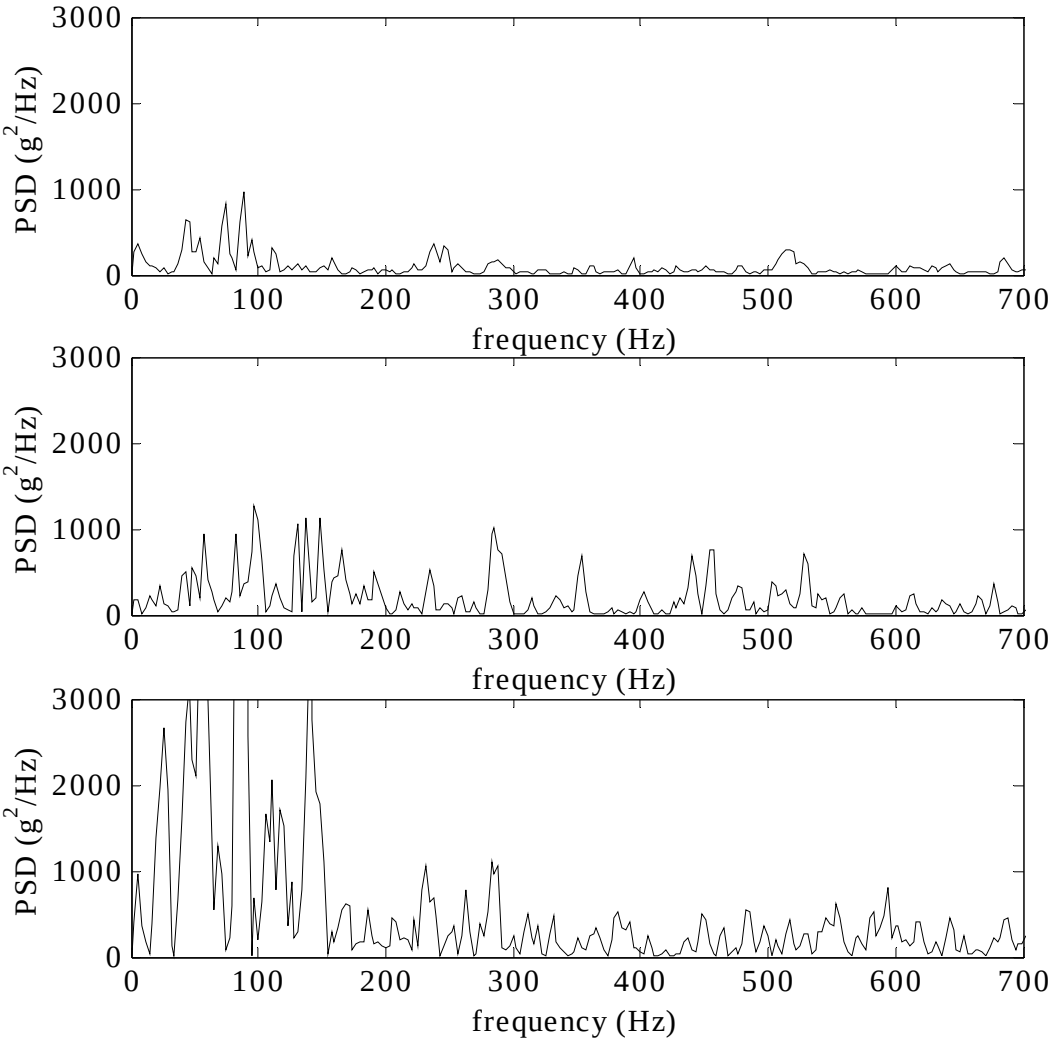

Figure B-1. PSD of Vertical Acceleration from Location 1 for (a) Spring, (b) Stick-Slip, and (c) Solid Load Transfer Mechanisms for the Loaded Tank Car

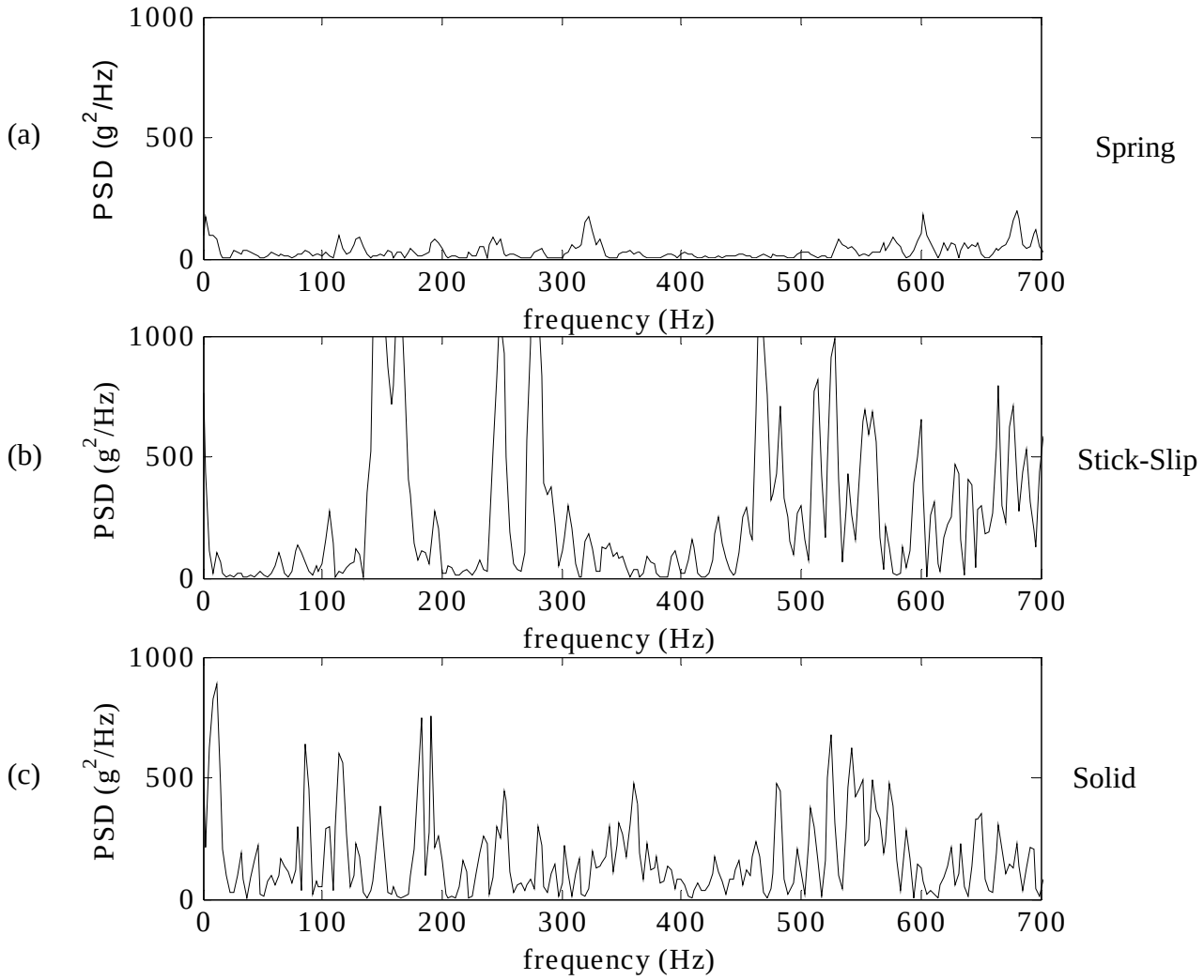

Figure B-2. PSD of Longitudinal Acceleration from Location 1 for (a) Spring, (b) Stick-Slip, and (c) Solid Load Transfer Mechanisms for the Loaded Tank Car

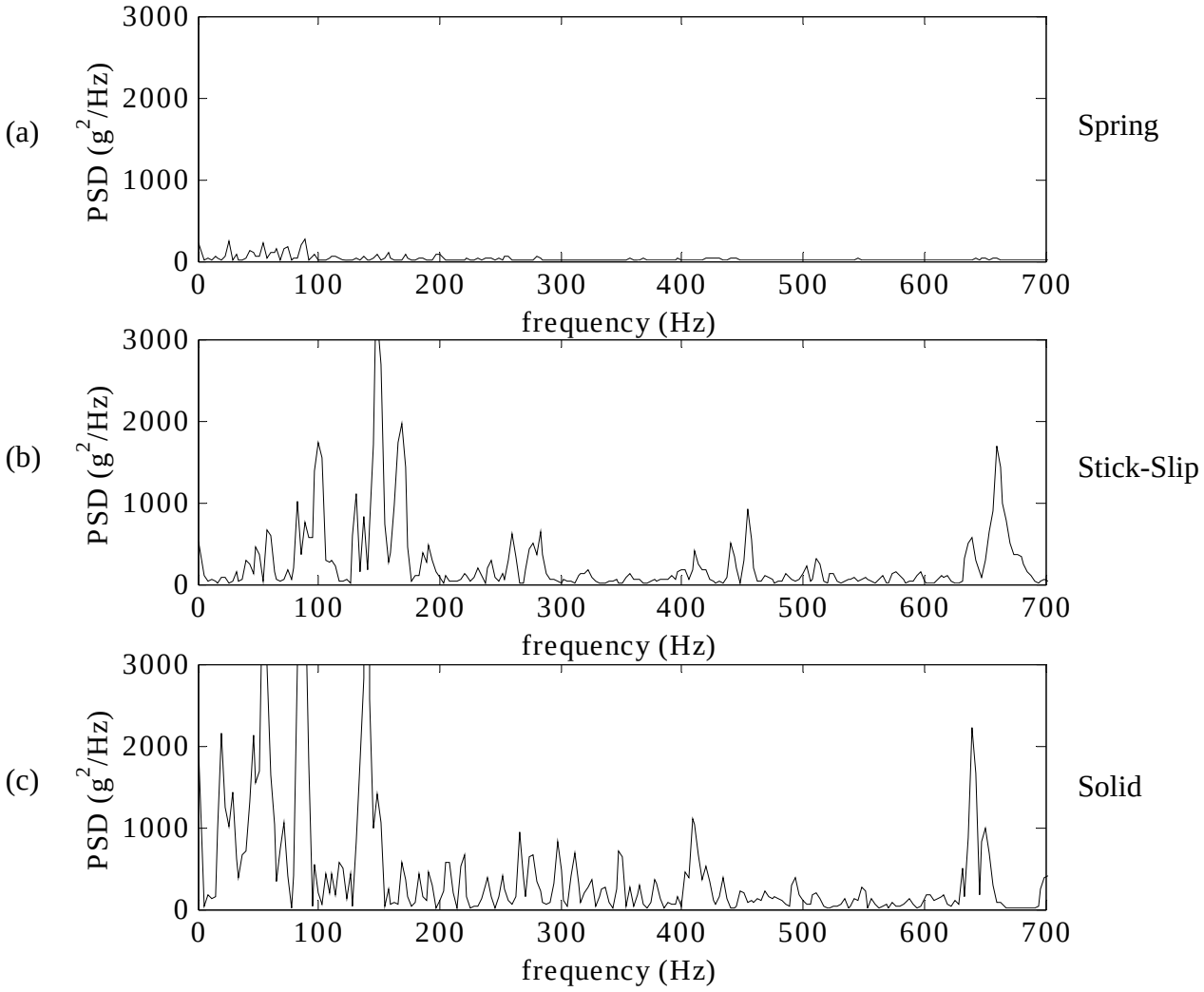

Figure B-3. PSD of Vertical Acceleration from Location 1A for (a) Spring, (b) Stick-Slip, and (c) Solid Load Transfer Mechanisms for the Loaded Tank Car

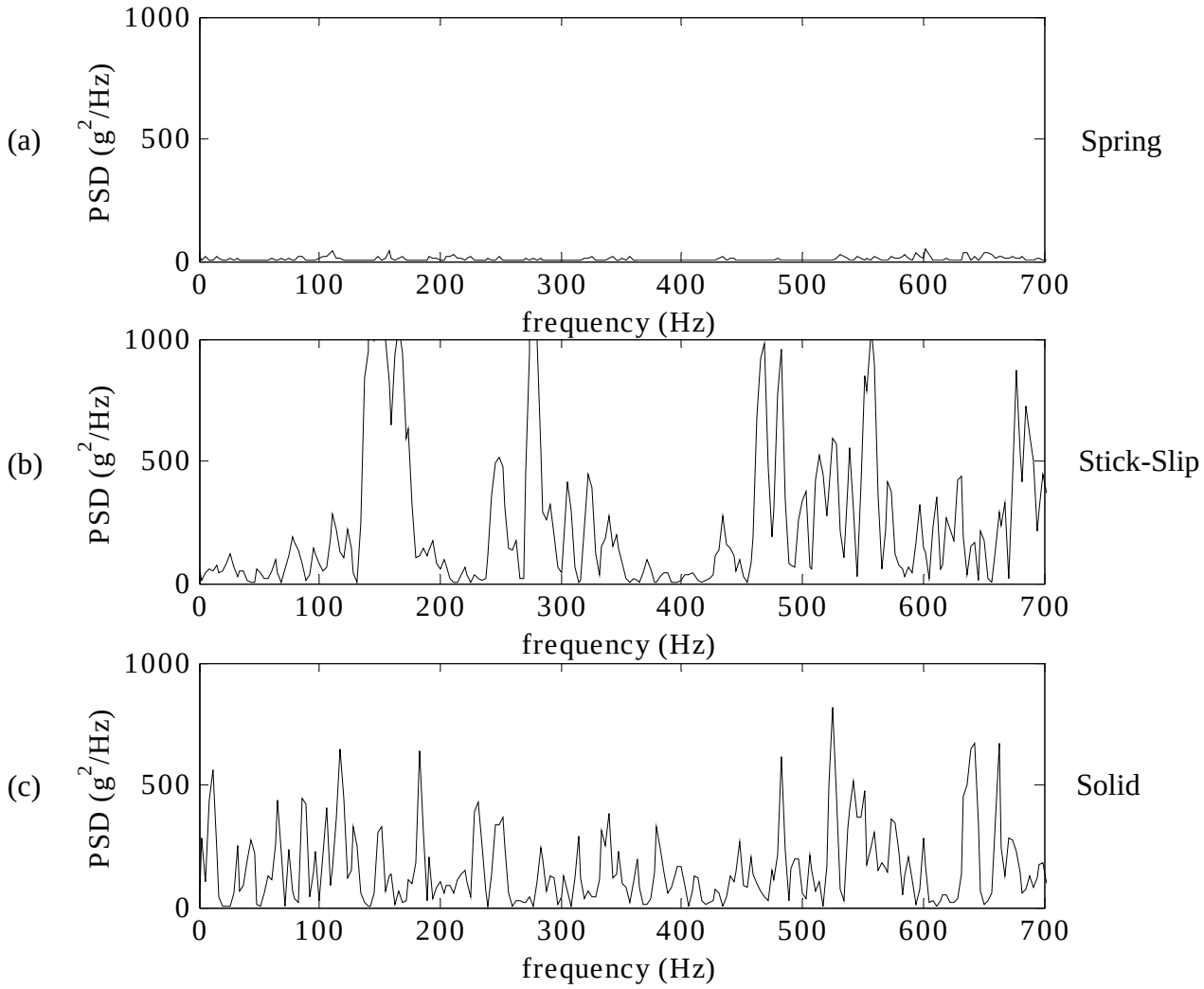

Figure B-4. PSD of Longitudinal Acceleration from Location 1A for (a) Spring, (b) Stick-Slip, and (c) Solid Load Transfer Mechanisms for the Loaded Tank Car

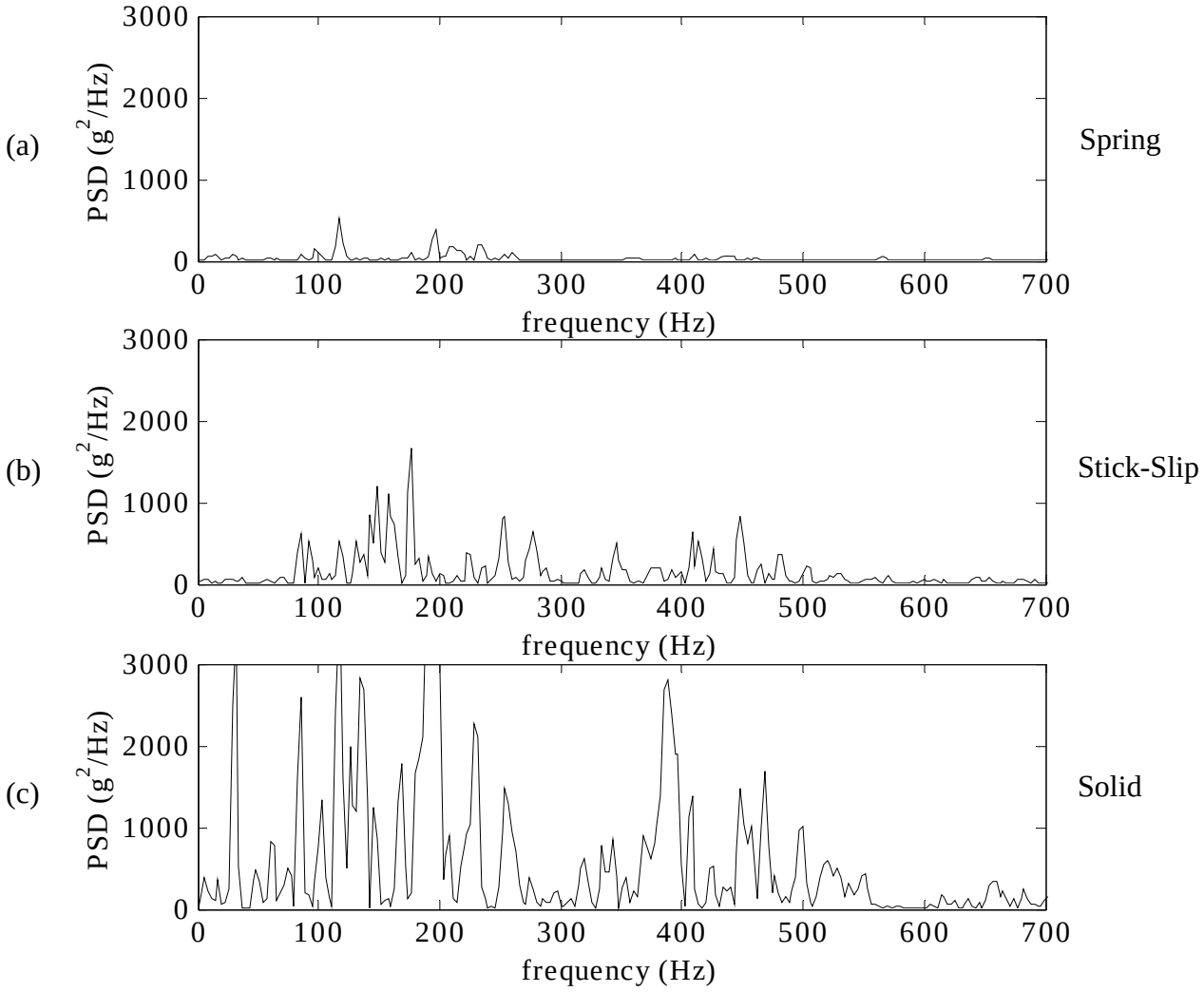

Figure B-5. PSD of Vertical Acceleration from Location 5 for (a) Spring, (b) Stick-Slip, and (c) Solid Load Transfer Mechanisms for the Loaded Tank Car

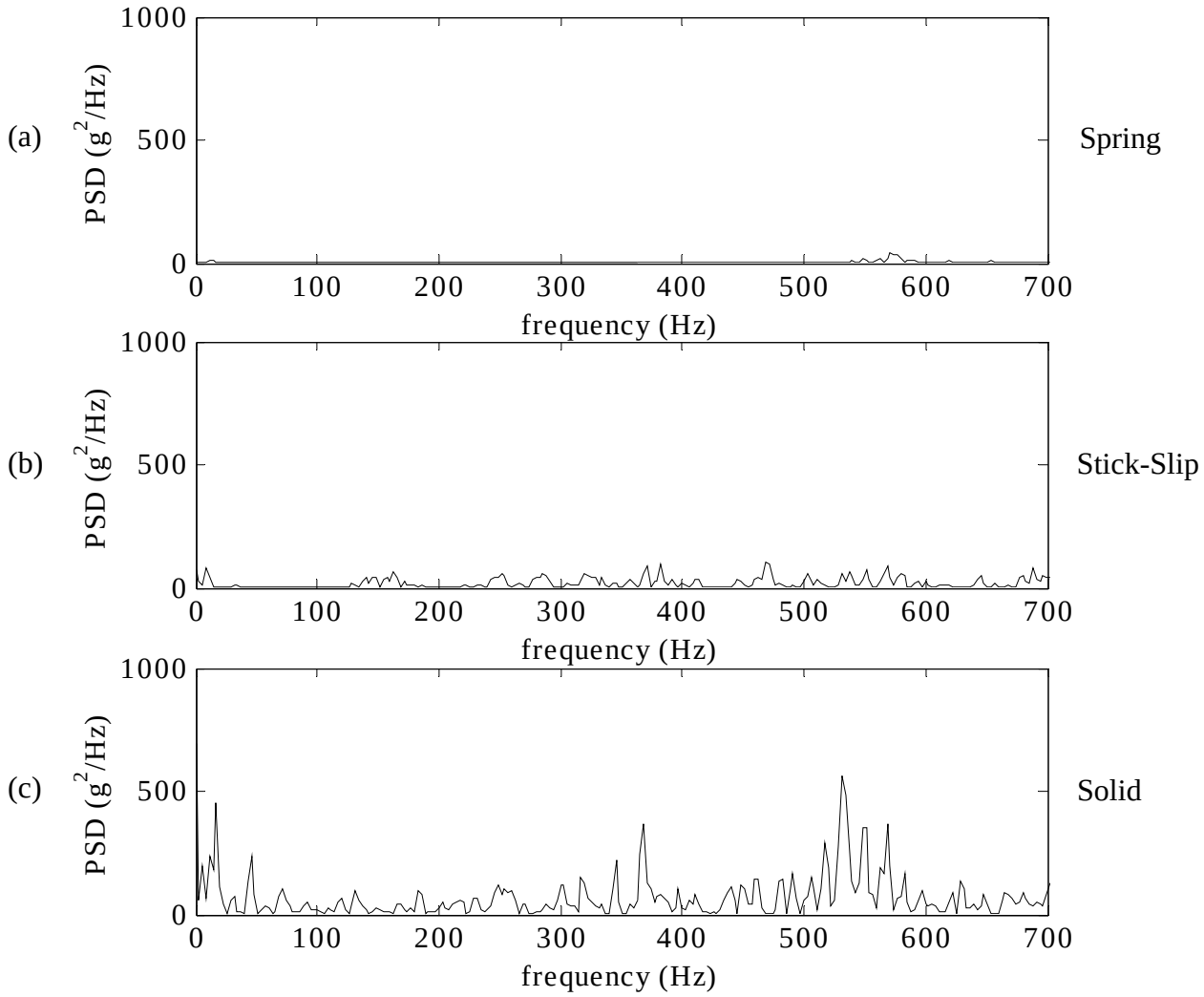

Figure B-6. PSD of Longitudinal Acceleration from Location 5 for (a) Spring, (b) Stick-Slip, and (c) Solid Load Transfer Mechanisms for the Loaded Tank Car

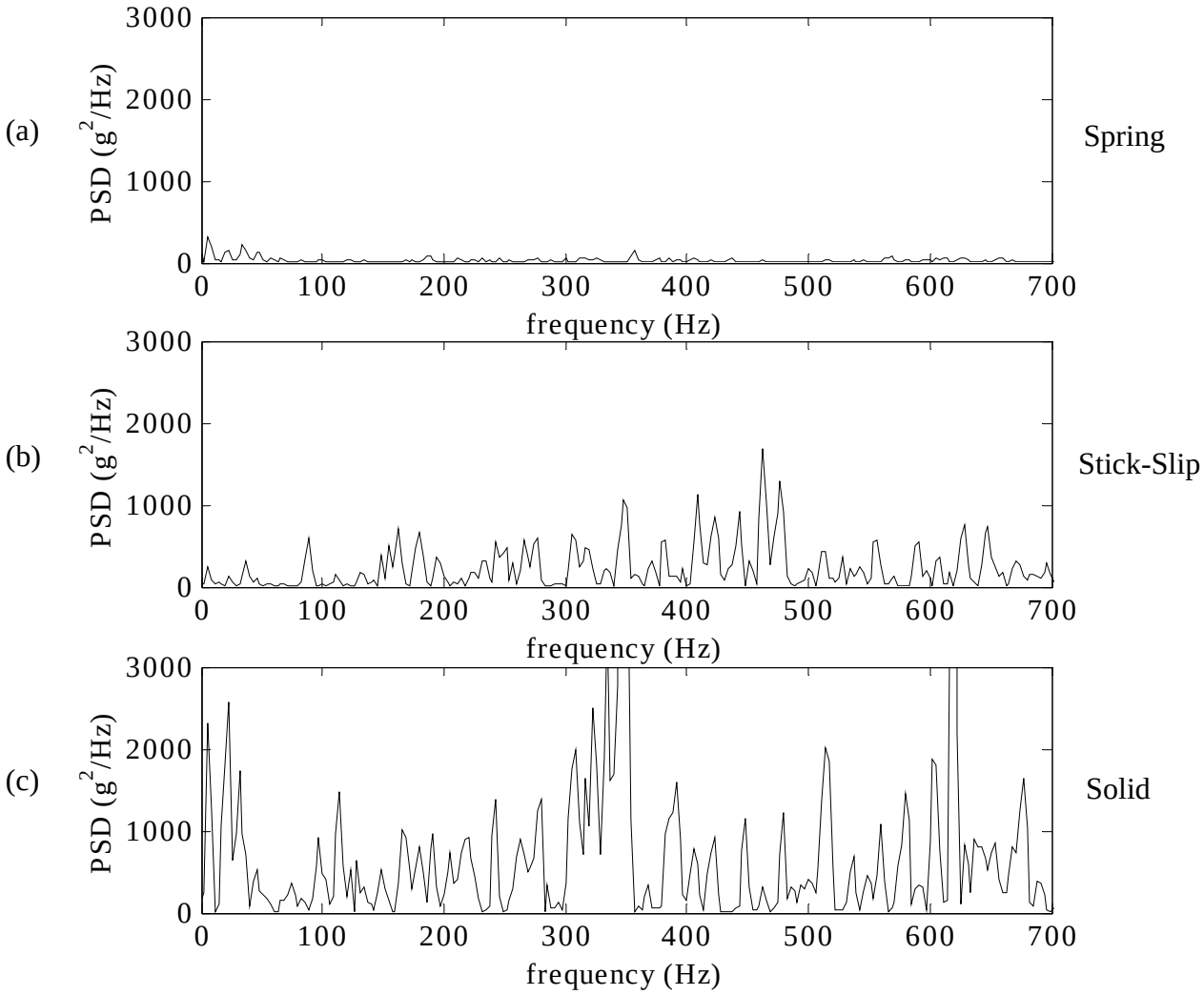

Figure B-7. PSD of Vertical Acceleration from Location 6 for (a) Spring, (b) Stick-Slip, and (c) Solid Load Transfer Mechanisms for the Loaded Tank Car

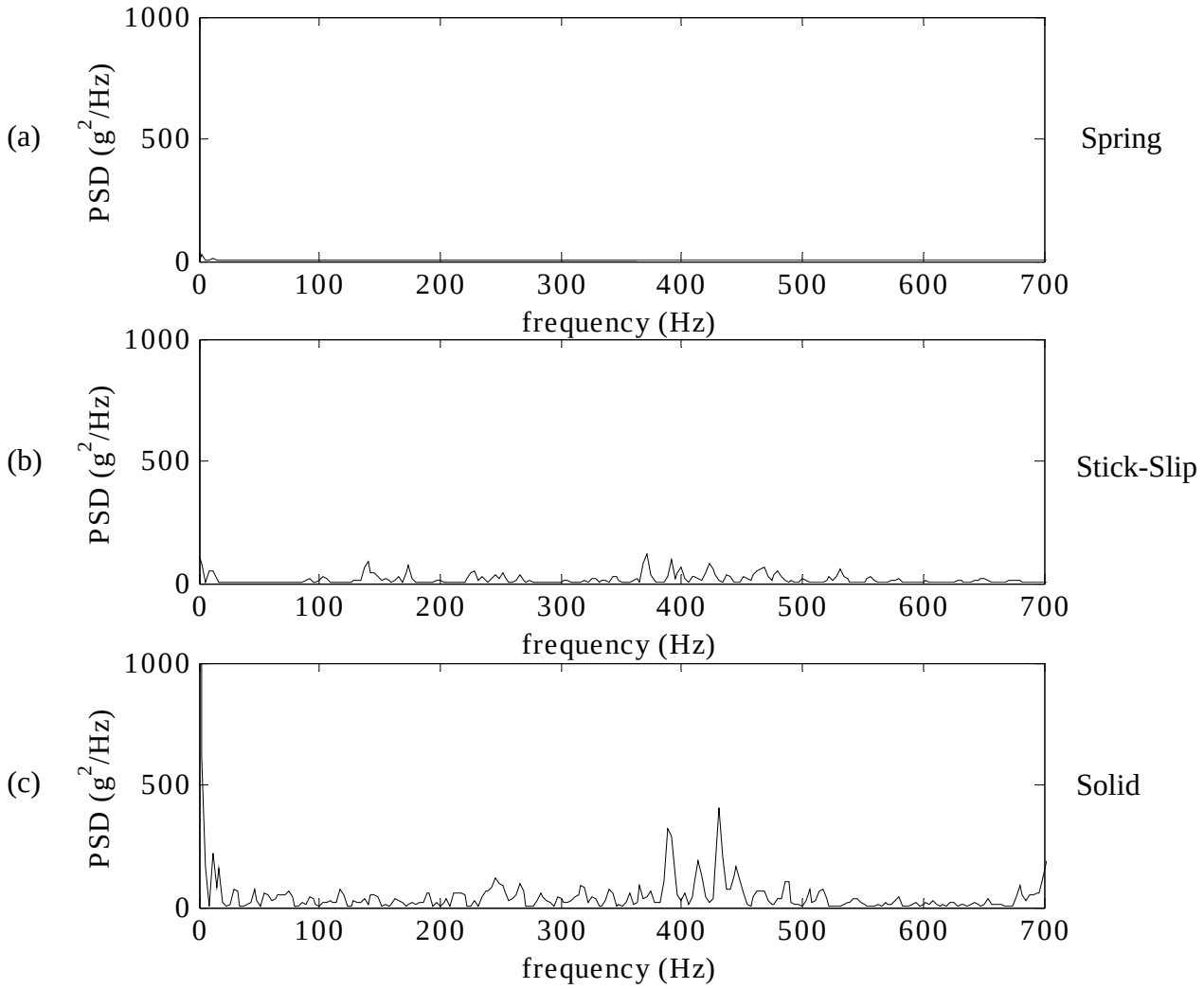

Figure B-8. PSD of Longitudinal Acceleration from Location 6 for (a) Spring, (b) Stick-Slip, and (c) Solid Load Transfer Mechanisms for the Loaded Tank Car

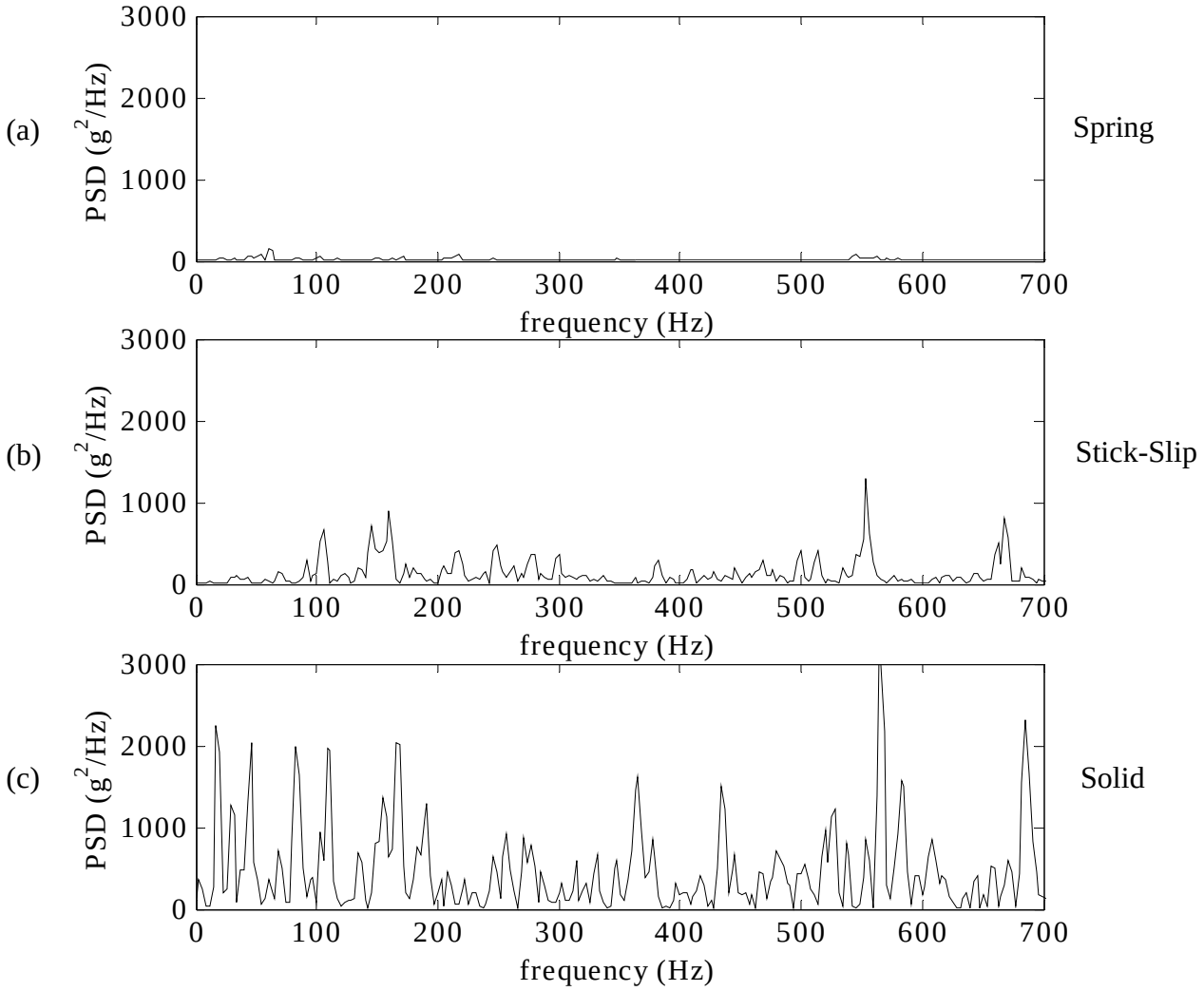

Figure B-9. PSD of Vertical Acceleration from Location 9 for (a) Spring, (b) Stick-Slip, and (c) Solid Load Transfer Mechanisms for the Loaded Tank Car

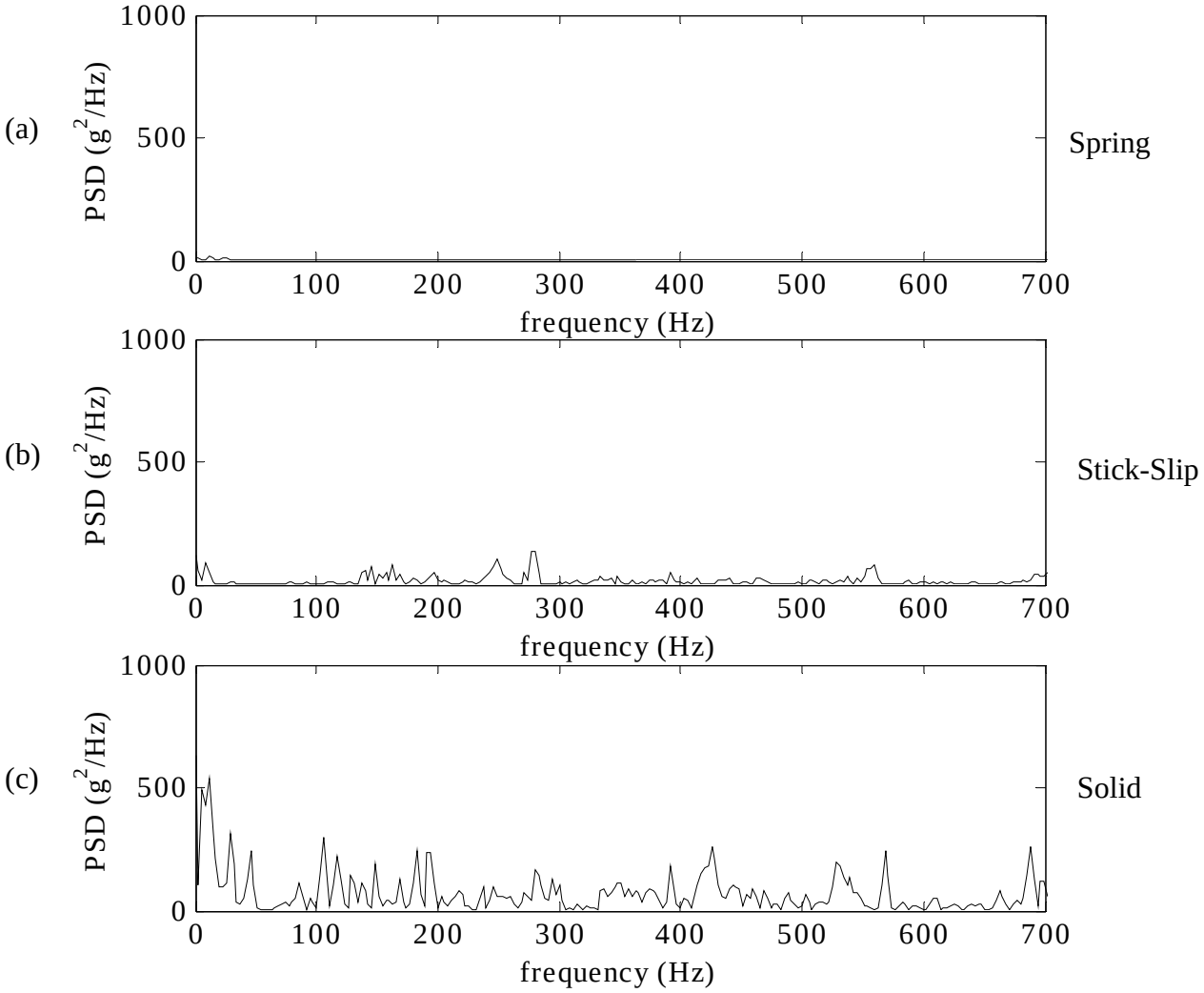

Figure B-10. PSD of Longitudinal Acceleration from Location 9 for (a) Spring, (b) Stick-Slip, and (c) Solid Load Transfer Mechanisms for the Loaded Tank Car

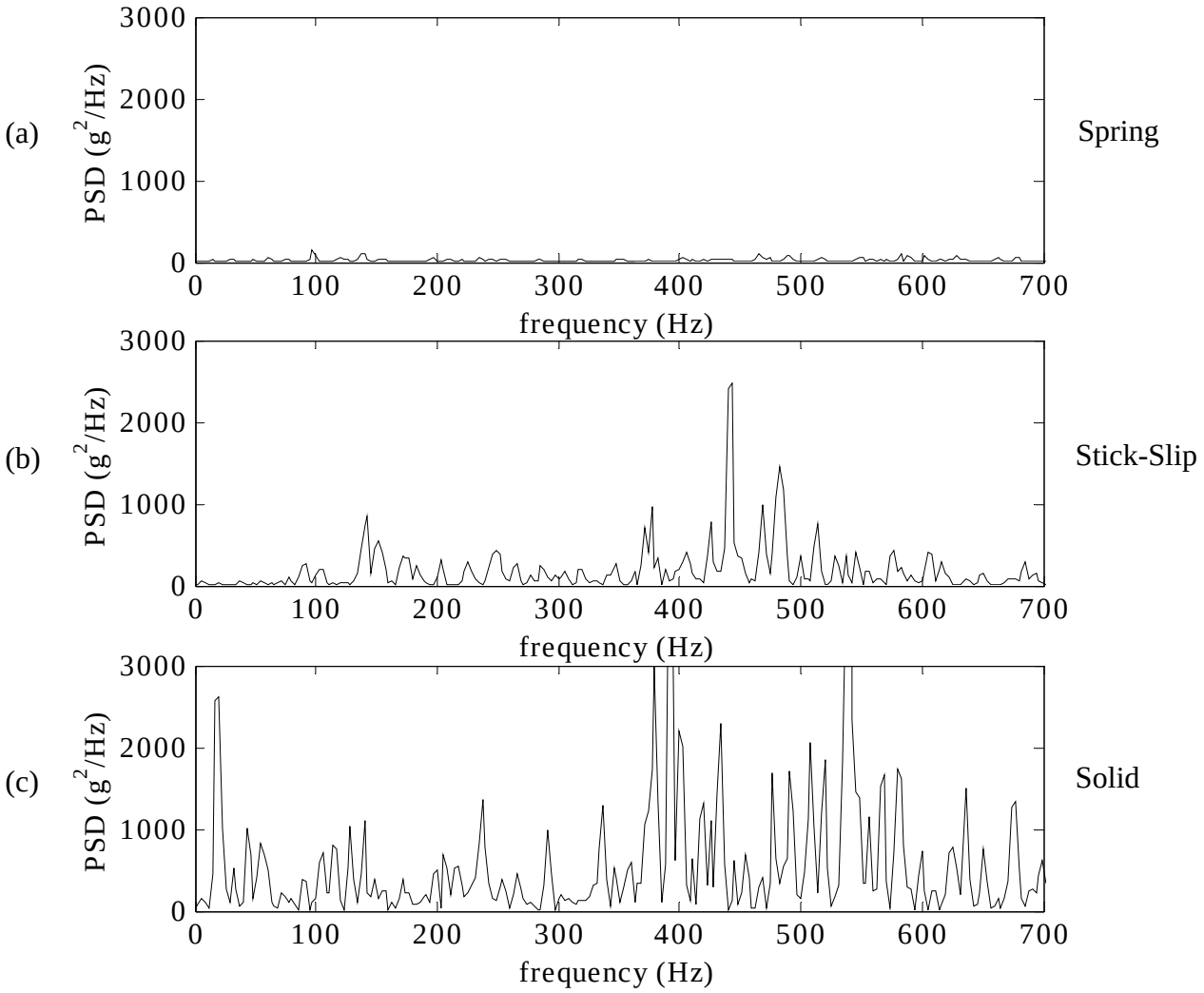

Figure B-11. PSD of Vertical Aceleration from Location 10 for (a) Spring, (b) Stick-Slip, and (c) Solid Load Transfer Mechanisms for the Loaded Tank Car

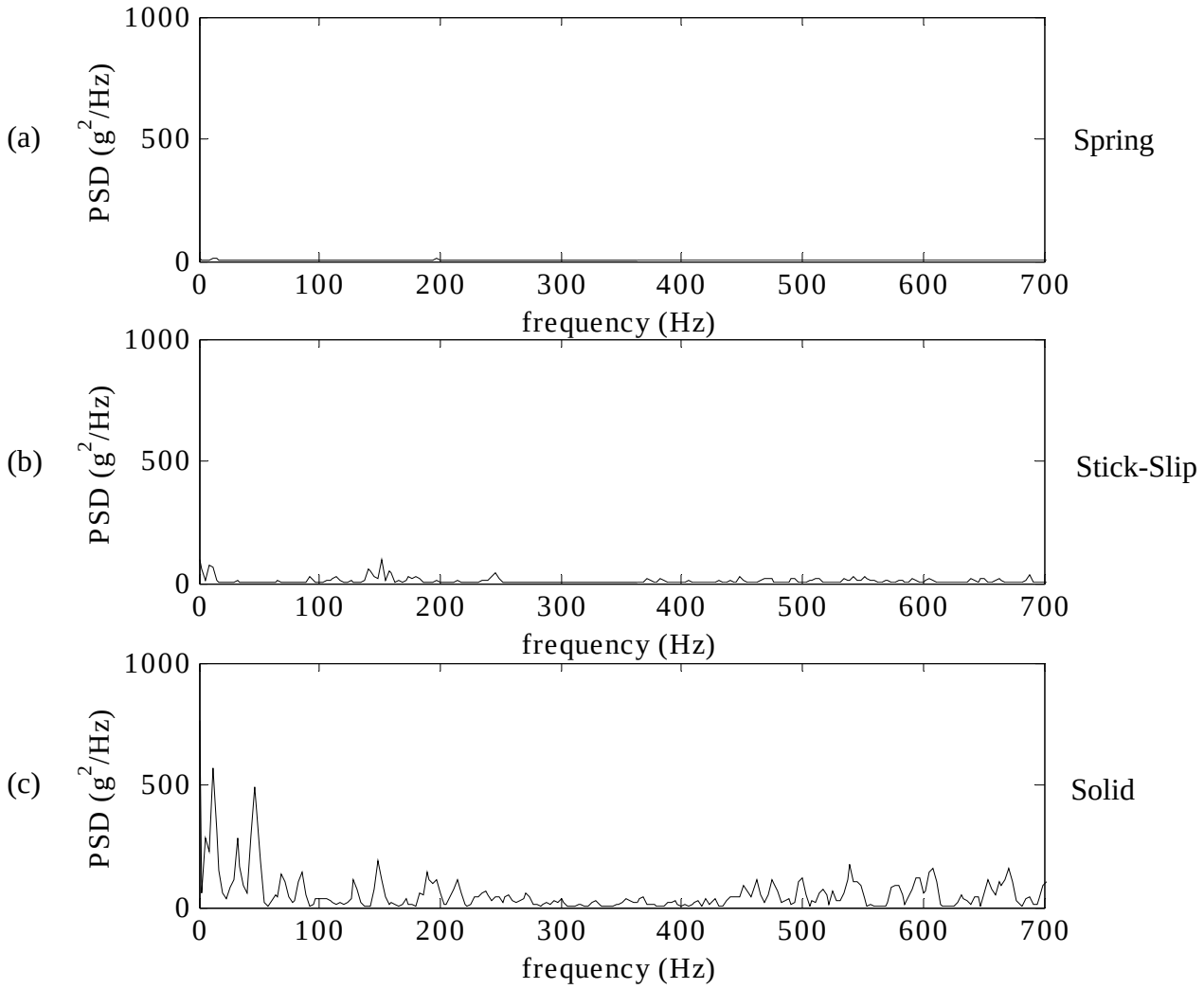

Figure B-12. PSD of Longitudinal Acceleration from Location 10 for (a) Spring, (b) Stick-Slip, and (c) Solid Load Transfer Mechanisms for the Loaded Tank Car

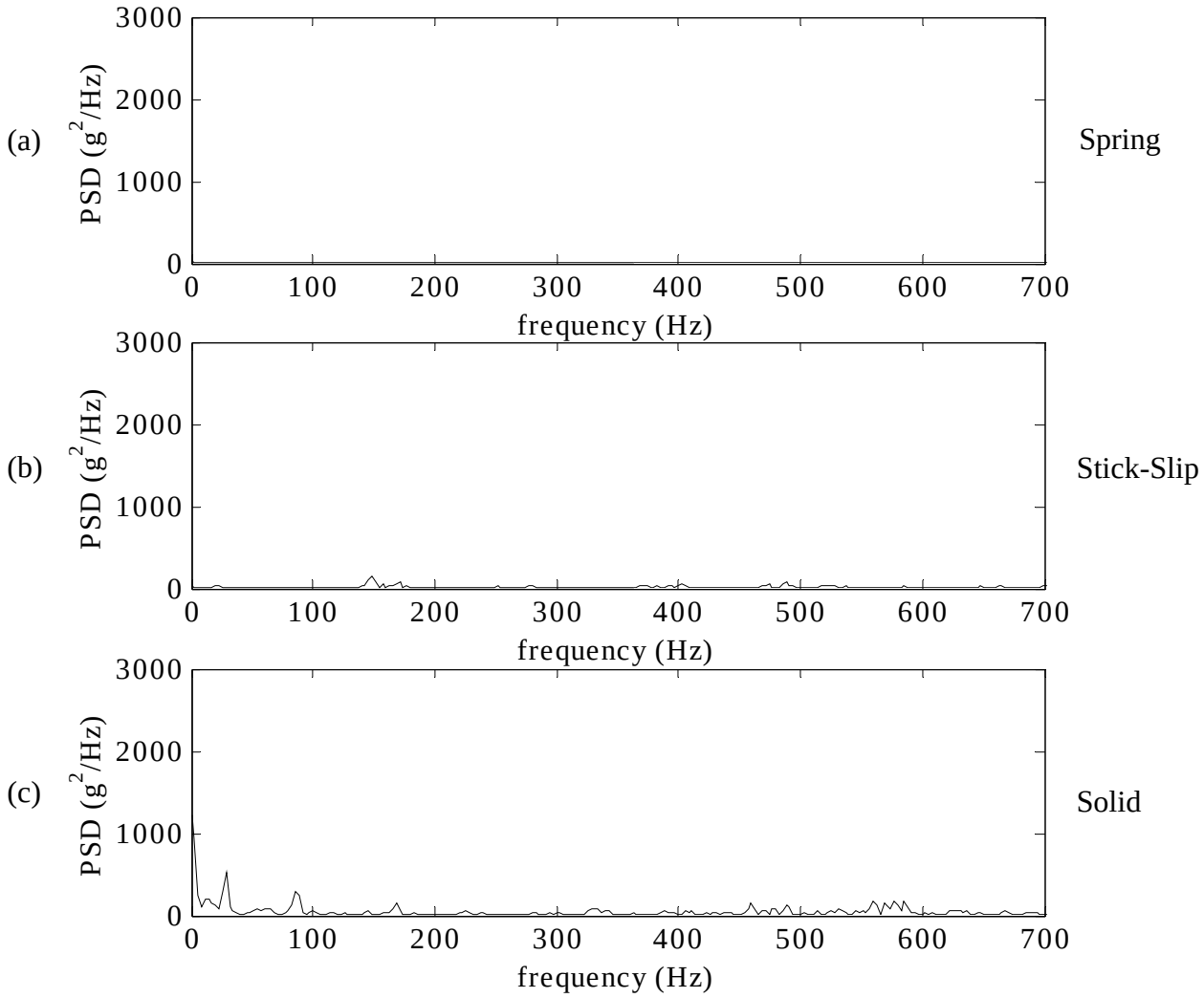

Figure B-13. PSD of Vertical Acceleration from Location 18 for (a) Spring, (b) Stick-Slip, and (c) Solid Load Transfer Mechanisms for the Loaded Tank Car

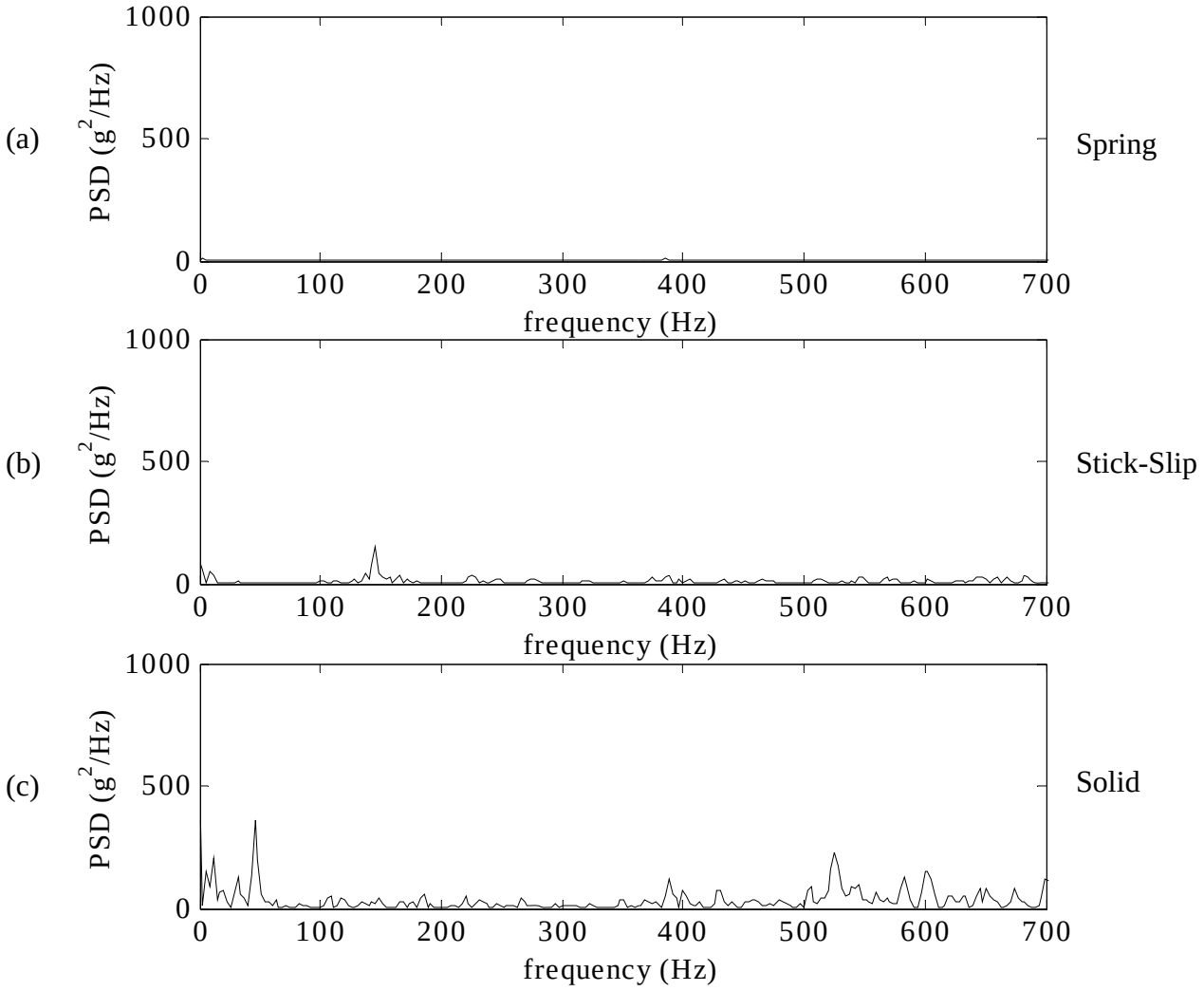

Figure B-14. PSD of Longitudinal Acceleration from Location 18 for (a) Spring, (b) Stick-slip, and (c) Solid Load Transfer Mechanisms for the Loaded Tank Car

Acronyms

AAR	Association of American Railroads
ACF	American Car and Foundry
FRA	Federal Railroad Administration
MPH	miles per hour
PSD	power spectral density
SRS	shock response spectrum